POLITECNICO DI MILANO

POLO REGIONALE DI LECCO

Facoltà di Ingegneria Civile, Ambientale and Territoriale

MASTER OF SCIENCE IN CIVIL ENGINEERING

FOR RISK MITIGATION

ROBUSTNESS OF SELF CONSOLIDATING STEEL FIBER REINFORCED CONCRETE.

SUPERVISOR: PROF. LIBERATO FERRARA.

Co-supervisors: PROF. PATRICK BAMONTE AND DR. ALESSIO CAVERZAN.

MASTER THESIS:

MUSA ABDISA MOHAMMED [Mat. 737745];

ACADEMIC YEAR 2009/10.

ABSTRACT

The applications of self consolidating steel fiber reinforced concrete (SCSFRC) are rising considerably worldwide due to several new advantages with respect to conventional concrete. One of the main obstacles of wider use of self consolidating steel fiber reinforced concrete is its sensitivity to small variations of the constituent materials, mix-proportions and other external factors. There is a great importance to have a robust mixtures which tolerate these deviations, i.e. should maintain its fresh and hardened state properties inside the specified limits. Allowable variations or errors as specified in EC 2 and ACI code for conventional concrete was applied to mix constituents of self consolidating steel fiber reinforced concrete to study the effects on its fresh and hardened state properties. Several mix designs were analyzed to verify whether these variations used in conventional concrete are still applicable to self consolidating steel fiber reinforced concrete. To achieve the aforementioned objectives, experimental tests were conducted at the level of cement paste, cement mortar and self consolidating steel fiber reinforced concrete. The fresh state performance, fiber dispersion and orientation, and hardened state properties of SCSFRC was considered for a thorough evaluation of robustness. Fresh state performance was measured by means of the slump-flow and V funnel test. Fiber dispersion was measured in the fresh state by fiber washing and in the hardened state by a non destructive magnetic probe test with ferrite core. The hardened state properties of self consolidating steel fiber reinforced concrete were measured by means of flexural tests, compression tests, tensile splitting tests performed on the specimens from each mixes. Moreover, the results from the fresh state and hardened state properties were correlated.

Keywords: robustness, rheology, self consolidating concrete, steel fiber, segregation.

ACKNOWLEDGEMENT

TABLE OF CONTENTS

LIST OF SYMBOLS

$\sigma_{N:}$ Nominal stress,

b:- width of the cross-section,

h:- height of cross-section,

m- meter

dm- decimeter

cm- centimeter

mm- millimeter

MPa- Megapascal

Sec.-second

c- cement

w- water

sp- superplastisizer

g- gram

LIST OF ABBREVIATIONS

SCC:- self consolidating/compacting concrete

FRC:- fiber reinforced concrete

SFRC:- steel fiber reinforced concrete

SCSFRC:- self consolidating steel fiber reinforced concrete

GGBF Slag:- Ground Granulated Blast Furnace Slag

COD:- Crack opening displacement

D_{final}- final spread diameter

T_{final}- final flow time

CHAPTER 1: INTRODUCTION

1.1 Research Background

Developed in Japan during1980's, self compacting concrete (SCC) is still relatively a new type of high performance concrete which is designed so that concrete can easily and freely flow around congested reinforcements, consolidating by its own weight and at the same time being cohesive enough to be placed without segregation or bleeding. Currently, SCC has gained wider use in many countries for different applications such as provision of high strength, improved quality and durability, eliminate problems associated with vibrations, less labor evolved.

Precast industry is particularly suited for the use of SCC. In a precast factory, concrete elements with complex geometric shape and dense reinforcement are often produced. The production of such elements using traditional concrete can only be executed with great effort; very strong external vibrators have to be mounted and in some cases casting has to be carried out in more than one step. On the other hand, in a precast plant it is easier to install a quality control system because of the high degree of automations and repetitions of similar process. For this reason, many precast factories have fully converted to the use of SCC (Walraven,2005).

Another technology that has been topic of interest in the 1950's and also resurrected in the 60's by Romualdi and Mandel is fiber reinforced concrete (FRC). Usually, fibers made of steel are dispersed into concrete for improving its properties such as control of both plastic shrinkage and drying shrinkage cracking, improved toughness, increased resistance to fatigue, spalling of concrete and improved flexural strength, abrasion and shear strength [Nedhi, 2004].

Currently, researchers are working to optimize the advantages offered by both SCC and FRC and have developed Self Consolidating Fiber Reinforced Concrete (SCFRC). This has been possible as a result of the positive synergy existing between both SCC and FRC [Nedhi]. Due to the numerous advantages and wide potential applications offered by this new technology researchers in recent times are shedding a lot of light investigating the characteristics, properties and the various applications of SCFRC.

An important advantage of SCSFRC is the elimination of vibration due to the self consolidating matrix. There is no effect of compaction on the fiber distribution and orientation in concrete and this has also provided further motivation to focus more on SCFRC in recent times. However, many researchers still have their attention drawn on the effect of increasing the amount

of fibers or fiber types on the mechanical properties of FRC. Other researchers in this field placed much attention on the ability of the SCC matrix to well disperse the fibers and have devised various methods to achieve their objectives. Fiber dispersion is hence the outcome of fresh state performance and casting process and may generally affect the mechanical properties in the hardened state.

The fresh and hardened state properties of SCFRC are highly influenced by the amount of water-cement ratios. For example, parameters likes the concrete strength depend mainly on the water cement ratio. Other properties such as workability, flowability and resistance to segregation also depend on the relative constituents mix of cement, water, admixtures and others. Therefore, the variations in the amount of mix constituents affects both fresh and hardened state properties of SCFRC. It is of great importance to have robust mixture that is as insensitive as possible to small variations of the constituent materials, mix compositions and other external factors. This has encouraged researchers to investigate SCSFRC in terms of robustness.

1.2 Problem statement

Large-scale SCSFRC production with good degrees of reliability has encouraged engineers to further study the stability of different mixture designs in terms of robustness. The fresh and hardened properties of SCFRC are mainly influenced by errors in the dosage of mix constituent which are unavoidable on the site. Therefore, the sensitivity of SCFRC in both fresh and hardened state to small variations of the mix constituents, mix-proportions and other external factors should be properly studied to assess the robustness. The variations allowed for the conventional concrete EC 2 and ACI code were applied to the SCSFRC, and it should also be clarified whether these tolerances are accepted for SCFRC.

1.3 Research Objectives

The following are the main objectives of this researches,

➤ Establishing the effects of changes in water, cement and admixture (superplasticizer) on the fresh state properties of SCSFRC. For this objectives, the experimental tests were performed on cement paste and mortar, SCC, SCSFRC in order to correlate the results of the larger scale of observation to those of the lower ones.

➤ Studying the effect of changes in cements, water and admixtures on the ability of the fluid mix to disperse fibers when flowing (dynamic segregation) and hold them in place when at rest (static segregation).

➢ Correlate the fresh and hardened state properties with fiber segregation resistance (static and dynamic) in fresh state as well as fiber dispersion and orientation in the hardened state.

1.4 Methodology

SCSFRC mix design and experimental procedures were established and tests such as Slump flow test, V-funnel tests were performed on the fresh mixes. The rheology of corresponding cement paste and mortar formulated from mix design of SCSFRC was investigated with the help of Marsh cone and Mini cone slump test in the laboratory. In addition, mechanical test such as bending test, compressive strength test, splitting tensile strength tests were performed on the hardened specimen of SCSFRC for the hardened state properties of SCSFRC. In addition, a magnetic probe was used in a non destructive way for concentrations and orientation of steel fibers in hardened SCSFRC specimen, and the results correlated with the ones obtained by washing out fresh concrete of nominally identical specimens and separating to weigh only fibers.

1.5 Outline of the report

This report is structured as follows:

Chapter 2: Literature review

Chapter 3: Methodology

Describes the constituent materials and investigated mix-design, the testing equipments and the procedure used.

Chapter 4: Discussion and Results

Presents the results and findings from all test phases and their discussions and analysis.

Chapter 5: Conclusion and Future development

Shows the summary of the whole project, deductions, conclusions and recommendations for future work arising out of the study.

CHAPTER 2: LITERATURE REVIEW

2.1 Self compacting concrete (SCC)

Durability of concrete has been an important topic of interest all over the world. However, the need for highly skilled workers for the manufacturing of such durable concrete in terms of its good compaction coupled with the gradual/eventual reduction of skilled labor culminated/led to the reduction of construction quality. So in order to maintain the same high standards of high compaction even in the absence of the desired highly skilled manpower, Self Compacting Concrete (SCC) then emerged as one possible solution in the early 1980s in Japan.

In order to achieve highly resistant and durable structures the concrete should be well and effectively compacted in the fresh state to reduce porosity, permeability to degrading agents and maintain durability and strength. SCC has since been the preferred choice due to its rheological qualities and its ability to be compacted to all corners of the formwork as a result of its viscosity and ability to flow under its own weight without the need of any vibration of any kind. The necessity of this type of concrete was proposed by Okamura in 1986. Studies to develop the SCC, including a fundamental study of the workability of concrete, have been carried out by Ozawa and Maekawa at the university of Tokyo (Ozawa 1989, Okumara 1993) [fig 2.1].
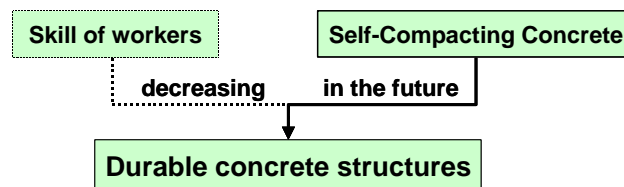
Fig. 2.1 Necessity of Self-Compacting Concrete

In the second half of the 1990s, the interest and use of the SCC spread from Japan to other countries including Europe, and Sweden was the first country in Europe to start the development of SCC in the early 1990s. Most of the major European countries are currently in the process of developing guidelines or specifications for the use of SCC [C. I Goodier]. In America SCC usage in commercial projects has been tremendous with current researchers focusing on the developing raw material requirements, mixture proportions, material requirements etc. [Khayat et al, 2001;Chan et al, 2003].

In 2003 the Precast/Prestressed Concrete Institute (PCI), formulated the definition for SCC as: A highly workable concrete that can flow through densely reinforced or complex structural elements under its own weight and adequately fill voids without segregation or excessive bleeding without the need for vibration" (Interim Guideline for the use of Self-Consolidating

Concrete in the Precast/Prestressed Concrete Institute member plants, TR-6-03, Precast/Prestressed Concrete Institute).

Also by the American Concrete Institute (ACI) SCC is defined as: "Highly flowable, non-segregating concrete that can spread into place, fill the formwork, and encapsulate the reinforcement without any mechanical consolidation"(ACI International, Committee 237 Self Consolidating Concrete, July 2003).

And finally by the American Society for Testing and Materials (ASTM) as: "Concrete that can flow around reinforcement and consolidate within formwork under its own weight without additional effort, while retaining its homogeneity" (ASTM Sub-Committee C09.47 Self - Consolidating Concrete, December 2003).

Self consolidating concrete (SCC) is characterized by:

- extreme fluidity as measured by slump flow diameter, typically between 650-750 mm,
- no need for vibrators to compact the concrete, and placement being easier,
- no bleed water, or aggregate segregation,
- Increased Liquid Head Pressure, which can be detrimental to Safety and workmanship as well as have significant effects on the design of the formworks,
- SCC can save up to 50% in labor costs due to 80% faster pouring and reduced wear and tear on formworks and others.

As of 2005, self-consolidating concretes account for 10-15% of concrete sales in some European countries. In the US precast concrete industry, SCC represents over 75% of concrete production. Departments of transportation in the US accept the use of SCC for road and bridge projects. This emerging technology is made possible by the use of polycarboxylates plasticizer instead of older naphthalene based polymers, and viscosity modifiers to effectively counteract aggregate segregation.

2.1. 1 Materials used in Self-Compacting Concrete

2.1.1.1 Aggregates

The size and content of aggregates affect the behavior and strength of concrete in various ways and its choice depends on the application of the final product. For SCC applications, usually lower content of coarse aggregate is used in comparison with the conventional vibrated concrete. According to [Okamura] this reduction also reduces the collision and contact forces between particles resulting in lower internal stresses when concrete flows, and further reducing the

blockage of the aggregate particles. [Okamura] again pointed out that in order to achieve this self consolidating behavior; the degree of packing of coarse aggregate should be limited to 50% whereas that of fine aggregates is 60% [fig 2.2].
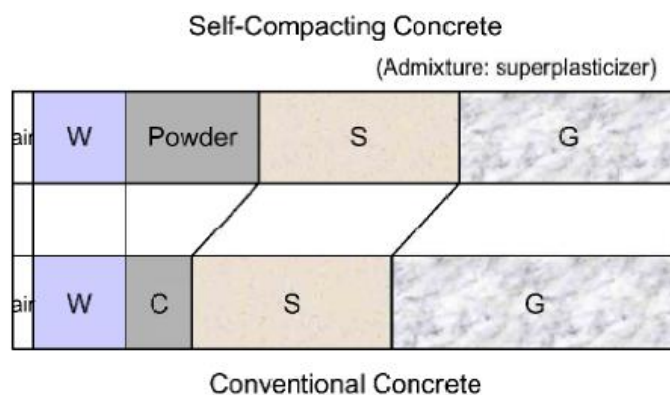
Figure 2.2 comparison of mix proportioning between SCC and conventional concrete.

For the size of the aggregate a review of technical and experimental study (about 70 cases) show that for SCC 70% were within 16-20mm aggregate size [Domone]. Also from [Domone] a coarse aggregate content of about 770kg/m^3 to 925kg/m^3 is usually used to give good results.

2.1.1.2 Powder Components (Cement and Filler)

A mixture of cement and filler is what is normally termed as Powder and usually should have particle size less than 0.125mm.With the addition of water a paste is formed and for SCC high deformability is achieved by increasing the paste content in the overall concrete mixture. According to [Domone] the most common powder blend used is Ordinary Portland cement and Limestone filler. Consequently most SCC contents comprise about (385kg/m^3 to 500kg/m^3) which gives satisfactory results [Khayat, Asaad et al,2004].

Other most commonly used filler are Class F fly Ash, Silica Fume, Ground Granulated Blast Furnace Slag (GGBFS). These materials reduce the permeability of the concrete and thereby increasing the durability and other aspects such as long term compressive strength. Whilst Slag is considered as cementitious material, Fly Ash and Silica fume are both regarded as Pozzolanic materials.

2.1.1.3 Fly ash

Fly Ash is a by-product of the combustion of ground or powdered coal exhaust fumes of coal – fired power stations. It is also called Pulverized Fuel Ash with its main components as siliceous (SiO$_2$) or aluminous (Al$_2$O$_3$) and Ferric Oxide (Fe$_2$O$_3$). Depending on the percentage of these components ASTM classifies Fly Ash into two types: Class C and Class F. Whilst Class F has 70% of the above constituents present and with a particle size range of 1 micrometer to 1 mm,

Class C type has about 50% of the above constituents and particle size of 10 micrometer. Fly Ash being a pozzolanic material does not hydrate on its own but reacts with Calcium Hydroxide, a byproduct from cement hydration to form the C-S-H gel with less influence from the presence of water. It is this C-S-H gel that may seal any available micro cracks.

2.1.1.4 Silica flume

Silica fume is a recent pozzolanic material and has been obtained as a by-product resulting from the use of high-purity quartz with coal in an electric furnace during the production of silicon. After oxidation of silicon, the condensed silica oxide that is filtered into particles then forms final slag. It has a particle range of 0.1 to 0.12 micrometer. Silica fume also generates high demand for water and may compose about 5-20% of concrete mixture by cement weight. Silica fume also reacts with free lime to form hydro –Silicates. Some researchers [Popovics] claim it can also improve the strength of the bond between the aggregates and cement matrix.

2.1.1.5 GGBF Slag

According to the ASTMC 989 GGBFS is a non metallic by product made up of mainly silicates and aluminum silicates of calcium and other bases developed together in a molten condition with iron in a blast furnace in a process of iron production. Percentage of slag in concrete mix may be up to about 50% by volume of the total cementitious material.

2.1.1.6 Admixtures

Admixtures are materials used to modify properties of concrete as a result of certain intended applications. They are usually materials other than water, cement or aggregate. Major types are Suplasticizers and Stabilizers. According to [Okamura] super plasticizers are the major contributors to the high deformability of the SCC. Another important super plasticizer is so-called the high-Range water Reducer, HRWR. Stabilizers are also used as admixtures and in most cases the major types used are the Air Entrained Agents (AEA) which increases workability and frost resistance as well. Another type of stabilizers includes Viscosity Modifying Agents (VMA) for stability of the concrete mix.

2.1.2 Characteristics of S.C.C in the fresh state

The main requirements in SCC production in order to achieve its peculiar advantage are high deformability, high passing ability and high resistance to segregation. Deformability is the ability of concrete to spread and also fill any space within a formwork. This is achieved basically through the flow on its own weight and casting energy. Passing Ability is also another key quality since in order for the fresh concrete to avoid blockage as a result of collision or contact between solid particles close to openings, the concrete has to maintain some features. This ability of

concrete to flow through tight openings without blockage is called its passing ability and this is obtained through the fine size coarse aggregate content. The resistance to segregation which is described as the opposition of SCC to migrate but rather to ensure homogenous distribuòn and this is achieved by the usage of Viscosity Modifying Admixtures.

2.2 Fiber reinforced concrete (FRC)

Fiber reinforced concrete (FRC) is a composite cement-based material that is characterized by an enhanced post-cracking tensile residual strength, also defined as the toughness in the following, due to fiber reinforcement mechanisms provided by fibers bridging the fiber the crack surface. As a matter of fact, fibers help in terms of concrete toughness and structural ductility, durability, high-temperature and fire sensitivity, impact and fatigue strength, and − last but not least-strength in tension [P.G. Gambarova]. Steel Fiber Reinforced concrete (SFRC) is mainly made from a mixture of cement, fine and coarse aggregate, Pozzolana, and other cementitious materials, admixtures to improve properties and uniformly disperse fibres. Steel fibers normally have lengths ranging from 12.7mm to 63.5mm.They are either round and produced from either cutting or chopping wire or flat and from shearing sheets. The steel fiber content normally varies from 0.25% to 2% by volume, which is 20 to 157 kg/m^3. The progress in FRC development and utilization has lately been systematic, albeit gradual, as shown by the results accumulated in the last 15 years [P.G. Gambarova].

2.3 Self consolidating steel fiber reinforced concrete (SCSFRC)

In the very last decade SCFRC has been used in a certain number of partially and full load-bearing structural applications, including slabs on grade, precast prestressed beams, roof elements sheet piles, tunnel segments, precast post-tensioned girders for slope stabilization [Barragàn et al, 2004].

So far the largest number of applications has dealt with steel fibers (Self Consolidating Steel Fiber Reinforced Concrete [SCSFRC]). The use of different types of steel fibers (straight, hooked-end, crimped etc.), with either circular, rectangular or even elliptic cross section has been reported, with fiber lengths L_f varying from 5 to 60 mm and aspect ratios L_f/d_f (where d_f is the diameter of the fiber cross section) from 30 to more than 100. The dosage of fibers employed in SCSFRC, depending on the application, varied from 25-30 kg/m^3 (0.32-0.38% by volume) for slabs on grade and façade panels, to 40-50 and 80 kg/m^3 (0.64-1.02% by volume), for housing units, tunnel segments and precast prestressed elements, up to more than 100 kg/m^3 (1.27% by volume) either in some structural applications (125 kg/m^3-1.59% by volume for sheet piles) and

lab-scale studies (up to 157 kg/m^3 – 2% by volume). Examples of lower dosages have been also reported: in this case the sole scope of fiber addition was the control of shrinkage cracking. The use of polymeric (mainly polypropylene) macrofibers (lengths between 25 and 54 mm), either alone or in combination with steel fibers, in volume percentages ranging between 0.25 and 1% by volume (2.3 – 9 kg/m^3), has been also reported with reference to lab-scale investigations [Krage et al].

In all the aforementioned applications, one of the main advantages of using fibers is represented by the possibility of partially replacing or even completely substituting the traditional welded wire mesh reinforcement (such as shear reinforcement in beams and roof elements), thus reducing the element thickness, since constraints due to minimum covers don't hold any more, and consequently structure self-weights.

Furthermore, the incorporation of (steel) fibers into self consolidating concrete may take advantage of its rheological stability and self-placeability, which leads to the elimination of compaction by vibration, to achieve a more uniform dispersion of fibers within structural elements, not even affected by their downward settlement and segregation [Krage, G. and Wallevik, O.H, 2007]. This requisite is of paramount importance for a reliable structural performance of elements made with fiber reinforced cementitious composites. Improper compaction and placement, furthermore complicated by the negative effects of fibers on workability, may in fact hinder the random dispersion of fibers within structural elements: spots with reduced or even nil amount of fibers may hence act as flaws, triggering early failure and activating unforeseen mechanisms, thus affecting the load bearing capacity and the structural performance as a whole, e.g. in terms of deflection stiffness, crack opening toughness etc.

It has also been recently recognized that, through a suitably balanced performance of the fluid mixture (mainly an adequate viscosity of the fresh concrete) fibers can be orientated along the casting-flow direction [Ferrara, L., et al, 2007]. By suitably tailoring the casting process to the intended application, the direction of the fresh concrete flow, along which fibers tend to align, may be made to match as close as possible to the anticipated stress pattern (direction of principal tensile stresses) within the element when in service. This would lead to a superior mechanical and structural performance which may most likely turn into optimized structure size and reduced self weights. Benefits may also follow in terms of time- and cost-effectiveness of the construction process as a whole, including, e.g. in the case of precast elements, costs for transportation, lifting equipments etc..

Finally, the synergy between self consolidating and fiber reinforced technologies is likely to improve the overall economic efficiency of the construction process: increased speed of construction, reduced crew size, cost and energy saving, better working environment, with reduced noise and health hazards, automation of quality control, also thanks to the reduction or elimination of the reinforcement detailing and placement operations etc. All what above said also highlights the great potentials of SCSFRC in the field of sustainability.

As a matter of fact the influence of the flow-driven fiber dispersion and orientation on the mechanical performance represents a key distinctive feature of self consolidating FRC as compared to traditional vibrated FRC which cannot be disregarded when analyzing engineering and mechanical properties of the material. To this aim a thorough understanding is required of the mechanisms underlying the connection between mix-design and fresh state performance, on one hand, and the dispersion and orientation of the fibers on the other, also in the sight of their monitoring and prediction to achieve the anticipated performance in the hardened state.

2.3.1 Mix-design method for Self Consolidating Fiber Reinforced Concrete

A mix design methodology relying on sound physical concepts allows one, through suitable selection and proportioning of raw materials and other constituents and by governing the aforementioned connections between fresh state behavior, fiber dispersion and mechanical properties, to achieve the required level of material performance, either in the fresh and hardened state.

A review of mix-design methods for plain SCC has been provided in [RILEM TC 174-SCC]. A common rationale underlying them is the concept of SCC as a "suspension" of a granular aggregate skeleton into a fluid phase, which may be either the paste or the mortar, depending on the fractions of aggregates considered in the former. On one hand the maximum aggregate diameter and the grading of the solid skeleton (e.g. the fine to coarse aggregate ratio) are optimized to achieve an optimum packing density. On the other, the composition of the cement paste, e.g. in terms of w/b ratio, cement replacement, superplasticizer dosage etc., has to be selected in order to achieve a performance in the fluid state characterized by suitable ranges of both the yield stress and viscosity, able to guarantee adequate fluidity of the resulting concrete mix, as well as resistance to static and dynamic segregation of solid particles. To this purpose optimum rheological properties of the fluid phase have to be sought as a function of the particle size distribution (maximum size, void ratio etc.) as well as of the relative volume fraction of the solid skeleton [V.K. Bui, J. et al, 2002]. A more dense suspension of the aggregates into the paste (higher aggregate/lower paste volume fraction) would require a lower yield stress and a

lower viscosity of the suspending fluid than a looser suspension (lower aggregate/higher paste volume fraction) to achieve the same target set of fresh state properties of concrete and vice versa.

In the case of fiber reinforced self consolidating concrete such a mix-design philosophy has to be adapted to include the influence of the fibers, as a function of their type and dosage, on the packing density of the solid skeleton.

Empirical assessment of the above mentioned effects has been reported [Ferrara, L. et al, 2007] e.g. to determine the optimal sand to total aggregate ratio (for a given type and dosage of fibers). [Grunewald, 2004] reported that, whereas the addition of fibers was detrimental to the packing density of a coarse aggregate (4-16 mm) solid skeleton, optimum packing density (between 75% and 80%) could be obtained, almost independently of the fiber type and dosage (up to 3% by volume) for a sand (0.125-4 mm) to total aggregate ratio equal to 50%.

Theoretical approaches have been also provided to account for the inclusion of fibers into mix-design methodologies previously developed for conventional concrete.

[Yu et al., 1992] proposed the concept of equivalent packing diameter to include non spherical particles into numerical tools for particle grading optimization. The shape and dimensions of a non spherical particles are related to the diameter of a fictitious sphere which does not results in a change of the packing density, when combined with an arrangement of spherical particles of the same diameter. For cylindrical particles (such as wirelike fibers) the equivalent diameter is defined as:

$$d_p = (3.1781 - 3.6821\,\frac{1}{\psi} + 1.5040\,\frac{1}{\psi^2})\,d_v \qquad (1)$$

where d_v is the volume diameter of the cylindrical particle, i.e. the diameter of a sphere having the same volume as the fiber

$$d_v = 1.145\left(\frac{L_f}{d_f}\right)^{\frac{1}{3}} d_f \qquad (2)$$

with L_f and d_f respectively denoting the length and diameter of the fiber. Parameter ψ is the so called "sphericity" and is defined as the ratio between the surface area of a sphere having the same volume as the particle to the surface area of the particle,

$$\psi = \left(\frac{d_v}{d_s}\right)^2 \quad \text{with } d_s \text{ diameter of a sphere having the same surface area as the particle.}$$

$$\psi = 2.621 \ \frac{\left(L_f / d_f\right)^{2/3}}{1 + 2\left(L_f / d_f\right)} \tag{3}$$

[De Larrard, 1999] proposed the concept of the "perturbed zone" to include the effect of stiff fibers into his Compressible Packing Model for the proportioning of concrete mixtures. With reference to the explicatory Figure 2.3, which geometrically details the concept of wall effect around a fiber, the packing density of a given fiber reinforced arrangement of particles is defined as,

$$\overline{\alpha} = (1 - \phi_f - N_f \, v_p) \, \alpha \tag{4}$$

where α is the unperturbed packing density, ϕ_f is the percentage of fibers of the granular skeleton, N_f is the number of fibers, v_p is the percentage of perturbed volume (in a given container, volume of particles).

De Larrard himself obtained good predictions for stiff (steel) fibers with aspect ratios up to 60, whereas accuracy was worse for higher aspect ratios stiff fibers as well as for flexible ones (polypropylene).
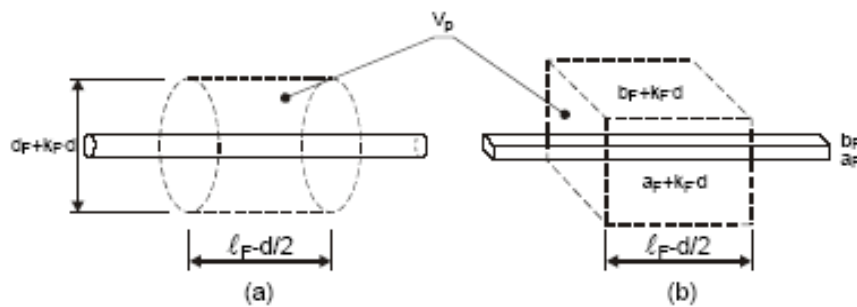
Figure 2.3: principle of the perturbed volume around a fiber according to De Larrard ($k_F = 0.065$)

[Grunewald, 2004] widely applied both the approaches obtaining good predictions for a wide range of fiber types (steel) and dosages (up to 3% by volume).

[Ferrara L., et al., 2007] proposed to include fibers into the optimization of particle size distribution of the granular skeleton (*e.g.* by means of theoretical "optimum" grading curves) as a fictitious aggregate fraction with 100% passing at an "equivalent fiber diameter" calculated through specific surface equivalence:

$$d_{eq\text{-}fiber} = \frac{3\,L_f}{1 + 2\,\dfrac{L_f}{d_f}}\,\frac{\gamma_{fiber}}{\gamma_{aggregate}} \qquad\qquad (5)$$

where γ_{fiber} and $\gamma_{aggregate}$ respectively denote the specific gravity of fibers and aggregates (average for fine and coarse). The definition is instrumental to the extension to the mix design of SCSFRC of the "rheology of paste model" [V.K. Bui et al, 2002] where, as above recalled with reference to plain SCC, optimum yield stress and viscosity of the paste are sought to achieve the target fresh state performance also as a function of the average diameter and packing density of the solid skeleton as well as of the relative volume fraction of paste and aggregates. This concept is synthetically accounted for through the average aggregate spacing d_{ss} (or equivalently, twice the excess of paste thickness) illustrated in Figure 2.4.

$$d_{ss} = d_{av}\left[\sqrt[3]{1 + \frac{V_{paste} - V_{void}}{1 - V_{paste}}} - 1\right] \qquad\qquad (6)$$

with d_{av} average diameter of the solid particles (aggregates and fibers) calculated as:

$$d_{av} = \frac{\Sigma_i\,d_i m_i + d_{eq\text{-}fibers} m_{fibers}}{\Sigma_i\,m_i + m_{fibers}} \qquad\qquad (7)$$

where the sum is extended to the different grain fractions of aggregates according to their particle size distribution.
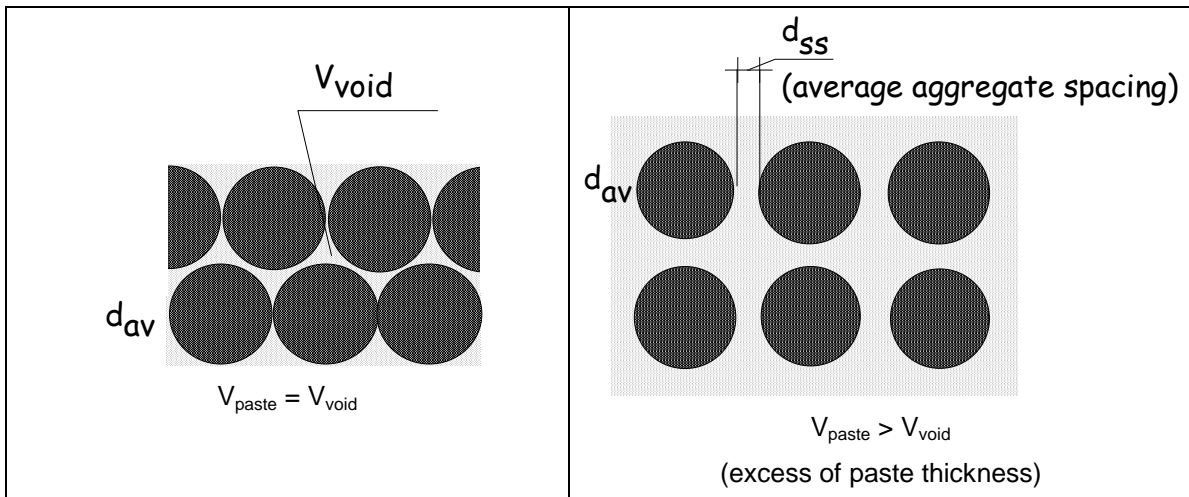
Figure 2.4 average aggregate spacing d_{ss} (according to [S.P. Shah et al, 2001, 2002])

Optimum yield stress (or inversely, flow diameter) to viscosity ratios for the cement paste are defined as a function of d_{ss}, which stands as an indicator of the "concentration" of the solid suspension.

(see the mix-design flow chart in Figure 2.5).

The mix-design flow chart for the extension of SCSFRC of the rheology of the paste model according to [Ferrara et al., 2007a].
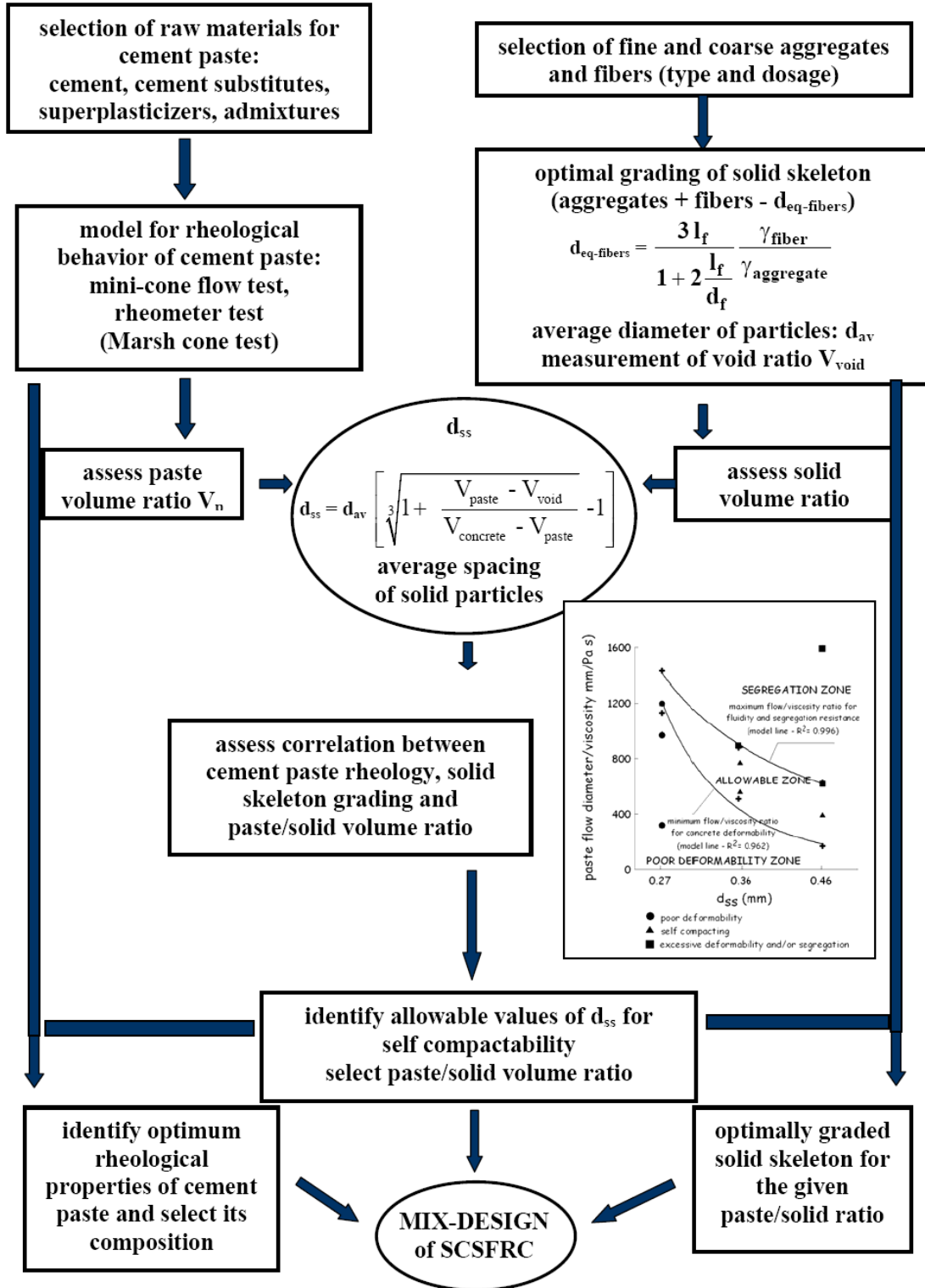
Figure 2.5: mix-design flow chart for the extension of SCSFRC of the rheology of the paste model.

2.3.2 Fresh state performance of SCSFRC

The addition of fibers to a concrete matrix affects its fresh state performance, due to both the large surface area of fibers, which requires more fluid phase (either paste or mortar) to be properly enveloped and lubricated, and the significant interparticle friction and interlocking between fibers as well as between fibers and aggregates [Bayasi, M.Z. and Soroushian, P, 1992]. Mix-design methodologies reviewed in the previous section more or less explicitly account for the aforementioned issues, providing tools to suitably design the composition of fiber reinforced concrete mixtures to achieve the target performance in the fresh state.

The concept of "fresh state performance" is, as well known, a rather broad one, encompassing either quantitative measures of fundamental rheological properties (yield stress and plastic viscosity) and multifold qualitative concepts, such as workability, placeability, compactability, flowability, finishability, pumpability, resistance to static and dynamic segregation etc. In the case of fiber reinforced SCC, the latter concepts have a peculiar importance: it has been infact recognized that a self consolidating concrete matrix, thanks to its suitably adapted rheological properties, may yield to a homogeneously random dispersion of fibers in structural elements, with no downward settlement due to vibration and manual compaction, and with the further possibility of orienting the fibers in the direction of the casting flow. The assessment of correlations between such qualitative concepts, fundamental rheological properties and mix design variables has been a major research focus, since it would enable to tailor the material composition to the desired application and to establish reliable testing procedures for quality control and material acceptance [Khayat, K., et al, 2004].

Extensive research has been conducted to this purpose for plain self consolidating concrete, with remarkable achievements, such as the correlation between yield stress and slump flow diameter [Roussel, N., 2006]. The acceptance worldwide of robust test equipments and methods (slump flow, J-ring, V-funnel, L-box and U-box) meant as representative of the different features contributing to the definition of the fresh state performance [prEN12350-8,9,10,12]. Some open questions are still debated, such as the correlation between the plastic viscosity and a reliable field test measurement [Ferrara, L. et al, 2010] or the most suitable rheometer configuration for the measurement of constitutive rheological properties of concrete mixtures [Domone, P., et al, 1999].

The extension and application of these concepts to self consolidating fiber reinforced concrete may be not straightforward, since some peculiar issues need to be considered, as it will be hereafter summarized and reviewed:

> ➢ the definition of test methods and equipments to measure the properties of interest, thereby including those which are specific to SCSFRC mixes (e.g. "fiber dispersing ability"); methods and measures must take into account the presence of fibers, as a function of their type and geometry, quantity etc, and testing devices may need to be modified accordingly;

> ➢ the proper quantification of the effects of fibers on the fresh state performance, as measured through the previously defined tests, and rheological properties, mainly as compared to plain SCC, ;

> ➢ the identification of relevant model parameters which would allow to quantify and predict the above mentioned effects still as a function of the fiber reinforcement variables.

2.3.2.1 Measuring the fresh state performance

Standard tests employed for plain SCC [prEN12350-8,9,10,12] such as slump-flow, V-funnel, L-box and U-box, J-ring, have been extensively applied also to SCSFRC. In the case of the slump flow test, the same tool as used for plain SCC and the same target values, either of the slump-flow diameter (600 ÷ 750 mm) and the time to a 500 mm spread $T_{50} \leq 5$ sec. have proved to be adequate for quite a broad range of fiber types and dosages.

As for the V-funnel, [Grunewald, 2004] reported the use of a "fibre funnel" with a nozzle almost twice longer (250 mm) and larger (125x125 mm^2) than the standard V-funnel (150x65x65 mm^3) used for plain SCC [prEN12350-9]; with such a device he obtained meaningful results avoiding any kind of blockage, even for the longest fibers and the highest fiber volume fractions employed (up to 80 kg/m^3 – V_f = 1% for 60 mm long fibers, with l_f/d_f = 80 and up to 160 kg/m^3 – V_f = 2% for 30 mm long fibers with l_f/d_f = 45). Standard V-funnel geometry was also successfully employed by several researchers for fiber dosages up to 1%, almost independently of the fiber length, aspect ratio, maximum aggregate size and mix-design proportions, whereas blocking most likely occurred for higher fiber dosages. In the majority of the surveyed studies steel fibers were employed, between 30 and 50 mm long and with aspect ratios around 50; studies dealing with either polyethilene or polypropylene fibers, always considered lower fiber volume fractions.

Passing ability of SCSFRC has been extensively evaluated by using either the L-box test and the J-ring test. Basing on the latter, [Groth] proposed some guidelines for the minimum bar spacing to avoid blocking of SCSFRC in the case of hooked end steel fibers with circular cross section.

As shown in Table 2.1 the ratio of the clear gap length to the fiber length increases either with the fiber content and the fiber aspect ratio. All the results reported in surveyed studies were found reasonably complying with the guidelines in Table 2.1

Table 2.1: minimum clear spacing to fiber length ratio to avoid blockage of SCSFRC in J-ring test

c/L_f [-]	L_f/d_f [-]	Max. m_f [kg/m³]	Max. m_f [lb/yd³]
≥ 3	80	30	50.59
	65	60	101.18
≥ 2	65	30	50.59
	45	60	101.18
≥ 1.5	45	30	50.59

[Grunewald, 2004] also highlighted the dependence of the blocking bar spacing on the mix-composition, and hence on the fundamental rheological properties of the SCSFRC: for the same amount of same type of fibers, the non-blocking bar spacing *decreased* with increasing the yield stress, which generally corresponded to a decrease of the paste volume and hence of the thickness of paste/mortar layer enveloping either fibers and coarser aggregate particles.

U-box test has been also tentatively used to measure the filling capacity of SCSFRC; the reliability of results depended on the length of fibers, due to the quite narrow gap between obstacles and to the quite demanding conditions the test itself imposes to the flow.

Caisson/filling box tests have been also reported [K.H. Khayat and Y. Roussel, 2000] in an attempt to correlate its results to those garnered from slump flow and V-funnel tests.

As a general remark about the evaluation of passing ability and filling capacity of SCSFRC, it has to be highlighted that one of the main goals the structural use of fibers aims to, is the reduction of reinforcement congestion, e.g. in beam column nodes, critical regions of beams and columns, support and end regions etc.). Such an issue has to be adequately taken into account when selecting the most appropriate test to evaluate the passing ability with reference to the specific application. In this framework a recent trend has come out to evaluate passing and filling ability employing a mock-up of the most critical structure detail, from the point of view of reinforcement congestion, plexiglass moulds allowing for visualization of the flow [Dhonde, H.B., et al, 2007]. Fiber washing and counting has been also reported in one of the referred studies to evaluate the fiber dispersing ability of the mixture and correlate to the filling capacity (Figure 2.6 and Table 2.2).

(a)

(b)

(c)

(d)
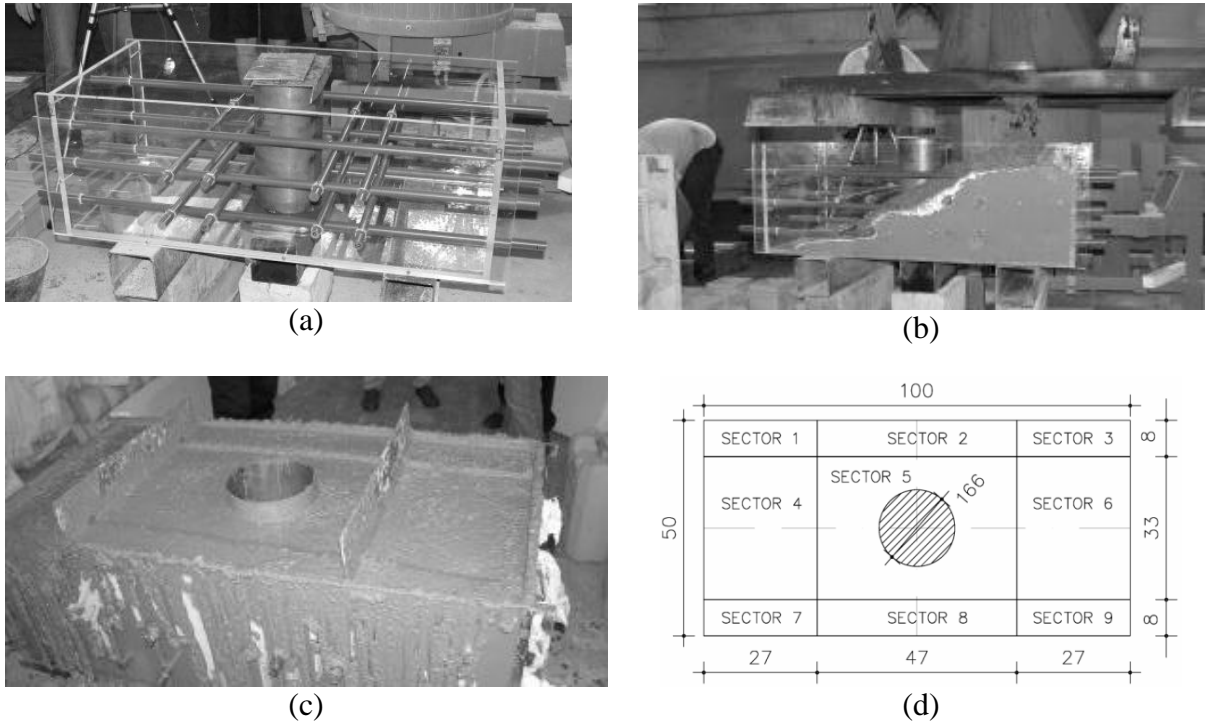
Figure 2.6: Plexiglas replica of a SCSFRC element (a), mould filling (b,c) and sector subdivision for fiber counting (c,d) (from [di Prisco, M et al, 2006])

	Test 1		Test 2		Test 3	
	Ratio	Scatter	Ratio	Scatter	Ratio	Scatter
Sector	[kg/m³]	[%]	[kg/m³]	[%]	[kg/m³]	[%]
1	40.01	-20.24	60.33	-7.73	44.43	-25.3
2	54.48	8.61	63.36	-3.10	69.33	16.56
3	54.16	7.98	68.12	4.19	53.62	-9.85
4	47.25	-5.79	61.15	-6.48	64.66	8.71
5	45.34	-9.62	64.12	-1.93	57.69	-3.01
6	50.35	0.37	76.00	16.23	61.94	4.13
7	46.58	-7.13	70.63	8.02	62.41	4.93
8	57.56	14-76	66.95	2.39	62.87	5.69
9	55.71	11.06	57.82	-11.57	58.37	-1.87
Mean	50.16		65.39		59.48	

Table 2.2: fiber content in different sectors of the plexiglass mould (Figure 2.6)

The issue of "fiber dispersing ability" has also recently started being considered as a relevant feature of the fresh state performance of SCSFRC. [Ferrara and Ozyurt, 2008] with reference to a Self Consolidating High Performance Fiber Reinforced Cementitious Composite, containing 100 kg/m³ of short steel fibers 13 mm long and with a diameter equal to 0.16 mm (maximum aggregate size 2 mm) have proposed a series of simple tests to evaluate the resistance to static

and dynamic segregation of the fibers, in the stream of similar approaches proposed for plain concrete [Shen, L. et al, 2009] (Figure 2.7 and Table 2.3).
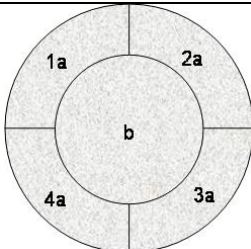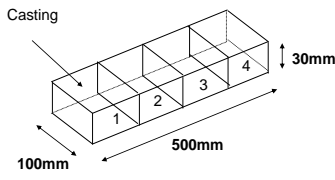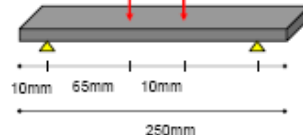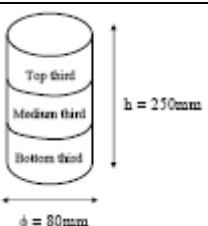
Mini-slump test	Channel flow test	Bending test	Cylinder test
Objective: to assess the abilityof the mix to disperse fibers under conditions of free flow	Objective: to evaluate material's ability to "drive" fibers longitudinally in the mould under conditions of constrained flow	Objective: to evaluate the effect of static segregation of fibers on the mechanical performance	Objective: to evaluate resistance to static segregation of fibers
Procedure: evaluate fiber content in different parts of the flow area.	Procedure: material is poured from one end and allowed to flow to other end. Measure fiber contents in sections 1 to 4.	Procedure: cast two nominally identical specimens and test either downside and upside down to casting sense. Modulus of rupture difference is evaluated.	Procedure: measure fiber content in the three sections (top-medium-bottom) and calculate Fiber Dispersion Gradient (FDG) along the height

Figure 2.7 - Test methods used to assess static and dynamic segregation of fibers of self-consolidating HPFRCCs [Ozyurt, N., et al 2009]

Fiber reinforced mix					Mini-cone fiber content kg/m^3		Channel flow fiber content kg/m^3				Bending test MOR diff (%)	Cylinder test FDG
	V_{paste}	w/b	SP% (by weight of binders)	Mini-cone slump flow diameter (mm)	a	B	1	2	3	4		
F5	0.65	0.18	3.0	368	81.3	138.2	99	106	104	94	69.8	0.89
F3	0.60	0.19	2.5	333	95.0	125.0	85	95	98	102	37.0	0.36
F1	0.55	0.20	2.0	=	Difficult mixing and casting						36.1	-0.10
F6	0.55	0.22	2.0	318	91.1	126.7	101	100	104	96	15.0	0.04

Table 2.3 - Results of tests for static and dynamic segregation of fibers of self consolidating HPFRCCs – correlation with mix-design variables and fresh state performance [Ozyurt, N., et al 2009]

2.3.2.2 Effect of the fibers on the fresh state performance and theology of SCSFRC: experimental assessment and physical modeling

The assessment of the aforementioned correlation among fresh state performance of SC-FRC, fiber dispersion related issues and mechanical properties in the hardened state requires, as a basic step, the effect of the fibers on the foremost and on the fundamental rheological properties of the fluid composite mixture to be quantified. To this aim dedicated analyses criteria have to be identified in order to draw comprehensive information from the huge amount of data nowadays available in the literature as due to intense research efforts.

In order to describe the effects of different types and contents of fibers on the multifold aspects of the fresh state performance, the so-called fiber factor $V_f l_f/d_f$ has been used by several authors [S. Grunewald, 2004]. As expectable, the higher the fiber content V_f and the higher the fiber aspect ratio l_f/d_f, the worse the fresh state performance of the SCFRC mix, i.e. the lower the slump-flow diameter and the higher both the yield stress and the plastic viscosity (see e.g. Figure 2.8). Furthermore, the higher the fiber factor, the larger the dispersion of experimental results.
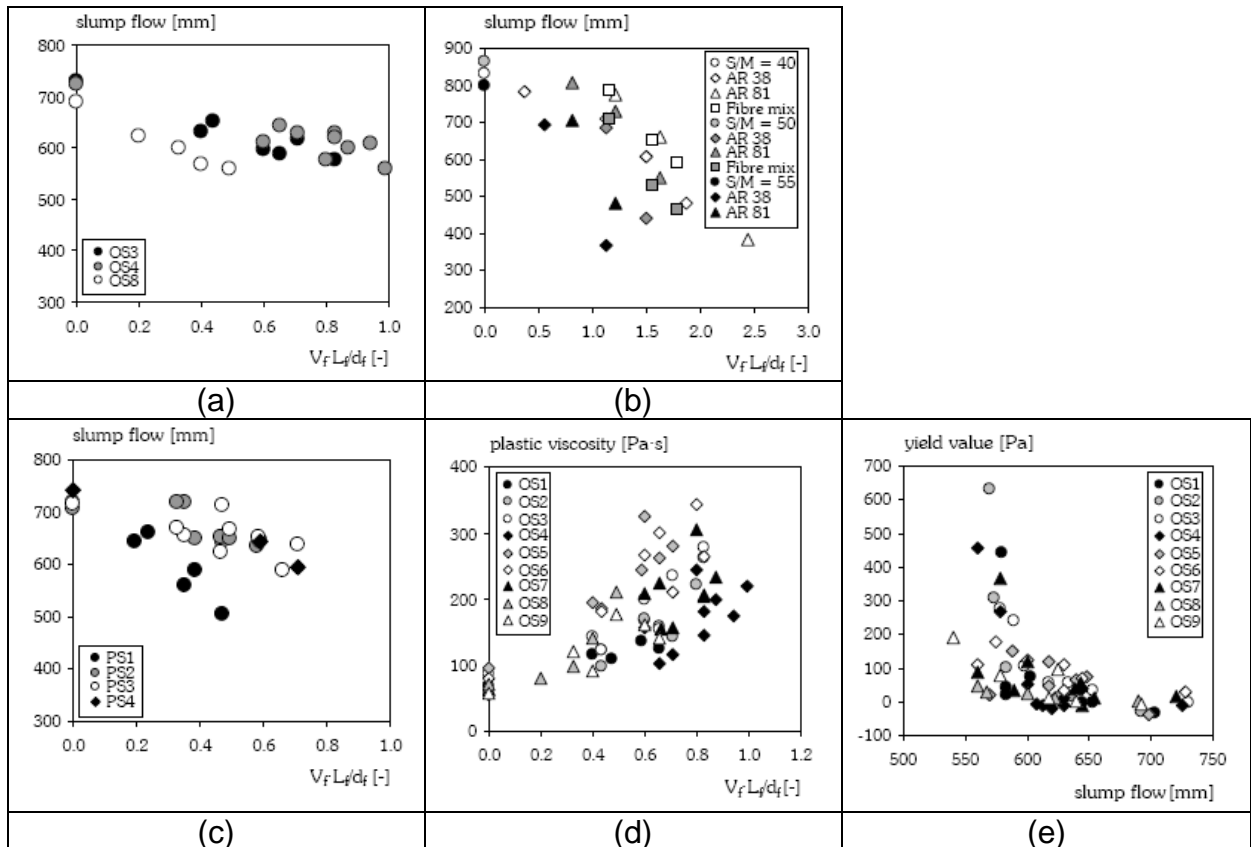

Figure 2.8: slump flow vs. fiber factor (a-c), plastic viscosity vs. fiber factor (d) and yield stress vs. slump flow (e) for different SCSFRC mixtures (from [S. Grunewald, 2004])

The rate of variation of the aforementioned properties with the fiber factor, and hence with respect to the unreinforced reference mixture, actually depends also on the global mixture composition [S. Grunewald – see also Figure 2.8]. This makes the comparison difficult among results obtained by different authors, even in terms of relative performance (to the reference plain SCC) because of the different approaches which may have been adopted in designing the mix composition.

A correction/modification to the criterion based on the fiber fraction along has been proposed by [Martinie et al., 2010], based on the concepts of packing regimes of rigid inclusions (either spherical, such as aggregates, and not spherical, such as fibers). The authors proposed to assume as a variable to judge about the influence of fiber addition on the rheology and fresh state performance of fiber reinforced cementitious composites, either the relative packing fraction of the fibers, i.e. the ratio between the actual packing density and the maximum one obtainable for the fiben type of fibers. The latter is defined as $\alpha\, d_f/l_f$, where factor α "should be of the order of 4". The main conclusions by the authors can be thus summarized, as long as in a mixture there are no inclusions other than fibers:

- if $V_f\, l_f/(\alpha d_f) < 0.8$ the influence of the fibers on the rheological behavior of the cementious composite is low;
- if $0.8 < V_f\, l_f/(\alpha d_f) < 1.0$ the rheological behavior of the cementious composite is likely to be strongly dominated by the contact network between the fibers and may be far stiffer than the one of its unreinforced reference material;
- for $V_f\, l_f/(\alpha d_f) > 1.0$ should not be able to flow anymore.

Theoretical approach based on the "number of fibre-fibre contact per fibre" has been recently proposed [Chalencon et al., 2010] and is likely to yield similar results.

Whenever, like in SCSFRC, fibers are not the only inclusion in the cementitious mixture, the authors [Martinie, L., et al, 2010] propose to take into account the interaction of the fibers with the packing density of the aggregates by referring to a total relative volume fraction, defined as the sum of the relative volume fraction of fibers and that of the granular skeleton, eventually limited to coarser aggregates. In the latter case the fresh state performance of the fiber reinforced composite has to be referred to that of the "suspending mortar", which also includes all the aggregates smaller than the those considered as forming the granular skeleton. The meaningfulness and reliability of such an approach clearly appears from Figure 2.9.
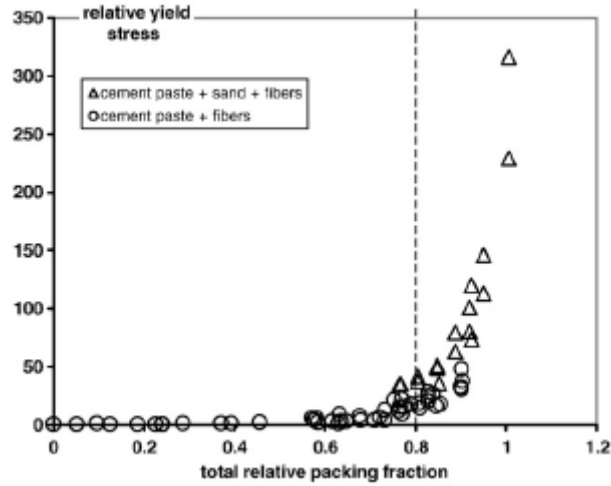
Figure 2.9: relative yield stress as a function of the total relative packing fraction. The dashed line corresponds to the theoretical random loose packing (from [Martinie, L., et al, 2010])

In the same framework, [Ghanbari and Karihaloo, 2009] recently proposed a predictive approach to the plastic viscosity of self compacting steel fibre reinforced concrete which proved likewise reliable.

The aforementioned approaches have evident strict correlation with the one based on the paste/mortar thickness, originally proposed by [van Bui et al., 2003] and widely employed also by other authors [S. Grunewald, 2004]. This provides sound physical interpretation of the fresh state performance, based on the rheological properties and amount of the fluid phase (either paste or mortar) exceeding that strictly necessary to fill the interparticle voids and hence enveloping and lubricating fibers and coarser aggregate particles (Figure 2.10).
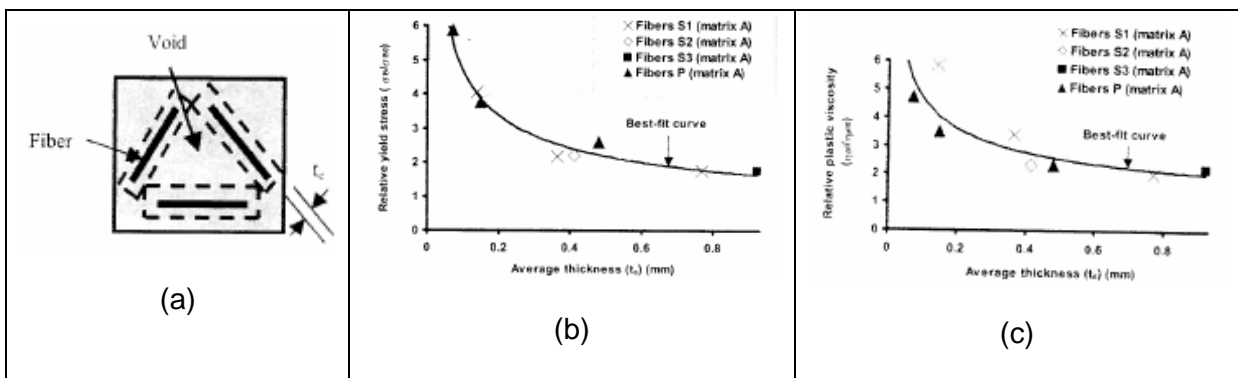
Figure 2.10: concept of average matrix thickness t_c (a) and relative yield stress (b) and plastic viscosity (c) of SCSFRC mixes vs. t_c (from [van Bui, K., et al 2003])

As a further support to the soundness of this criterion, recently, [Chalencon et al., 2010], by means of detailed X-ray microtomography analysis, showed that the "microstructure and local rheology" of the mortar phase in a fiber reinforced cementitious composite "is not affected by the

22

presence of fibres or fibre bundles and that its rheology within the fibre suspensions plays a key role on the rheology" of fibre reinforced mortars and concretes.

The role of the excess paste/mortar layer thickness on modeling the performance of SCFRCs in the hardened state, initially addressed by [Voigt et al., 2004] with reference to drying shrinkage of conventional SFRC.

2.3.3 Dispersion and flow-induced orientation of fibers: experimental evidence, monitoring techniques and predictive modeling

One of the most interesting outcomes of the synergy between self-consolidating and fiber reinforced concrete technologies is represented by the random dispersion and, in case, tailored orientation of fibers which can be obtained thanks to the superior fresh state performance of the composite. Dedicated experimental investigation, performed either at the lab-scale [S. Grunewald et al] and on full scale precast elements, tunnel segments and precast beams; underwater slabs and tunnel segments[di Prisco et al, 2006].

The influence of the flow width and length and the length of the fibers on the fiber orientation was also systematically studied by a few authors [Ozyurt, N et al] who showed that:

> ➢ longer fiber tend to orient better than shorter.
>   it has to be remarked that the flow conditions in [S. Grunewald] (a long precast beam) and most of all the positions along the flow in which the fiber orientation was monitored, were such to exclude any wall effect. Whenever lab specimens are considered, wall effects due to the moulds may significantly affect the results, the longer the fibers the more sensible to such an influence [Kooiman, A.G, 2000];
> ➢ orientation along the flow direction increases with the distance from the casting point;
> ➢ orientation effectiveness along the flow direction tends to decrease with increasing flow width to fiber length ratio;
> ➢ as expectable by increasing the thickness to fiber length ratio the through thickness orientation becomes less negligible.

[Ferrara L., et al., 2010] also highlighted that, due to the transition along the flow thickness, from a pure shear flow, at the bottom interface with the formwork, to an extensional flow, on the free surface, the effectiveness of fiber orientation may vary along the depth of the element cast.

In the majority of the reported investigations, fiber dispersion and orientation was monitored by counting the fibers on (fracture) cross sections of specimens (in case obtained by sawing or

core-drilling at different positions of larger cast elements), e.g. after toughness tests. Manual counting was rather easy for lower dosages of longer fibers with average aspect ratios [Ferrara L., et al., 2007] whereas image analysis techniques were required for higher dosages of shorter fibers with higher aspect ratios or whenever a quantitative information on the orientation of fibers with respect to the plane of the cut has to be sought [S. Grunewald, 2004].

X-ray pictures of cores or of thin slices obtained by sawing the specimens (as dictated by the absorption properties of the material) were also taken in several investigations [Vandewalle, L., et al, 2008] and provide immediate and effective visualization of the fiber orientation. Obtaining quantitative information from X-ray pictures may be cumbersome, either due to the loss of the third dimension and, most of all, in the case of higher percentages of short fibers.

All the reported investigations were by the way instrumental at highlighting the need for a time and cost effective, even non-destructive, method for the on-site monitoring of fiber dispersion, which could be implemented into quality control procedures.

Electrical methods based on the effect of fibers on the conductivity of the composite have received much attention in the very last years. Among them, the Alternate Current Impedance Spectroscopy (AC-IS) was intensively investigated and proved to be a reliable tool for the purpose at issue [Ozyurt, N., et al, 2006]. The method is based on the frequency dependant behaviour of cementitious composites reinforced with conductive, such as steel and carbon, fibers. These were infact shown to be insulating under Direct Current (DC) and low frequencies of Alternate Current (AC) while they are conductive under high frequencies of AC. The method consists of applying to the specimen a voltage excitation over a range of frequencies (e.g. 10 MHz-1Hz) and measuring the amplitude and phase of the output current. When the calculated real and imaginary parts of the impedance Z are plotted on the so-called Nyquist diagram, fiber reinforced cementitious composites exhibit the so called dual-arc behavior (Figure 2.11), where the rightmost cusp, occurring under low frequencies (fibers act insulating), gives the resistance of the matrix, R_m, also detected on the single arc behavior in the case of unreinforced composites, and the leftmost cusp, occurring under high frequencies (fibers are conductive) corresponds to the resistance of the fiber reinforced composite R. In order to define fiber dispersion and overcome the drawback of the sensitivity to moisture conditions of the specimen/structure sample, the so-called matrix normalized conductivity is used:

$$\frac{R_m}{R} = \frac{\sigma}{\sigma_m} = 1 + \left[\sigma_{fibers}\right]V_f \tag{8}$$

24

where σ and σ_m are the conductivity of the fiber reinforced composite and of the matrix respectively and [σ_{fibers}] is the intrinsic conductivity of the fibers which, in the case of highly conductive fibers, only depends on their geometrical properties (fiber aspect ratio) [Douglas, J.F. and Garboczi, E.J , 1995].
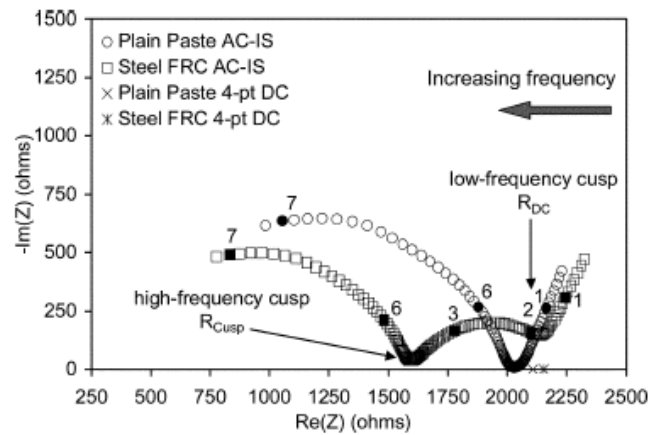

Figure 2.11 sample Nyquist plots for plain and FRC cement paste (from [Torrent, J. M., et al, 2001])

A wide assessment of the method was performed at the lab-specimen scale, also through comparison with the much more time-consuming image analysis, showing its sensitivity to orientation and to sources of non-uniform fiber dispersion, such as clumping, segregation etc. [Ozyurt, N., et al, 2006].

[Ozyurt et al., 2006] also attempted an industrial scale application with reference to SCSFRC precast elements, confirming the ability of the mix to guarantee a uniform dispersion of fibers as well as to orient them along the casting flow direction. In the same framework [Ferrara et al., 2008] applied the method to check the different abilities by vibrated SFRC, self consolidating SFRC and segregation consolidating SFRC in dispersing and orienting the fibers in 600 mm square slabs, meant as representative of precast slab. With reference to the set-up shown in Figure 2.12, the plotted values of the matrix normalized conductivities highlights the influence of the fresh state performance of the mix in achieving randomly uniform dispersion and tailored orientation of fibers.

The extension of the frequency range needs the employment of expensive instrumentation. Furthermore, the method is very sensitive to moisture gradients within the specimen/sample as well as to the contact impedance between the electrodes and the material. To overcome this problem, the two electrodes should be cast into the concrete, but restricts the applicability of the method to laboratory tests only. Some authors have proposed to minimize the contact impedance
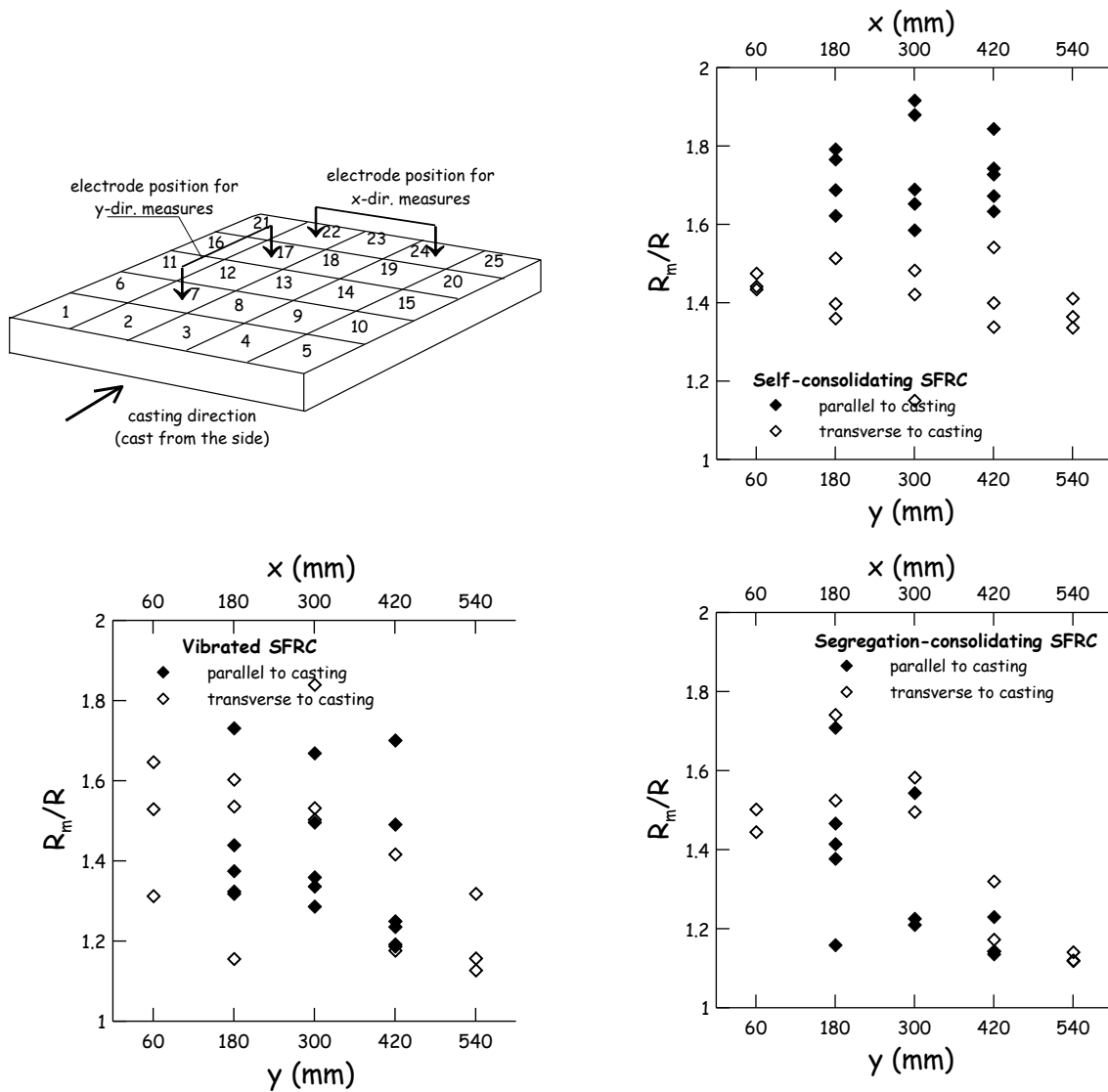
Figure 2.12: scheme for AC-IS measurements on 600 mm square slabs and matrix normalized conductivities for SCSFRC, vibrated and segregation consolidating SFRC plates ([Ferrara, L., et al, 2008])

between the superficial electrode and the material by employing conductive solutions (generally water and NaCl) [Ozyurt, N., et al, 2006; Ferrara, L., et al, 2008].

Methods based on low-frequency resistance measurements have also been employed [J.F. Lataste , et al, 2008], with a four-electrode configuration aimed at reducing the effects of the poor electrical coupling. However, this method cannot provide quantitative information about the actual fiber concentration, because the resistivity of the cement is highly affected by the aging, the moisture content, as above recalled, and the presence of electrolytes in the pores other than the amount of conductive fibers.

The inclusion of steel fibers in a homogeneous concrete matrix affects the effective permittivity of the mixture. Its value depends on the volume fraction of the fibers and their aspect ratio. The effective permittivity can be estimated employing a coaxial probe and microwave reflectometry techniques [Van Damme, S. et al]. Assuming that the fibers are randomly oriented and because of their known aspect ratio, it is possible to assess their concentration. This method has proven to be very effective; however, it is not applicable to SFRC featuring a preferential fiber orientation.

A new method for the detection of fiber density and orientation has been also recently presented [Faifer, M., et al, 2010]. It is based on the employment of a probe sensitive to the magnetic properties of the steel fibers. The presence and the relative position of steel fibers modify the magnetic circuit of the probe thus resulting in an impedance variation. In this way, by measuring the inductance of the magnetic probe it is possible to assess the fiber concentration and average orientation. The performance of the method has been theoretically and experimentally analyzed with reference to a self-consolidating high performance fiber reinforced cementitious composite slabs. Besides its good sensitivity, the method is also characterized by ease of use, since it just require to lean the probe on the surface of the specimen, without any particular care about the coupling. This guarantees a high degree of repeatability and low uncertainty in the measurements, even on vertical elements or slabs accessible from the bottom. This method has been employed in assessing fiber concentrations and orientations in this research projects, robustness of SCSFRC, and will be further discussed under chapter 3.

Methods based on the study of heat transients and hence on the effects of the fibre on the thermal properties of concrete have been also tentatively applied for non-destructive assessment of fiber concentration, thanks to the influence of fiber volume fraction on the thermal diffusivity of the composite [Felicetti, R. and Ferrara L., 2008]. Temperature fields within a structural element may be easily surveyed through IR thermography, but the slow propagation of temperature variations in thick members, which makes difficult to provide a controlled input excitation over large areas, may limit the applicability of the method. Further validation on well controlled benchmarks is needed.

Computer Axial Tomography has also been applied to the investigation of fiber dispersion [Molins Borrel, C., et at, 2008]. Among the pros of the method surely its non-destructiveness has to be highlighted, together with the fact that after analysis a nice 3D visualization of the actual fiber arrangement can be obtained (Figure 2.13). The need of dedicated equipment and analysis

software still stands as the major drawback to a wider use of the method, also at an industrial scale. Figure 2.13:
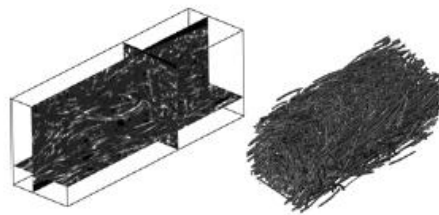

Figure 2.13: Three different orthogonal slices through a reconstructed FRC specimen from a CT-scan and 3D reconstruction of the steel fibres only [Molins Borrel, C., et at, 2008).

2.3.4 Engineering and mechanical properties of SCSFRC

Once sufficient confidence was gained about the technology for producing robust self consolidating fiber reinforced concrete, thanks to intensive research efforts, investigation focused on the structural application of this new material, thereby including measurements of several different mechanical properties, as might have been required by the specific application. In this section, studies on the mechanical properties of SCSFRC will be reviewed and their major outcomes and results summarized, mainly focusing on the comparison with ordinary SFRC.

2.3.4.1 Fiber matrix bond

Engineering and mechanical properties of fiber reinforced cementitious composites are actually the outcome of the toughening effect exerted by the dispersed wirelike reinforcement: this effect depends on the fiber geometry and quantity, filament strength, dispersion and orientation with respect to the applied stress and on the fiber-matrix bond. Approaches aimed at predicting the mechanical response of FRCs from pull-out behaviour of single fibers and distribution data [Armelin. H.S.,and Banthia, N.,1997] have received renovated attention in the very last year's [Jones, P.A., et al, 2008].

Experiences on the pull-out behaviour of single fibers from SCC matrices have been reported by [Grunewald, 2004; Cunha et al., 2010]. Comparative investigation between SCC and vibrated concrete (VC) matrices featured by same compressive strength, resulted in comparable pull-out forces (Figure 2.14). Interestingly, [Grunewald, 2004] reported average SCC/VC shear stress ratios comparable to the splitting strength ratios between the same concrete matrices.
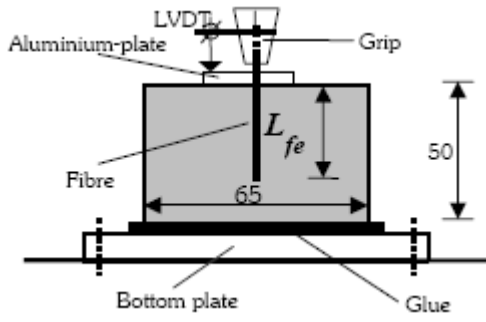
(a)
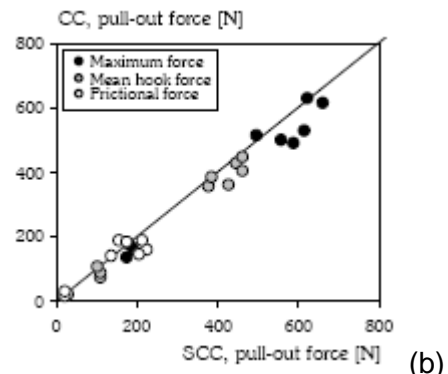
(b)

Figure 2.14: Test set-up of the single fibre pull-out test (a-from [Markovic, U., et al]) and comparison of pull-out forces of steel fibres from SCC and CC matrices [Grunewald, 2004]

The role of fiber type (straight, hooked-end), embedded length and inclination angle on the pull-out behaviour in SCC matrices has been also recently investigated by [Cunha V.M.C.F.et al., 2010] providing sound confirmation to the consolidated knowledge on the topic (Figure 2.15); no comparative investigation with ordinary concrete was in this case performed.
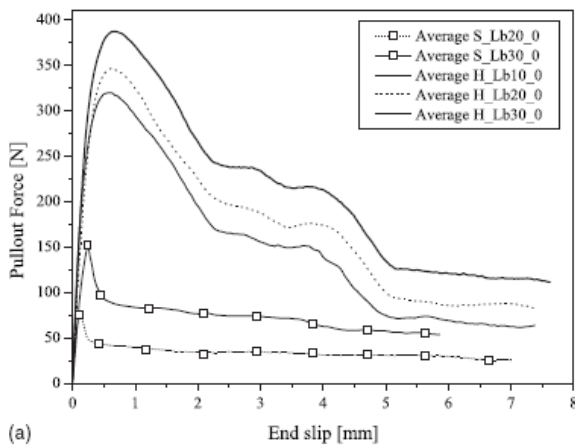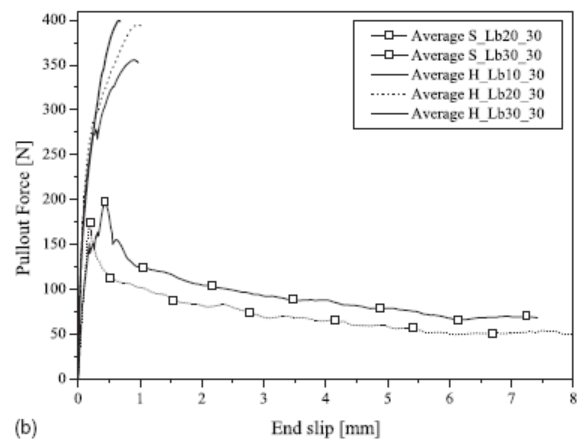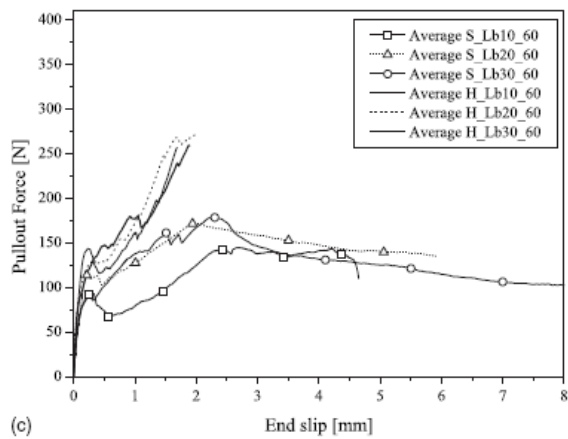
Figure 2.15: average pull-out vs. slip curves for straight (S) and hooked-end (H) fibers for different embedded lengths (Lb) and fiber inclination angles: 0° (a), 30° (b) and 60° (c) [Cunha, V.M.C.F. et al, 2010]

2.3.4.2 Compressive strength and stress-strain behavior

As well known from the literature on conventional vibrated SFRC [Balaguru, P. N. and Shah. S.P.,1992], fibers have negligible effects on the compressive strength of the fiber reinforced composite, whereas they affect the post-peak behaviour, mainly as a function of their dosage. This has been confirmed also for SCSFRC [Aoude, H., et al, 2009].

Interestingly, the compressive strength gain with time was found faster for SCSFRC than for conventional vibrated SFRC having the same 28-days compressive strength (e.g. same strength class) [Dhonde, H.B., et al, 2007] or than what obtainable through predictive models, also with reference to same strength class [Cunha, V.M.C.F, et al,2008; Pereira, E.N.B., et al, 2008] (Figure 2.16). Similar findings were obtained also for plain SCC as compared to vibrated concrete having the same strength class [Ferrara, L., 2009]. This was most likely attributed to the reduced w/cm ratio [Cunha, V.M.C.F, et al, 2008; Pereira, E.N.B., et al, 2008] or to the higher content of cementitious materials [Dhonde, H.B., et al, 2007] as well as to the presence, when applicable, of limestone microfiller, whose extra-fine particles act as nucleation sites for the formation of calcium silicate hydrates [Ferrara, L., 2009; Domone, P.L., 2007].

Young modulus of SCSFRC was found to be lower than what predictable through models calibrated on conventional vibrated concrete for the same strength class [Cunha, V.M.C.F., et al, 2008]. This also agrees with related findings for plain SCC and vibrated concrete, because of the higher paste content and lower maximum aggregate diameter which feature the mix-design composition of the former [Domone, P.L., 2007] (Figure 2.17).

The inset equations read:

$$f_{cm}(t) = f_{cm}(28) \cdot \exp\left\{0.2\left[1-\left(\frac{28}{t}\right)^{0.5}\right]\right\}$$

$$R^2 = 0.945$$

$$f_{cm}(t) = f_{cm}(28) \cdot \exp\left\{0.052\left[1-\left(\frac{28}{t}\right)^{0.89}\right]\right\}$$

$$R^2 = 0.991$$
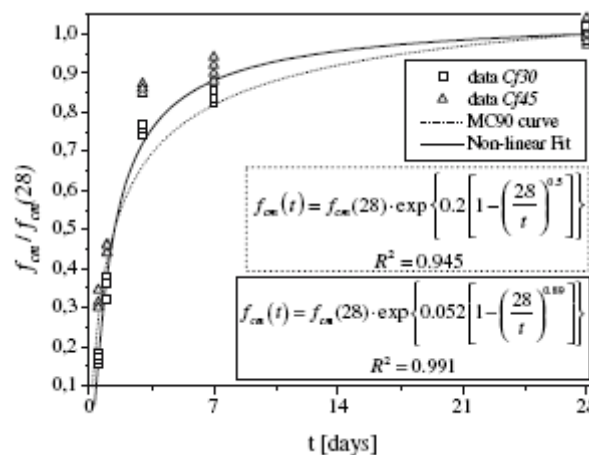
Figure 2.16: influence of aging on the compressive strength of SCSFRC – experiments and modelling

(a)

(b)
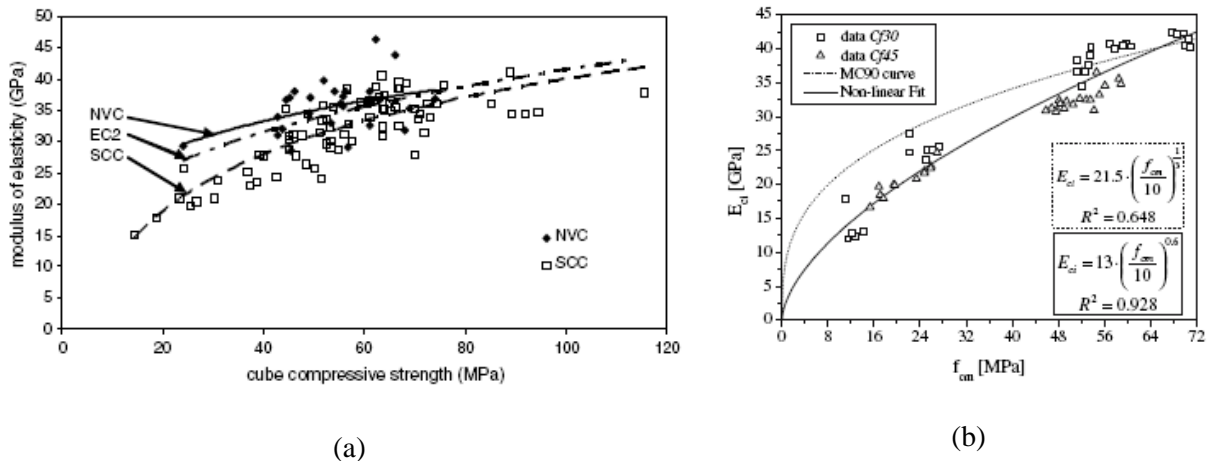
Figure 2.17: relationship between modulus of elasticity and compressive strength for plain (a – [Domone, P.L.]) and fiber reinforced (b – [Cunha, V.M.C.F., et al, 2008])SCC and normal vibrated concrete (NVC) – experiments and modelling

[Dhonde et al., 2007] also found that fibers slightly enhanced the modulus of elasticity, in the case of SCSFRC mixtures, pointing out this as an additional advantage of using fibers in SCC, due to its intrinsic higher deformability.

"Top column" effect on compressive strength and modulus of elasticity was investigated by [Torrijos M.C., et al., 2008]: with reference to the variability of the above said properties along the height of a 2.5 m high column, they found poorer values in the highest 50 cm, reasonably constant values holding elsewhere; the trend of the above said properties was also interestingly related to the trend of the material density and of the fiber content along the column height (Figure 2.18).

(a)

(b)

(c)

(d)
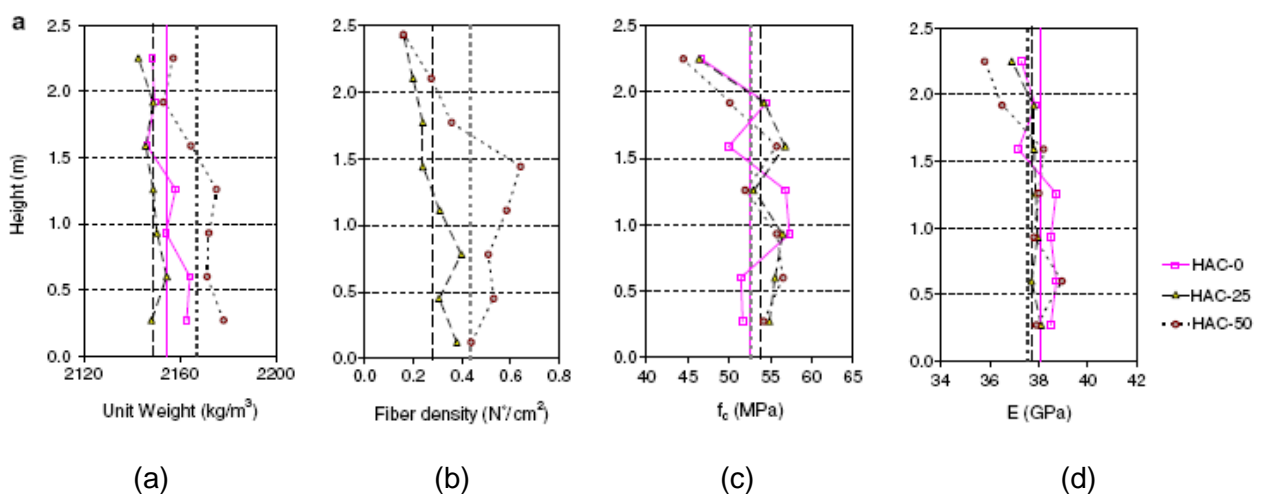
Figure 2.18: top-column effect on material density (a), fiber content (b), compressive strength (c) and modulus of elasticity (d) for SCSFRC [Torrijos, M.C., et al, 2008]

2.3.4.3 Biaxial compressive strength and deformation behaviour

[Mohammed and Eliot, 2007] performed a pioneer study on the behaviour of SCSFRC under biaxial compressive stress states, employing 100x100x50 mm specimens, obtained from larger 100 mm side cube specimens. Two fiber volume percentages (0.5% and 1%) were considered in the investigation. Hooked end fibers 35 mm long and with aspect ratio equal to 65 were employed. It was found that fibers increased the ultimate biaxial strength (respectively 24% and 55% for V_f = 0.5% and 1% at a stress ratio equal to 0.5 whereas no significant increment was measured for uniaxial strength with V_f = 0.5% and a 25% increment for V_f = 1%). Fibers were also found to positively affect the biaxial to uniaxial strength ratio, which was 39% and 51% respectively for V_f = 0.5% and 1%, as compared to 12% for plain SCC (Figure 2.19). Fibers, as expectable, also increased stiffness and ductility in the major principal compressive stresses under biaxial stress states as well as changed the mode of failure from tensile splitting to shear-type. Results were found in good agreement with previous studies on vibrated SFRC under biaxial stress states [Yin, W.S., et al 1989; Traina, L.A. and Mansour, S.H., 1991] – where it was also found that fiber aspect ratio may affect the biaxial/uniaxial strength ratio.

Figure 2.19: test set-up employed for biaxial tests on SCSFRC (a) and absolute and normalized failure envelopes (b) [Mohammed, R.N. and Elliot, K. S]
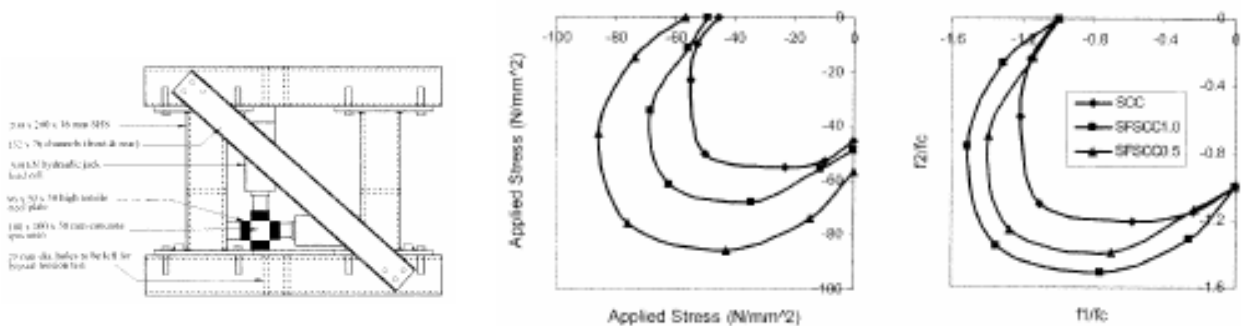
2.3.4.4 Tensile and flexural strength and fracture properties

The major advantage of using fiber reinforcement in a concrete matrix is the improvement of the tensile and flexural fracture properties due to the crack-bridging effect. The effectiveness of the fracture toughness enhancement depends on several variables, such as fiber type and geometry (L_f/d_f), dosage, bond with the concrete matrix and also, if not primarily, on the dispersion of the fibers and on their alignment to the direction of the principal tensile stresses [Soroushian, P. & Lee C.D., 1990]

The addition of fibers into a self compacting concrete may benefit from its superior fresh state performance, which does not require mechanical vibration and/or manual compaction, to achieve a randomly uniform dispersion, with no fiber-free spots and controlled downward settlement [Ferrara, L. and Meda, A., 2006, Cunha, V.M.C.F., et al]. Comparative investigation between vibrated and SC-SFRC highlighted the importance of the latter's rheological stability and of the mechanical vibration and consequently induced fiber downward settlement in the former on the dispersion of splitting tensile strength [Ozyurt, N., et al 2007] (Figure 2. 20).
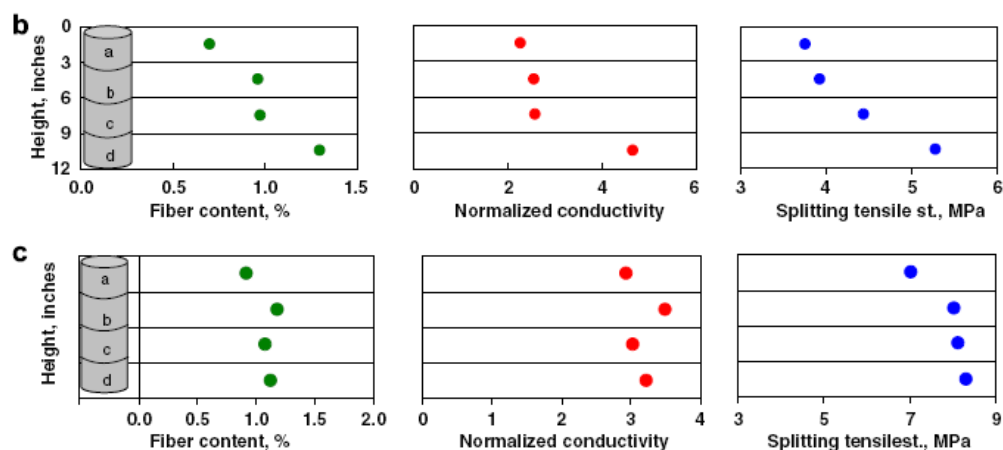
Figure 2.20: variation along 300mm high cylinder of fiber content, matrix-normalized conductivity (AC-IS method) and splitting tensile strength for vibrated (b) and SC SFRC (c) (1% by volume of 40 mm long steel fibers) [Ozyurt, N., et al 2007]

Similarly, [Cunha V.M.C.F, et al.] reported comparable content of fibers along a 300 mm high cylinder and related correlation to fracture toughness parameters (residual stresses at different crack openings) in direct tension (tests performed on circumferentially notched 150 mm high cylinders obtained from top and bottom part of the higher cast one – Figure 2-21).
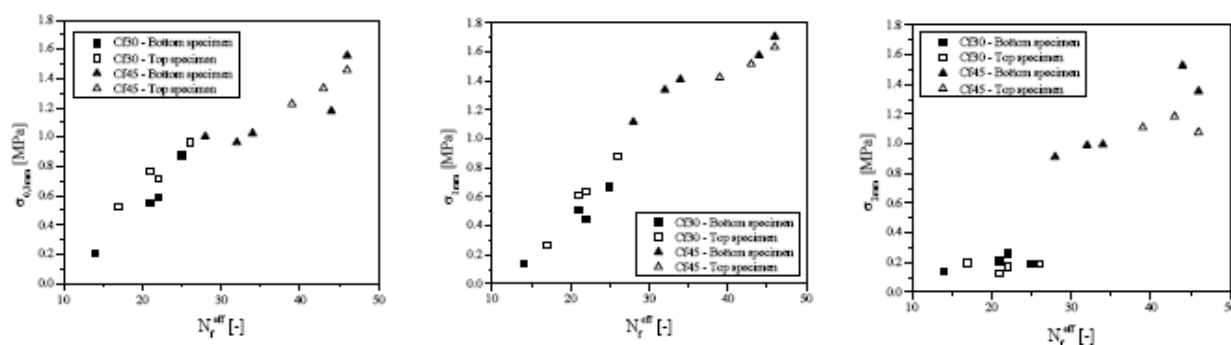
Figure 2.21: correlation between tensile post-cracking residual stresses and number of fibers on fracture surfaces (specimens containing either 30 and 45 kg/m^3 hooked end 60/80 steel fibers obtained from top and bottom of higher cast columns) [Cunha, V.M.C.F., et al]

In a similar framework, the role of a "flow-driven" orientation of the fibers, due to the "tailored" specimen casting procedure, can be called to justify the superior flexural toughness of

SCSFRC with respect to similar (same concrete strength and fiber content) vibrated SFRC (Figure 2.22) obtained by [Grunewald], irrespective also of the similar fiber pull-out strength (see also Figure 2.14). Also [Pons et al.] reported, for vibrated and self consolidating mixtures with different kinds of hybrid fiber reinforcement, better flexural performance of the latter, attributing it to better fiber matrix-bond, even if neither single fiber pull-out tests were performed nor fiber dispersion/orientation information, as related to casting procedure, was provided.
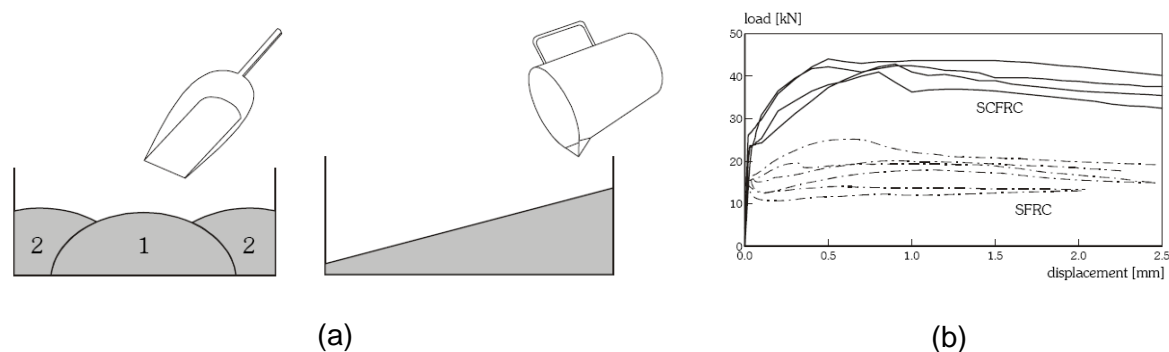
Figure 2.22: mould filling method for SFRC (left) and SCSFRC (right) beam specimens (a) and results of 3-point bending tests (b) (beams 150x150x550 mm with a 25 mm notch at mid-span) [S. Grunewald].

[Velasco R.V et al., 2008] also reported positive effects of the orientation of fibers driven by the fresh concrete flow on either the tensile strength and peak strain in direct tension tests (dumbbell specimens) on self consolidating concretes reinforced with up to 2.5% by volume 65/35 steel fibers.

Correlation among the performance in the fresh state, the effectiveness of fiber dispersion and flow-induced orientation and the resulting mechanical (hardened state) performance in bending was investigated by [Ferrara et al., 2008]. Figure 2.23 shows the results of 4-point bending tests performed on beam specimens cut from the slabs shown in Figure 2.12; cutting was done in such a way that the beam axis resulted, when applicable, either parallel or orthogonal the main flow direction during casting. A higher dispersion characterizes the results obtained from either vibrated SFRC and poorly designed SCSFRC (prone to segregation), whereas randomly uniform dispersion and a tendency to flow driven alignment of fibers can be highlighted for SCSFRC beams. Sensitiveness to fiber downward settlement due to either mechanical vibration or poor performance in the fresh state also appears from the results (beams tested upside down to casting), together with the effectiveness of properly designed SCC mixture to control the phenomenon.
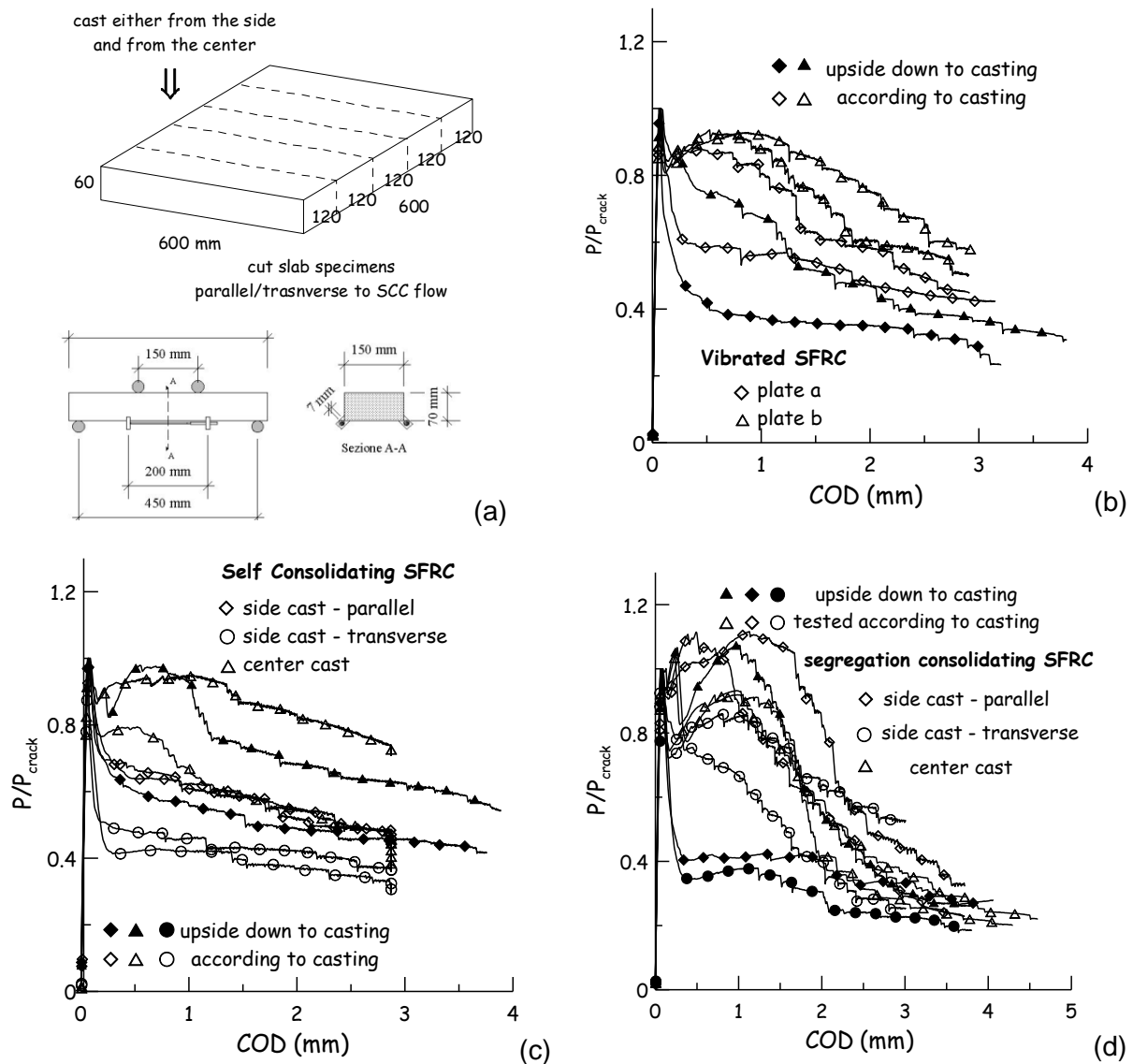
Figure 2.23: scheme for beam cutting from slabs and 4pb test set-up according to [Ferrara, L., et al, 2008]; normalized load vs. COD for vibrated b) self-consolidating and segregation consolidating (c) SFRC

Quantitative correlation between flexural toughness parameter and the fiber density/fiber orientation number on the fracture surface has been also provided by several authors [Stahli, P., et al, 2008; Ferrara, L., et al, 2010; Torrijos, M.C.,et al, 2010]. In all the reviewed studies, specimen casting was carefully designed in order to trigger the orientation of fibers along the direction of flow of the fresh concrete. Similar experience were performed by [Grunewald, 2004], with reference to splitting tensile strength, and by [Ferrara et al., 2010] for tensile strength and fracture toughness parameters measured by means of a novel testing technique (Double Edge Wedge Splitting Test) proposed for HPFRC.

Moreover, research has highlighted the following needs which still have to be deeper investigated:

➢ The procedure employed to manufacture the specimens which have to be employed for the identification of material properties has to be conceived in such a way to "mimic" as close as possible the casting of structural elements. In this way the flow-governed fiber dispersion and orientation which will likely to occur in the structure to be can be reliably reproduced at the lab specimen scale; this would allow the material property identification relevant to the intended application;

➢ The material anisotropy resulting from the flow-induced fiber orientation should be suitably taken into account not only as far as structural design calculations are concerned but also in the design-oriented identification of material properties.

Whereas the former issue is addressed, though in a general way by codes and recommendations, provisions specifically addressing the latter are so far lacking.

Interesting results on the effectiveness of flow induced fiber orientation were also obtained by [Hegger J., 2008] with reference to "puzzle strip" shear connectors (Figure 2.24). By placing concrete so that a fiber orientation perpendicular to the connector shear plane could be achieved, an ultimate capacity about 340% higher was obtained than when fibers were likely to orient themselves parallel to that plane (Figure 2.24 on page 37). In the referred study few information about material detail is available (a "nearly" self consolidating concrete reinforced with 0.5% by volume of steel microfibers) which does not make possible to draw any further quantitative conclusion.

2.3.4.5 Creep

The increase of long term deformations due to the higher paste content has been always standing as a major concern with reference to structural performance of SCC [Domone, P.L., 2007]. A very recent study [Buratti, N: and Mazzotti, C., 2009] has shown that even a limited amount of steel fibers (25 kg/m^3 steel fibers 50 mm long and with a 1 mm diameter were used) added to a normal strength self consolidating matrix ($f_{c,cube}$ = 40 N/mm^2) can be effective in reducing the long-term accumulation of deformations (published results refer up to 7 months), either in terms of deflections and crack openings.
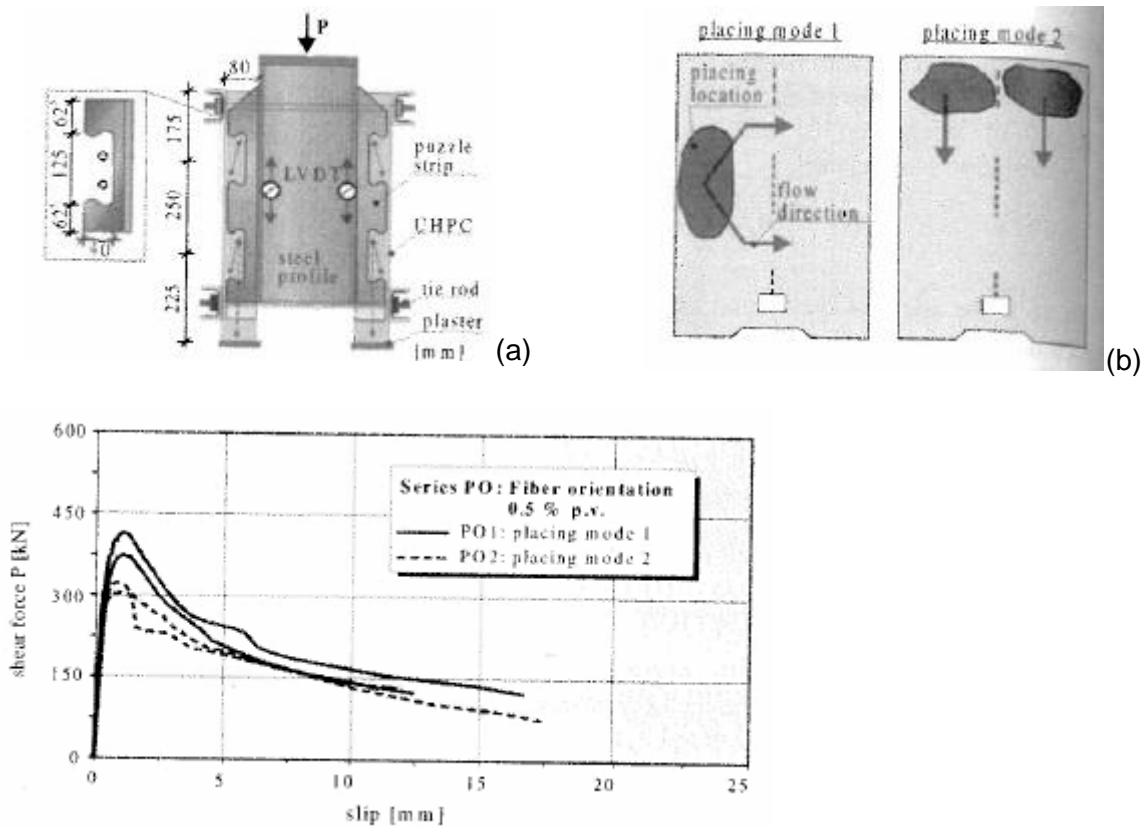
Figure 2.24: geometry and test set-up of puzzle-strip shear connectors made with SC-HPFRC (a); casting modes (b) and load-slip behaviour

2.3.4.6 Plastic and drying shrinkage

The higher content of cement and cement paste is also responsible for higher shrinkage cracking potential of SCC, as compared to conventional vibrated concrete [Domone, P.L., 2007]. Fibers, either steel and plastic, have been shown to effectively counteract the aforementioned phenomenon, either reducing the total cracking area and maximum/average crack width, as far as plastic shrinkage is concerned [Forgeron, D. and Omer, A.], as well as, with reference to free and restrained drying shrinkage, reducing both the time for the first crack to appear and its progressive opening with time [Kwon, S.H., et al, 2007; Carlsward, J. and Emborg, M.]. Steel fibers (hooked end macro fibers) were found to be more effective, in this respect, than either polypropylene and PVA fibers, when the same volume fraction was added to the same matrix [Carlsward, J. and Emborg, M.]. Results quantitatively agreed with similar experiences on conventional vibrated concrete as far as the effect of fibers is concerned on either plastic [Naaman, A.E., et al, 2005] and drying shrinkage [see e.g. Voigt, T., et al, 2004], as a function of their volume fraction, type, aspect ratio etc.

37

2.3.4.7 High temperature

Very few studies have been found in the literature dealing with the behaviour of SC-FRC exposed to high temperatures and all focus on special applications, as detailed after. Their findings could be usefully interpreted with reference to published results on the behaviour of either plain SCC and vibrated SFRC when exposed to high temperatures.

As a matter of fact, plain SCC and vibrated concrete have shown similar behaviour under high temperatures [Bamonte, P., et al, 2008], with reference to either the relative decay of mechanical properties with respect to room temperature conditions and to the higher sensitivity to temperature exposure with increasing strength. As for ordinary SFRC, a recent comprehensive study [Colombo, M., et al, 2010] has shown that either first cracking strength and post-cracking strengths (equivalent/residual) decay with temperature according to the same trend as tensile strength of plain concrete up to 400°C. Beyond that value, and up to 600°C they show an almost constant trend, which may lead to conclude that, for the examined case (average strength concrete reinforced with 50 kg/m^3 hooked end steel fibers 30 mm long and 0.67 mm in diameter) the pull-out mechanism, including hook straightening) is likely to be less affected by temperature that the matrix strength.

[Romano et al., 2007] investigated the behaviour of a self compacting refractory concrete (produced with calcium aluminate cement thermally treated to 588°C) reinforced with either 0.7% and 1% by volume of steel fibres (25 mm long and 0.51 mm in diameter): two temperatures were investigated (110°C and 650°C) but no room temperature data were provided for comparison.

[Caverzan A., 2010] investigated the residual behaviour of a self consolidating high performance fiber reinforced cement mortar (max d_a = 2mm) containing 100 kg/m^3 straight steel fibers (13 mm long and 0.16 mm in diameter); 4 different temperatures were considered, namely 20°C, 200°C, 400°C and 600°C.

In both studies the aforementioned general statements about the thermal degradation of SCC and SFRC properties were substantially confirmed. Caverzan also highlighted that fiber oxidation, occurring between 400°C and 600°C was responsible, in his case, of a stronger degradation of mechanical properties beyond 400°C, contrary to what reported in [Colombo, M., et al, 2010] for SFRC employing steel hooked-end macrofibers (see also [Biolzi, G., et al, 2004]).

2.3.5 Special FRCSS

2.3.5.1 Lightweight fiber reinforced SCC

[Hela and Hubertova, 2007] investigated fresh and hardened state properties of lightweight aggregated SCC reinforced with different amounts of different types of fibers. As far as mechanical properties are concerned, only data about and flexural strength were provided, Comparing two mixes, one with only LWA (ρ = 1430 kg/m^3) and the other with blended NWA and LWA (ρ = 1740 kg/m^3), the effect of fibers was found to be stronger in the former, consistently with an expectable more brittle behaviour of the plain matrix due to the less effective crack arrester role of the larger amount of LWA.

2.3.5. 2 Glass fiber reinforced SCC

Different SCC mixtures reinforced with 0.6 kg/m^3 of high dispersion glass fibers were tested [Suresh Babu et al., 2008] and the effectiveness of the glass fiber reinforcement on the behaviour of r/c beams in bending was assessed. As expectable the addition of fibers resulted in higher ultimate loads, deflection and curvatures and lower crack openings, either at service and ultimate state.

2.3.6 Structural Performance of SCSFRC

2.3.6.1 Bond with reinforcement

Fibers are known to positively affect the steel to concrete bond thanks to the crack bridging effect provided by fibers, which may be as effective as the confinement due to transverse reinforcement. A specific study [Cheung, A.K. and Leung, C.K.Y., 2008], focused on the bond between steel reinforcement and a self-consolidating high performance FRC provided results coherent with the aforementioned statement. No comparative investigation with vibrated SFRC was performed to highlight peculiarities, if any, of SCSFRC.

2.3.6.2 Tension stiffening

Crack bridging effect of fibers has also positive outcomes on the tension stiffening effect, making it possible even to further increase the tie bearing capacity beyond the yielding of steel rebars [Abrishami, H.H. and Mitchell. D., 1997]. A study steel fiber reinforced self consolidating concrete ties [Aoude, H., et al, 2008] confirmed previous findings related to vibrated SFRC. Fiber effect was well accounted considering uniform dispersion and orientation across cracks.

2.3.6.3 Column in compression

Fibers have been shown to be able to effectively (at least partially) replace transverse reinforcement, e.g. closely spaced hoops which are needed to provide confinement in critical regions of columns in buildings and structures susceptible of high seismic excitation [Aoude, H.,

et al, 2009]. A reduction of the not seldom too congested reinforcement which would be required in such cases may lead to improved constructability, which is likely to furthermore benefit from the use of a SCC matrix. Moreover, fibers delay cover spalling, thereby resulting in a greater material integrity at larger strains (even if the effect was not such to prevent the buckling of longitudinal reinforcement). This was confirmed by a recent study [Aoude, H., et al, 2009] in which SCSFRC columns were testes, characterized by different arrangement of transverse hoop reinforcement and different amount of fibers (1%, 1.5% and 2% by volume). It has to be remarked that in the referred study, for the largest amount of fibers the fresh state behaviour of the concrete was hardly definable as self-compacting/consolidating (slump flow diameter 360 mm), despite this may have not affected the reliability of the results and related conclusions. An explanation for this could be given considering that the addition of larger and larger amount of fibers to the plain SCC matrix was not at all compensated by a reduction of the (coarser) aggregate content, e.g. in the framework of the equivalence of solid particle lateral surface.

2.3.6.4 Beams in shear

A significant number of experimental investigation on vibrated concrete structural elements has shown that the inclusion of randomly distributed and orientated, short discrete steel fibers results in improved shear resistance. This is due to either the crack growth controlling effect provided by the fibers, as well as by a greater effectiveness in crack arresting mechanisms and better distribution of tensile cracks due to the smaller spacing existing between fibers than between stirrups [Aoude, H., et al, 2009]. In the post-cracking regime, fibers, bridging shear cracks, may also potentially change the failure mode from brittle to ductile. The addition of fibers is hence effective to supplement or replacing conventional shear reinforcement (stirrups), also offering substantial time- and cost savings over it, which tends to be labor intensive. Moreover, due to the resulting reduction in reinforcement congestions, the use of fibers may be extremely useful in thin webbed elements or thin slabs, where stirrups are both uneconomical and difficult to implement. Further advantages in terms of constructability due to the use of SCC matrices makes it extremely attractive the addition of fibers into SCCs to improve shear resistance.

[Greenough and Nehdi, 2008] performed an extensive investigation on the shear behaviour of SCSFRC slender beams, studying the influence of fiber type (steel, polypropylene), length (30 and 50 mm) and aspect ratio (respectively 43 and 50), fiber anchorage (flat- or hooked-end) and fiber content (0.5%, 0.75% and 1% by volume). The addition of higher and higher amounts of fibers resulted in a reduction of the coarse aggregates, as aforementioned, as well as in adjustments of HRWRA snf VMA dosage, to achieve the same target slump flow diameter (always ranging between 625 and 650 mm).

As expectable, the addition of fibers, with respect to the plain concrete unreinforced reference beam, resulted in higher cracking and maximum loads and (mainly in the case of steel fibers) in increased peak and ultimate deflections, hence in increased ductility. What is even more interesting is the fact, clearly shown by the authors with reference to a wide database (31 experimental cases), that FRSCC beams always have, as compared to the plain reference case, better shear strength improvement over that of conventional FRC beams. Furthermore, the higher the fiber content, the more relevant the relative improvement (Figure 2.25).

Figure 2.25: comparison between the relative increase in shear strength of FR-SCC and FRC beams (from [Greenough, T. and Nehdi, M.])
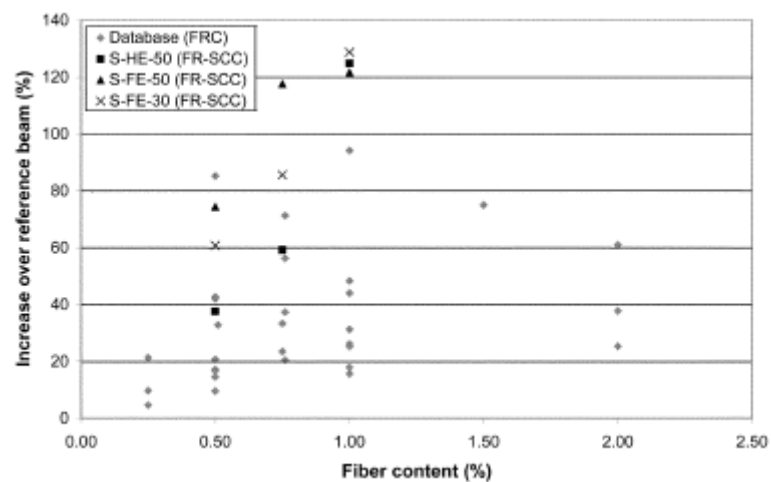
The authors claim this is likely due to the denser microstructure of the matrix and to the enhanced properties of interfacial transition zone, but also to the "self compacting ability of SCC", which may have reliably led to better fiber dispersion (even if the authors do not explicitly state this). The authors also provided a suitable modification to the current ACI code provisions for shear capacity of slender beams, explicitly including in the formula the effect of fiber orientation. Significantly, to support the aforementioned conclusion, assuming a random orientation of fibers, predictions for FRSCC beams always underestimate the measured shear capacity, which is not the case for either vibrated plain and fiber reinforced concrete beams.

With the authors: "it is believed that by optimizing the mixture design [and the casting process], substantial improvements in the ultimate shear strength of FR-SCC beams over that of traditional FRC beams can be achieved, and this aspect deserves further research".

2.3.6.5 Impact resistance

The higher energy dissipation capacity imparted by fibers to a fiber reinforced cementitious composite leads to improvements in impact resistance as well as guarantees material and structural integrity [Bindiganavile, V., et al., 2002].

Impact resistance of SCSFRC elements (beams and slabs) has been recently investigated in a few specific studies: [He X. and Yang] employed SCC reinforced with PP fibers (up to 1.2 kg/m^3 − 1.25% by volume), 12 mm long ad 0.031 mm in diameter, whereas Jiang et al. [Jiang, Z., Banthia, N. and Delbar, S.] used cellulose sheeted fibers, 6 mm long and 0.02 mm in diameter, up to 3.6 kg/m^3 (2.4% by volume). Drop weight and impact pendulum tests confirmed that the presence of fibers increased number of blows to 1st crack and to failure, enhancing energy dissipation capacity.

A material level investigation about the effect of strain rate, also coupled to the effect of high temperature, on the tensile behaviour of a self-consolidating high performance FRCC (reinforced with 100 kg/m^3 straight steel fibers 13 mm long and 0.16 mm in diameter), has been also recently performed [Caverzan, A., 2010].

CHAPTER 3. RESEARCH METHODOLOGY

3.1 Introduction

The research methodology followed in the investigation of robustness of SCSFRC is presented in this chapter. The first step is defining the constituent materials used in the experimental investigation and the testing equipments, test methods and procedures are then explained in detail. When studying the robustness of SCSFRC in fresh state properties, the experimental tests such as slump flow test, V-funnel tests were instrumental in determining the fresh state behaviours like flowability, deformability, workability and segregations resistance. On the other hand, the hardened state properties such as flexural strength and compressive strength were determined through mechanical tests.

3.2 Materials

The constituent materials used in experimental investigations of robustness of SCSFRC are cement, water, admixture (superplasticizer), fine aggregate (sand), coarse aggregate (gravel) and steel fibers. The description and specification of these materials are the following.

3.2.1 Cement

We have used cement in experimental investigations of cement paste, cement mortar, SCC, and SCSFRC. Portland cement CEM I 42.5 [European standard EN197-1:2000] was used in all steps of this research.

3.2.2 Water

Drinking tap water available in the laboratory of Polo Regionale di Lecco, Politecnico di Milano was used in all of experiments.

3.2.3 Aggregates

Aggregates form the solid skeleton of cement mortar, SCC, SCSFRC. Both fine aggregates (sand) and coarse aggregates (gravel) were used. Dry natural sand specific gravity of 2.63 and crushed gravel with specific gravity of 2.71 were used in this work. Grading curves of the aggregates are given in the table 3.1.

3.2.4 Chemical admixtures (SP)

A polycarboxilate based chemical admixtures (superplastisizer) with specific gravity of 1.09 was employed.

3.2.5 Steel fibers [Reinforcement]

Hooked-end Steel fibers with commercial designation of DRAMIX ZP 306 were used. They are supplied in glued packages, bundled together by water soluble glue which dissolves at contact with water during concrete mixing. The properties of the fibers are given in table 3.2.

Table 3.1 Grading size distributions of the aggregates,

Sieve size (mm)	Percentage passing	
	0÷4	4÷8
0.063	1.7	0.1
0.125	6.5	0.2
0.25	21.4	0.2
0.5	53.7	0.3
1	69.2	0.3
2	81.8	0.4
4	98.8	10.9
8	100.0	96.1
16	100.0	100.0
31.5	100.0	100.0
63	100.0	100.0

Figure 3.1: DRAMIX ZP306

Table 3.2 Material constituents for SCSFRC mix design

Material	Type	Quantity
Cement	CEM I 42.5	523.6 kg/m^3
Water	Pure water	200 l/m^3
Admixtures (Superplasticiser)	polycarboxylate	7.81 l/m^3
Steel fibers	Straight Fibers (hooked)	50 kg/m^3
	Length, L_f	35 mm
	Diameter, d_f	0.55 mm
	Aspect ratio, L_f/d_f	65
Fine aggregare (Sand)	Sand (natural)	850 kg/m^3
Course Aggregates	Gravel	886 kg/m^3

3.3 Robustness definition

A critical factor in the SCSFRC production process is its sensitivity to small batch-to-batch changes in one or more of the constituents, which may lead to variability of the performance. The concept of concrete robustness was introduced, which corresponds to the tolerances of SCC production, to daily fluctuations of materials [EFNARC., 2005]. In the European guide lines for self-compacting concrete, the robustness of SCC is defined as the capacity of concrete to retain its fresh properties when small variations in the properties or quantities of the constituent materials do occur.

It should be noted that the European definitions of robustness differs from the one suggested by the American researchers [Bonen et al., 2007]. According to the ACBM research team [Bonen et al., 2007], robustness is regarded as the ability of the given mixture to maintain both fresh properties and uniformity pre- and post-casting of one batch or successive batches. This is a broader definition since it includes the ability of mixture to resist changes in materials properties and mix proportions, due to batching inaccuracies, but also the ability to resist to changes during transport and placement (dynamic stability) and post placement (static stability). According to [Bonen et al. (2007] robustness is a time dependent property and it should be regarded according to the applications.

The author's opinion is that, to make clearer, the concepts of robustness (related to properties after mixing), dynamic stability (related to properties during transport and casting) and static stability (related to properties from the end of casting to setting time) should be discussed separately. In the present work the European definitions was adopted and generalized as the capacity of the SCSFRC to retain its performance requirements, which is of interest for specific application (fresh and hardened properties), when small variations in properties or quantities of the constituent materials occur.

3.4 Factors affecting properties during production

During production, there may be a number of factors that individually or collectively contribute to the balance between SCSFRC fresh state properties, namely, deformability, passing ability and resistance to segregation. Variations in the concrete properties can be attributed to variability of the constituent materials [Bonen et al., 2007], accuracy of the weighing materials [Bonen et al, 2007] and changes in the mixing energy [Emborg, 2000; Takada,2004]. Changes in the environment conditions, like temperature and humidity were also found to affect the rheological properties of SCSFRC after mixing.

3.4.1 Variability of constituents materials

The coarse to fine aggregate ratio in the mix and the maximum size of the aggregates are determining factors for the passing ability of SCSFRC, for a given reinforcement spacing [EFNARC., 2005]. Changes in the moisture content or water absorption of aggregates will change the target rheological properties of paste and, consequently, of concrete. Moisture content of fine aggregates normally is greater than that of coarse aggregates.

3.4.2 Inaccuracy in weighing of the materials

Deviations in the mix proportions can occur due to inaccuracy of weighing equipment which can affect workability of SCC [Bonen et al., 2007] and, generally, larger errors are introduced when batching small load sizes. Normal weighing tolerances regulated by the national and international standards are in general acceptable for the production of SCC. Accuracy of admixtures dosing equipment may vary depending on the type of dosing equipment and its set up [RILEM, 2006].

3.4.3. Mixing energy

The main influencing factors of mixing efficiency are: raw materials, the concrete mixture itself (type of constituent materials and mix-proportions), the loading sequence, the mixing sequence, mixing speed, mixing time, type of mixer, batching volume and cleanliness of the mixer before loading.

SCC (and hence SCSFRC) is less tolerant to changes in the mixing protocol than conventional concrete because it contains a higher amount of fines - not to speak about fibers - which depends on the mixing energy to be efficiently dispersed. SCC and SCSFRC typically requires a longer mixing time or mixing energy than conventional concrete but it is possible to reduce the mixing times by increasing the mixing speeds or by changing the configurations of the paddles in the mixer [RILEM,2006]. Admixture manufacturers recommend that the superplastisizer should be diluted in water before adding to concrete, allowing a better dispersion of the relatively small quantity of admixture within the concrete (RILEM, 2006)

3.4.4. Tolerances established for amounts of concrete constituents

In the European Guidelines for SCC, it is suggested that compositions with plus and minus 5 to 10 L of the target water content, be tested and the respective changes in the fresh state properties be measured in order to check the robustness of the SCC [EFNARC, 2005]. The variations applied to the cement, water and admixture (SP) are shown in the table below.

Table 3.3a: Tolerances for conventional concrete,

Constituents	Tolerances established for concrete	
	ACI,%	EC 2,%
Cement	±1	±3
Water	±3	±3(5)*
Admixture (SP)	±3	±5

Table 3.3b: Tolerances for studying robustness of SCSFRC in the present investigation,

mix. no	Cement variation(±2%)	Water variation ((±5%)	SP variation (±3%)
mix1	Reference mix (0%)	Reference mix (0%)	Reference mix (0%)
mix2	Reference mix (0%)	Reference mix (+5%)	Reference mix (0%)
mix3	Reference mix (0%)	Reference mix (-5%)	Reference mix (0%)
mix4	Reference mix (+2%)	Reference mix (0%)	Reference mix (0%)
mix5	Reference mix (-2%)	Reference mix (0%)	Reference mix (0%)
mix6	Reference mix (0%)	Reference mix (0%)	Reference mix (+3%)
mix7	Reference mix (0%)	Reference mix (0%)	Reference mix (-3%)

The behaviour of highly flowable concretes, such as SCC and SCSFRC, is getting closer to the behaviours of a suspension, which allows a multi-scale approach to mix-design [Flatt et al., 2006]. The properties of the matrix (water, paste or mortar) and solid inclusions (cement and cementitious material, fine or/and coarse aggregate) can be used to predict the properties of the composite material (paste, mortar, SCC, SCSFRC). This type of approach is not possible with traditional concrete, since its behaviour is dominated by grain to grain contacts. For a more scientific approach, a rheometer can be used to study rheology of cement suspensions. Unlike measurements from the empirical tests, rheological parameters are fundamental physical quantities, mutually independent and not dependent on operator or equipment.

3.5 Rheology of cement paste and mortar

In the concrete industry, workability is defined as "the ease and homogeneity for which the concrete or mortar can be placed, consolidated and finished" . Ideally, concrete workability should be characterized by its rheological properties, thus establishing a materials science basis. These properties are usually defined as the Bingham parameters: yield stress and plastic viscosity.

The Bingham equations used to describe cementitious suspension behaviour:

$$\begin{cases} \tau = \tau_o + \mu\gamma & \dot{\tau} \geq \tau_o \\ \dot{\gamma} = 0 & \tau \leq \tau_o \end{cases} \qquad 3.1$$

Where τ is the shear stress (Pa), $\dot{\gamma}$ is the shear rate (1/s), τ_o is the yield stress (Pa), and μ is the plastic viscosity (Pa·s).

The yield stress is the critical shear stress required to initiate deformations (flow). The plastic viscosity describes the resistance to flow once the yield stress is exceeded.

3.6 Rheological model for fresh concrete

It has been shown that the most common workability test used, the slump cone test [prEN12350-8], correlates well only with the yield stress. There are no standard tests of fresh concrete that relate directly to the plastic viscosity. Hence, the workability of concrete is not completely measured or specified by current standard tests. As a result, the concrete industry is unable to specify workability in terms of rheological properties, because the plastic viscosity cannot be easily and uniquely measured. Therefore, a different approach to compare the results from various rheometers has become necessary.

3.7 Experimental tests

The Mini-cone slump test and the Marsh cone test are conducted to determine the rheological parameters such as yield stress and plastic viscosity of cement paste and mortar.

3.7.1 Marsh cone test

The Marsh cone tests is the workability test used for specifications and quality control of cement pastes and mortars. The time required for a certain amount of materials to flow out of the cone is recorded. This measured flow time is related with the so called fluidity of the tested material. The longer the flow time, the lower is the fluidity.

The following procedure has been performed,

➢ Close the nozzle, and pour 1 L cement paste into the cone,
➢ the orifice is opened, and stop watch is started,
➢ the fluid mixture flow out of the cone, and the time required for the cement paste to flow out is recorded which corresponds to the volume of 250mL, 500mL, 750mL, 1000mL.
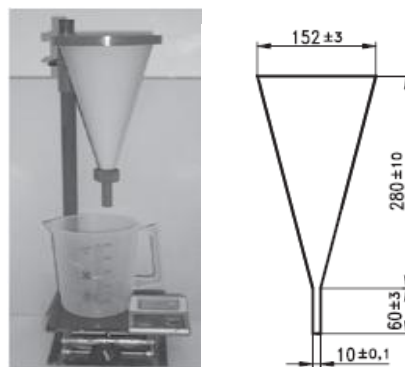

Figure 3.2 Image and geometry of the Marsh cone (EN 445)

3.7.2 Mini-cone slump test

The Mini-cone slump measures the deformability of cement paste and mortar. This Mini-slump truncated cone has a bottom diameter of 100 mm , a top diameter of 70 mm, a height of 60 mm and has the volume of 0.344 L, fig 3.3.
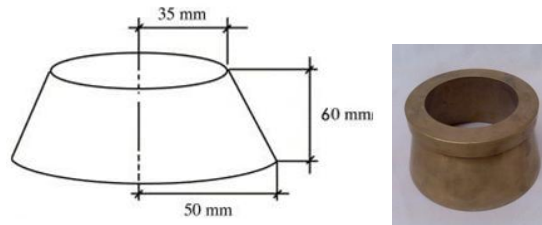

Fig.3.3 characteristics dimension of Mini-cone.

The cone is placed in the center of a square glass plate on which the diagonals and medians are traced. The cone is filled with cement paste/mortar and then lifted. The average spread of the paste, as measured along the two diagonals and two medians, is measured. Cement mortar or paste under the action of gravity tends to spread on the plate of support until a balance between internal forces and external resistance (i.e. when at any point the tangential component of stress due to gravity is below the threshold shift $\tau < \tau_o$) is reached. A digital recording of the flow has also been performed and the movies were processed using photo flash to obtain more accurate and meaningful information about radial spreading (such as time to final spread, spread velocity, etc.). Video recording is required because the rheological behavior of pastes makes it difficult to determine the final diameter and final time of spreading. In fact, for more viscous mixtures these parameters are more easily identifiable, while for more fluid ones where surface tension plays an important role, can be more difficultly captured merely with naked eyes the moment when the flow actually stops.

3.7.3 Mix proportions for cement pastes and mortar

The robustness of cement pastes and mortars, as formulated from SCSFRC mixes, has been first of all investigated.The mix design of cement paste and cement mortar, as formulated from the SCSFRC mix, was shown in tables 3.4a and 3.4b.

Table 3.4a Mix proportions for cement pastes in robustness investigation,

Table 3.4b Mix proportions of cement mortar for robustness investigation,

Table 3.4a Mix proportions for cement pastes in robustness investigation,

mix.no	Cement,kg	Water,kg	Superpla,kg	mix combination
P1	1.330	0.552	0.0199	C ±0 ,W±0,SP±0
P2	1.297	0.563	0.0194	C ±0 ,W+5%,SP±0
P3	1.365	0.540	0.0204	C ±0 ,W-5%,SP±0
P4	1.344	0.548	0.0197	C +2 %,W±0,SP±0
P5	1.315	0.557	0.0201	C -2% ,W±0,SP±0
P6	1.329	0.552	0.0204	C ±0 ,W±0,SP+2%
P7	1.331	0.552	0.0194	C ±0 ,W±0,SP-2%

Table 3.4b Mix proportions of cement mortars for robustness investigation,

Mix no.	Cement,kg	Water, kg	SP, kg	Sand, kg	mix combination
m1	0.737	0.300	0.0110	1.197	C ±0 ,W±0,SP±0
m2	0.727	0.310	0.0109	1.180	C ±0 ,W+5%,SP±0
m3	0.748	0.290	0.0112	1.214	C ±0 ,W-5%,SP±0
m4	0.748	0.299	0.0110	1.192	C +2 %,W±0,SP±0
m5	0.727	0.301	0.0111	1.202	C -2% ,W±0,SP±0
m6	0.737	0.300	0.0113	1.197	C ±0 ,W±0,SP+2%
m7	0.738	0.300	0.0108	1.197	C ±0 ,W±0,SP-2%

3.7.4 Mixing procedure

The control of mixing procedure is very important to provide a uniform and reproducible starting condition for cement paste and mortar. The basic assumptions of this research was that cement paste may be considered as the fluid phase of cement mortar, and the cement mortar is the fluid phase of the self-compacting concrete The mixing protocol detailed in Table 3.5 has been followed in this stage of the investigation.

Table 3.5a Mixing protocol employed for cement pastes

Time	Cement pastes
0 min	mix constituent materials(cement + sp +water),
0-8 min	= Mix at low speed,

Table3.5b Mixing protocol employed for cement mortars.

Time	mortars
0-1 min	mix constituent materials (cement + sand),
	add water and SP,
1-8 min	= Mix at low speed (water +sp)

3.7.5 Identifications of rheological parameters from the mash cone and mini slump test.

Roussel et al provided analytical relationship for the correlation between the Mini slump diameter and yield stress of the cement pastes.

$$\tau_0 = \frac{7200}{128} \frac{\rho g \, V^2}{\pi^2 \, D_f^5}$$

3.2

where V is the volume of the tested sample (0.344 lt for the mini-cone dimensions here employed). It is worth here remarking that Eq. 3.2 neglects the effects of surface tension, which may anyway play a not negligible role in the case of highly fluid suspensions, as in some of the cases herein investigated.

Plastic viscosity is believed to be correlated to the Marsh cone flow time. Roussel and Le Roy have proposed to use the Marsh cone as a complete rheological apparatus, to identify either the yield stress and the plastic viscosity, from results of tests performed employing two different nozzle diameters. The theoretical approach, based on the assumption of a uniform flow, results in the following equations for the calculation of the yield stress and viscosity from the measured flow times:

$$\tau_0 = \rho \, \frac{a_{v1} \, T_2 - b_{v1} \, T_1}{a_{v1} \, b_{v2} T_2 - a_{v2} \, b_{v1} T_1}$$

$$\mu = \rho \, \frac{T_1 \, T_2 \, (b_{v2} - a_{v2})}{a_{v1} \, b_{v2} T_2 - a_{v2} \, b_{v1} T_1}$$

3.3

where coefficients a_{vi} and b_{vi} depend on the cone geometry, nozzle diameter, amount of material filling the cone and amount of material flown out at the measured time. Subscripts 1,2 to the tests performed employing two different nozzle diameters. Unconsistent results, such as

negative values of the yield stress, were obtained in some cases. For this reason, if not correct, employed the value of the yield stress τ_0 obtained from Eq. 3.2. In this case, Eq.(2) can be greatly simplified: allowing thus an immediate evaluation of the plastic viscosity.

$$\mu = \frac{T(\rho - b_v \tau_0)}{a_v} \quad , \qquad 3.4$$

where the parameters a_v and b_v are the geometric parameters as shown below,

$$a_v = \frac{8.V.\tan(\alpha)\,(3.h.\,(H_o.\tan(\alpha) + r)^3 + H_o.r.\,(H_o{}^2.r.\tan^2(\alpha) + 3.H_o.r.\tan(\alpha) + 3.r^2}{(3.\pi.r^3.\tan(\alpha).g.r.(h + H_o)).(H.\tan(\alpha) + r)^3}$$

$$b_v = \frac{\pi.r^3.\ln\,(8.r^3.\ln(H_o.\tan(\alpha) + r) - 8.r.\ln\,(r) + 8.h.\tan\,(\alpha)}{(3.\pi.r^3.\tan(\alpha).g.r.(h + H_o))} \quad ,$$

and H_o is the height of full cone, α is the angle of the cone, h is height of nozzle, r is the radius of nozzle. Coefficients a_v and b_v obviously depend on the cone geometry, nozzle diameter, total amount of material filling the cone and amount of material flown out at the measured time.

3.8 Self consolidating concrete (SCC)

SCC is defined primarily in terms of its fresh properties, therefore, the characterization and control of fresh properties are critical to ensure successful SCC performance. Fresh properties influence not only workability but also hardened properties like strength and durability. Furthermore, SCC is a complex material exhibiting several sensitive interactions between the constituents materials and further work is needed to better understand the effect of mixture parameters governing its fresh properties.

The key workability requirements for SCC are filling ability, passing ability and segregation resistance. The former describes the ability of concrete to flow under its own weight and completely fill form work. Passing ability describes the ability of concrete to flow through confined conditions, such as the narrow openings between reinforcement bars. Segregations resistance(or stability) describes the ability of concrete to remain homogeneous both during transport and placing (in dynamic conditions), and after placing until setting (in static conditions) (ENFRAC, 2005). Additional information can be given about concrete mix viscosity, which is also important in understanding passing ability and segregation resistance, but is not essential for defining a fresh concrete as being self compacting concrete.

3.9 Self consolidating steel fiber reinforced concrete (SCSFRC)

SCC incorporating steel fiber poses difficulty in mixing, transporting, and placing. To better understand the behavior of steel fiber reinforced concrete, the experimental tests are conducted on the on the fresh state properties to assess filling ability, passing ability and fiber segregation (static and dynamic).

3.9.1 Mix proportions

It is mentioned that errors in weighing admixture and cement is influential on many properties of SCC [W. Rigueira et al]. Errors in weighing water have proven to have important influence on concrete properties, as this factor has been revealed as influential for many of the response variables considered by the ANOVA [analysis of variance]. Although the importance of errors in weighing water is of the same level as those in weighing cement or admixture (all three affect a similar number of response variables), the fact that water is less precisely weighed in real production than cement or admixture, as the corresponding part of our study reveals, makes it a primary factor to be considered when assessing the robustness of SCSFRC. It has been also been mentioned that the variation of aggregates does not have great influence on the properties of the SCC [W. Rigueira et al]. According to the variations of mix-constituents referred above, the following SCSFRC mixes have been designed and cast as the main part of the present robustness investigation.

Table 3.6 mix design of SCSFRC,

mix	cement	water	SP	Sand	gravel	steel	pate	mortar
no.	kg	kg	kg	kg	kg	fiber,kg	ratio	ratio
mix 1	23.57	9	0.35145	38.25	39.87	2.25	0.2906	0.6282
mix2	23.56515	9.45	0.35145	38.25	39.87	2.25	0.2934	0.6297
mix 3	23.56515	8.55	0.35145	38.25	39.87	2.25	0.2877	0.6267
mix 4	24.01515	9	0.35145	38.25	39.87	2.25	0.2934	0.6297
mix 5	23.12	9	0.35145	38.25	39.87	2.25	0.2877	0.6267
mix 6	23.56515	9	0.36045	38.25	39.87	2.25	0.2906	0.6282
mix 7	23.56515	9	0.34245	38.25	39.87	2.25	0.2905	0.6282

3.9.2 Mixing of constituents

Self-compacting steel fiber reinforced concrete was mixed in a horizontal mixer [fig. 3.4]. The weight of the materials was taken with a digital weight balance. Mixing sequence was as follows,

➢Mixing cement, sand, and coarse aggregates for 1 minute,

➢ Adding water and Sp and then mix for four additional minutes,

➢ Adding extra water and fiber and then mix three more minutes.

Fig 3.4 SCC, SCSFRC mixer- Polo Regionale di Lecco.

3.9.3 Experimental tests for SCSFRC and SCC.

The fresh state behavior of concrete has includes the workability, flowability, segregation resistance, etc and has been characterized through the following tests.

3.9.3.1 Slump cone tests

Slump-flow test describes the flowing ability of a fresh mix in unconfined conditions. Test results are the slump-flow diameters (SF, expressed to the nearest 10mm) and the time needed to reach the 500mm spread (t_{500}, expressed to the nearest 0,5s). which respectively give an indications of the filling ability and relative viscosity of SCC, respectively [fig. 3.5].

The slump-flow test principle, apparatus, procedure, result computation and precision are further described in prEN 12350-8 (CEN, 2007f).
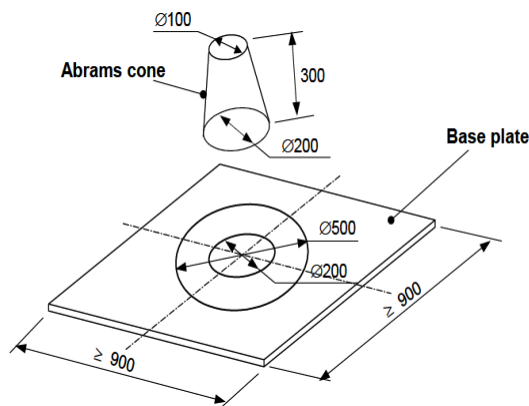

Figure 3.5- Base plate and Abrams cone

3.9.3.2 V-funnel test

The V-funnel test is used to assess the viscosity (and filling ability) of SCC (see figure 3.6). The test results is the time taken for concrete to flow out of a V-shaped funnel (Tv, expressed to the nearest 0,5sec). The V-funnel test principle, apparatus, procedure, result computation and precision are further described in prEN 12350-9 (CEN, 2007d).
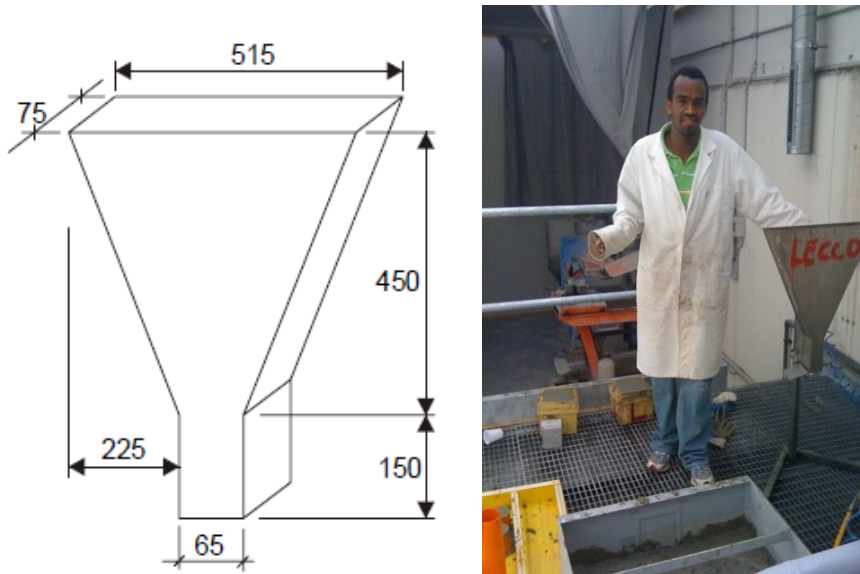

Figure 3.6: V-funnel dimensions and tests, Polo Regionale di Lecco.

3.9.3.3 Dynamic fiber segregations

3.9.3.3.1 Confined flow channel,

Beams were cast with the SCSFRC mixes in a channel of 1500mm long, 150mm wide, and 60mm deep as shown in figure 3.7. Two beams were cast for each mix from which the first cast was allowed to harden and the second cast specimen was divided into nine equal sections in fresh state.
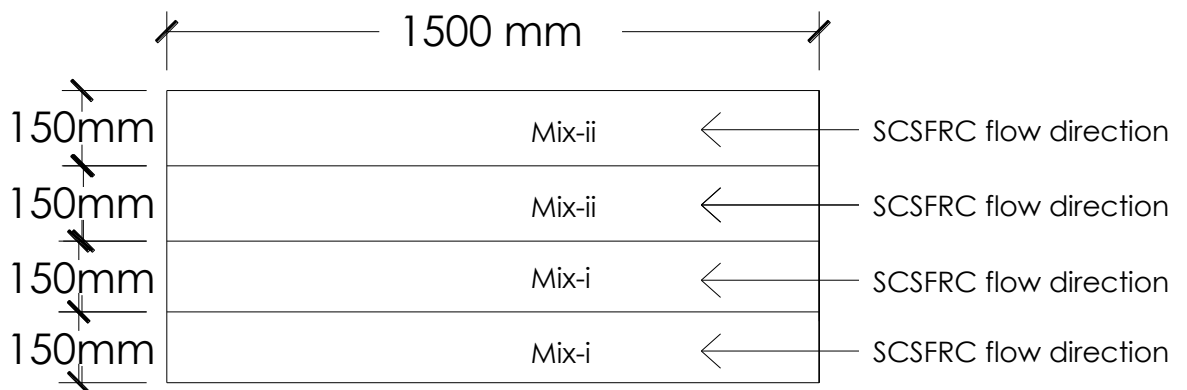

Figure 3.7a Channel flow- beam specimen

Concrete was cast with an inclined pipe, 1.5 m long, to provide the necessary force to achieve full casting of the long beam specimens.

Figure 3.7b Channel flow- beam specimen

The fibers in each nine section was separated out by washing fresh specimens in water, and then weighted to compute concentrations of fibers along the beam length 1500 mm.

3.9.3.3.2 Free surface flow

After having performed the slump flow test on SCFRC, the ability of the mix to disperse fibers in a free surface flow was evaluated by dividing its spread diameter section into three: the inner 20cm diameter, 20cm to 50 cm diameter and outside 60cm diameter section. The amount of fiber are computed by separating the fibers out of the concrete in this sections. [fig. 3.8]
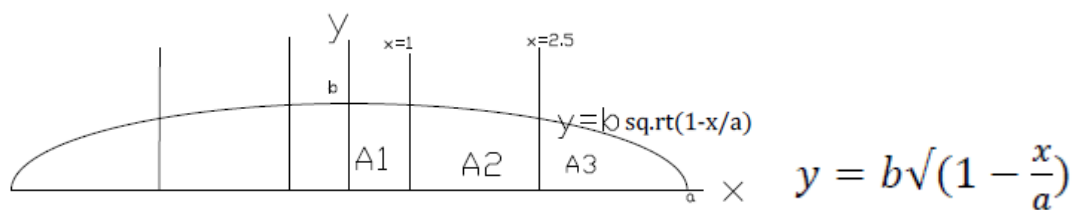

Fig 3.8 Geometric profile for final slump concrete profile

Computations of volume,

The parabolic approximations to the final geometric shape of the self-compacting steel fiber reinforced concrete on the horizontal plate, where a is the maximum x-axis or the radius of the slump and b is the maximum y-axis or the height of slump concrete at the center of the plate.

The areal moment of inertia was used to compute the sectional volume as shown in the table below by rotating the corresponding cross-sectional areas about y-axis.

56

Table 3.7a The volume inside 20cm diameter,

Mix No	slump diamter	Slump radius,a,dm	slump ordinate,b, dm	∫dA1 Area	∫xdA1 $\bar{x}A$	centroid $\bar{x}$	volume V1
1	60	3	0.36	0.332	0.160	0.483	1.008
2	80	4	0.20	0.192	0.093	0.488	0.587
3	20	10	-	-	-	-	-
4	56	2.8	0.42	0.378	0.182	0.482	1.145
5	62	3.1	0.34	0.312	0.151	0.484	0.949
6	68	3.4	0.28	0.262	0.127	0.486	0.798
7	45	2.25	0.65	0.569	0.271	0.476	1.703

Table 3.7b The volume between 20cm and 50 cm diameter

Mix No	slump diamter	Slump radius,a,dm	slump ordinate,b, dm	∫dA2 area	∫xdA2 $\bar{x}A$	centroid $\bar{x}2$	volume V2
1	60	3	0.36	0.347	0.580	1.671	3.645
2	80	4	0.20	0.230	0.392	1.708	2.463
3	20	10	-	-	-	-	-
4	56	2.8	0.42	0.375	0.621	1.654	3.899
5	62	3.1	0.34	0.333	0.559	1.678	3.512
6	68	3.4	0.28	0.294	0.497	1.692	3.123
7	45	2.25	0.65	0.402	0.604	1.500	3.792

Table 3.7c The volume outside 50cm diameter

Mix No	slump diamter	Slump radius,a,dm	slump ordinate,b, dm	∫dA3 Area	∫xdA3 $\bar{x}3A$	centroid $\bar{x}3$	Volume V3
1	60	3	0.364398505	0.04958836	0.133889	2.7	0.841247
2	80	4	0.204974159	0.12552053	0.389114	3.1	2.444873
3	20	10	-	-	-	-	-
4	56	2.8	0.41831461	0.02738512	0.071749	2.62	0.450812
5	62	3.1	0.341268111	0.06005518	0.164551	2.74	1.033906
6	68	3.4	0.283701258	0.08757786	0.250473	2.86	1.573766
7	45	2.25	0.647819565	0	0	0	0

Note: for SCSFRC mix number 3, i.e. less water, the final slump diameter was less than 50 cm and there was not samples in the section outside 50 cm diameter.

3.9.3.4 Static fiber segregation

The fresh SCSFRC was cast in a plastic cylinder of 240 mm height and 80 mm diameter, and allowed to rest. It was possible that, due to the difference between their specific weight and that of the suspending fluid matrix, fibers segregate, also depending on the yield stress of the matrix. Static segregation was hence measured by these tests as follows.

The plastic cylinders are filled from the top while keeping the cylinders height vertical. The fibers volume distribution along the cylinder height are computed by dividing the cylinders into three equal sections. The weight (g) or concentrations (gm/dm^3) of fibers in each section is used to compute the fiber segregation index.

3.9.4 Casting of SCC and SCSFRC specimen

SCCs and SCSFRCs specimens are cast to study their properties in the hardened state. The specimen are casted in accordance with the type of mechanical tests to obtain the hardened parameters like flexural strength, compressive strength, tensile strength. FOr bending tests, the 1.5 m long beam described before was used and three beam specimens, each 500 mm long were obtained by cutting it. Furthermore, the cubic samples of dimensions 150 mm were for cubic compressive strength and the cylinder samples of diameter 80 mm and height 80 mm for tensile splitting strength tests were casted for each mix.

3.10 Fiber dispersion and orientation in hardened state flow

The fiber dispersions and orientations in hardened SCFRC specimens were determined by using a non-destructive magnetic probe test performed on the hardened beam specimens and cylinder specimens of SCSFRC. The fibers concentrations computed using this method were correlated with the concentrations computed by washing beam section specimens in fresh state or crushed in the hardened state.

3.10.1 Magnetic probe test

Since the fiber orientation and fiber concentrations significantly affects the mechanical strength of fiber reinforced concrete, the appropriate methods needs to be developed to assess these parameters. In this research a magnetic probe sensitive to the magnetic properties of the steel fiber in the concrete was employed. The set up consists of low cost sensor employing a C shaped ferrite core. Four coils have been wound on it: two provides the generation of the magnetic flux and two allows the picking up the emf. By leaning the probe on the SCSFRC specimen surface and by measuring the variations of mutual inductance between the pairs of

winding, it is possible to discriminate the average orientation of the fibers, and to obtain information on concentrations [fig. 3.9, 3.10].

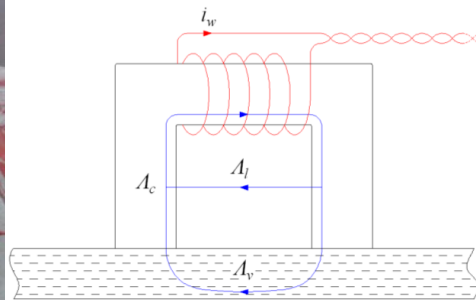Figure 3.9 : magnetic probe   Fig. 3.10. Layout of the magnetic probe.

The main disadvantages of this method is that it does not give the reliable information regarding the size of the fiber. This happens since this feature can better be analysed looking at the variations in power loss rather than change in the inductance. In fact, the power loss are strictly related to the dimensions of the fibers. In the measurement proposed by [Faifer et al, 2010] the estimations of power loss due to the steel fibers was masked by the ohmic resistance of the winding.

The performance of the method has been theoretically and experimentally analysed to provide adequate tool as non-destructive test on the hardened specimen of Steel fiber reinforced concrete. This kind of research activity has also been carried out by researchers of Politecnico di Milano, involving experts from both department of structural engineering and electrical engineering [fig. 3.11].
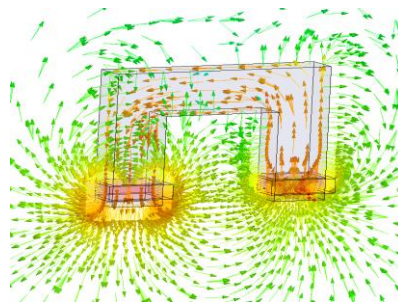

Fig. 3.11 – FEM simulation of the magnetic flux density[Faifer et al, 2010]

3.10.2 Measurement setup

An automatic measurement system has been implemented in order to evaluate the probe parameters (figure 3.12).
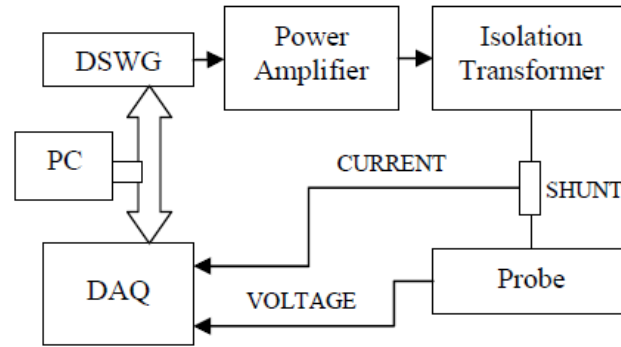
Figure 3.12: the scheme of the measurement system

The system has been developed following a virtual instruments (VI) approach. It allows injecting and measuring the current *ie* through the excitations circuit, and to measure the emf vs induced in the sensing winding. Then, it provides the computations of probe parameters *Lm* and *Pm* from the acquired current and voltage waveforms. The excitation signal has been generated by a means of a DSWG(digital signal waveform generators), followed by a power amplifier. An isolation transformer has been employed to electrically decouple the signal generation from the measurement section of the device. This isolation allows avoiding ground loops, thus improving the performance of the measurement system. The power amplifier has been set in order to inject a sinusoidal current of about 0.6A rms in the order of frequency 1khz to 10khz.

Therefore, through the measurement of the mutual inductance Lm, it is possible to obtain information about the fiber concentrations and orientations. From practical point of view, these evaluations require to execute the same measurements, but to process the data in two different ways.

For analysis of the SCSFRC beams, the proposed method requires to collect the inductances obtained by rotating the probe along its axis. Therefore, the average of this measurement is computed for the estimation of fiber concentrations. In this way, we can compute also the fiber clumps that results in a local increase of the average mutual inductance. However, the evaluation of the fiber orientations requires identifying the directions along which *Lm* has the maximum value. The informations about the fiber dimension can be extracted through a combined analysis of *Lm* and *Pm* [Faifer et al, 2010].

3.11 Hardened state properties of SCSFRC

After a non destructive magnetic tests had been performed on hardened specimens of beams and cylinders, another experimental tests such as bending test, crushing strength and tensile splitting strength tests were performed on all of the hardened specimens.

3.11.1 Crushing of hardened specimen

After performing the magnetic probe test to estimate the fiber concentrations and orientations, the cylinder specimen was cut into three equal parts and then crushed with heavy weight hammer. The steel fibers were separated from crushed specimen and weighed to calculate concentrations in each parts. Moreover, the measured inductances using the magnetic probe test were correlated with the actual steel fiber concentrations determined by crushing the samples.

3.11.2 Four point bending tests

The main effects of reinforcing concrete with steel fibers is the enhancement of the toughness of the material since the strength is not affected to a large extent but rather the post-peak mechanical behavior is dramatically changed even for relatively low fibers volumes.

The most straightforward way to characterize a material regarding the post-peak behavior in tension is by performing uniaxial tension tests under closed-loop displacement control ; however, the bending test is preferred to the former since such a test is relatively complicated to carry out and also since many applications in which SFRC is used are designed for bending, not pure tension, and hence the post peak bending behavior is of primary importance. As a result the flexural toughness was evaluated in this study by mean of four point bending test.

Procedure for Bending Tests: Un-notched beam specimen (CNR DT 204, UNI U73041440)

Tests were performed controlling the crack opening displacement (COD), measured over the 200 mm base length astride the mid-span. From the nominal stress vs. COD curves the effectiveness of the consolidating mix in orienting the fibers along the casting direction clearly appears.
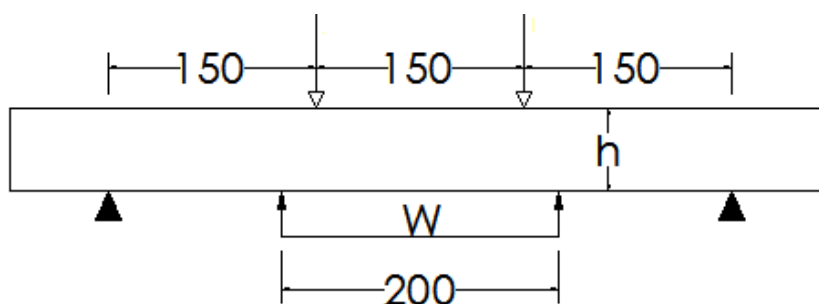

Figure 3.13 four point bending test

For the stress-COD response, besides the first cracking strength f_{If} (see below), the following post-cracking, equivalent stress have been computed. (CNR-DT 204-Tab. 2.4):

> feq_1, in the COD range $3w_1$-$5w_1$, where w_1 is the COD at first cracking, identified as the maximum load in the crack opening range 0-0.1 mm;

> feq$_2$, in the COD range 0.8w$_u$-1.2w$_u$, where Wu is the ultimate crack opening displacement, assumed equal to 3mm.
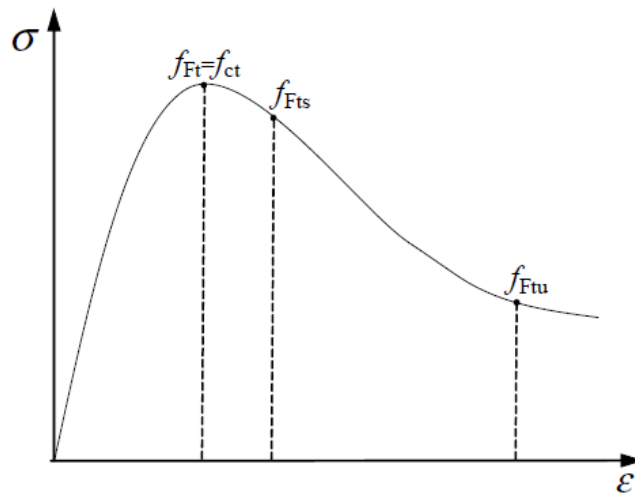

Figure 3.14 stress-strain diagram

3.11.3 Tensile Splitting strength test

The apparent tensile strength measured depends on the shape and size of the test specimen. The effect of cylinder size on the measured tensile strength was not found to be significant, possibly due to the variability of the data. It is recognized good practice to include measurement of density prior to the determinations of tensile splitting strength, as a check on compaction.

The European standard specifies a method for the determination of the tensile splitting strength on cylindrical test specimens of hardened concrete.
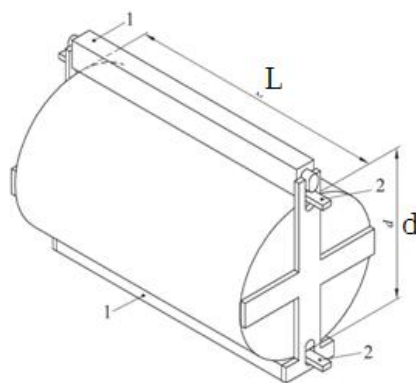

Figure 3.15 splitting test- cylinder specimen

The splitting tensile strength was measured for plain SCC, without fibers, since we wanted to have a reference for the tensile strength of the matrix alone eventually to be compared to f$_{lf}$ measured form bending tests on SCSFRC.

Principle

A cylindrical specimen is subjected to a compressive force applied to narrow region along its length. The resulting orthogonal tensile force causes the specimen to fail in tension.

Expression of the results

The tensile splitting strength is give by formula

$$f_{ct} = \frac{2 \times F}{\pi \times L \times d}$$

Where f_{ct} is the tensile splitting strength, in megapascals(MPa) or in N/mm^2,

      F is a maximum load in N, L is the length is of the line of contact of specimen in mm,

     d is the designated cross-sectional dimension, in mm.

express the tensile splitting strength to the nearest 0,05MPa. Or (M/mm^2)

3.11.4 Compressive strength tests

The compressive strength tests were performed on the specimens of SCSFRC. The dimension of the a cube specimen is 150mm. The compressive strength is not affected by the presence of steel fibers in SCSFRC specimen since it is mainly function of matrix strength.

Fig. 3.16 Compression test setup, Polo Regionale di Lecco.

CHAPTER 4: RESULTS AND DISCUSSIONS

4.1 Introduction

The results from the investigations of the robustness of SCSFRC and discussions in all the steps of our experiments are presented in this chapter. The experimental discussion startes from the cement paste and mortar since they are the basic ingredients of SCC and SCSFRC. This gives useful information regarding the robustness in fresh and hardened state of SCSFRC.

4.2 Rheology of cement paste and cement mortar

The rheology of cement paste and cement mortar was studied through the Mini-cone slump and Marsh cone tests as discussed in previous chapters. The final diameter of the Mini cone can be related with the yield stress and together with the Marsh cone flow time, the corresponding viscosity can be estimated.

4.3 Experimental results for cement paste and mortar

4.3.1 Results for cement paste

The fresh characteristics of the cement paste from both Marsh cone and Mini-cone test are shown in the table below.

Table 4.1: Experimental results for cement paste,

cement paste	Cement Kg	water kg	SP, kg	mix variati	Slum dia Df,m	Sh.stre N/m2	Final time,se	Visco. Pa-s	Ratio w/c	sp/c
Mix 1	1.330	0.552	0.0199	000	0.455	6.73183	19	0.675	0.415	0.01497
Mix 2	1.297	0.563	0.0194	0+0	0.48	5.15209	16	0.575	0.434	0.01497
Mix 3	1.365	0.540	0.0204	0-0	0.43	8.92992	23	0.802	0.396	0.01497
Mix 4	1.344	0.548	0.0197	+00	0.415	10.6647	24	0.825	0.407	0.01469
Mix 5	1.315	0.557	0.0201	-00	0.50	4.20088	15	0.544	0.423	0.01526
Mix 6	1.329	0.552	0.0204	00+	0.466	5.97393	16	0.572	0.415	0.01535
Mix 7	1.331	0.552	0.0194	00-	0.4425	7.73791	19	0.669	0.415	0.01458

4.3.1.1 March cone test

It can be observed from figure 4.1 that decreasing the amount of water affects the fluidity of cement paste. Increasing the amount of cement is comparable with the effect of decreasing the amount of water; however, the effect of water is more noticeable.

Fig. 4.1 Flowability for cement paste.
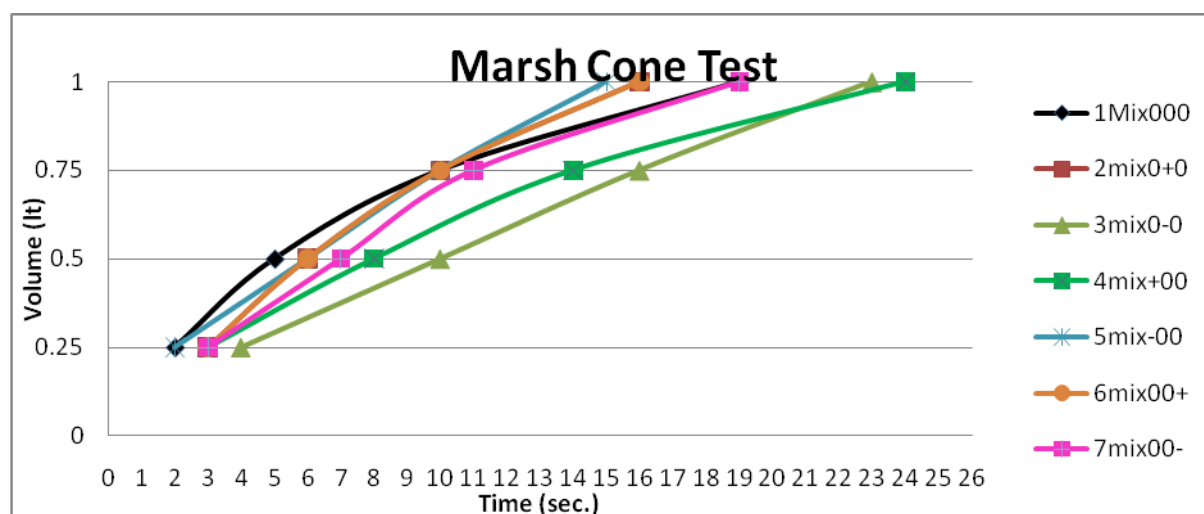
4.3.2 Results for cement mortar

The Marsh cone tests conducted for the cement mortar showed that it takes too much time for the flow of the mix in the mouth of the cone. For this reason, we decided to conduct only the mini cone test for cement mortar and video recording was taken.

Table 4.2 Experimental results for cement mortar

Mix	cement	water	SP	Sand	Mix	Mix ratio		Slum dia.	Yield st.	Viscosity
no.	C, kg	W,kg	SP,kg	S,kg	Prop.	w/c	sp/c	Dfinal,m	N/m2	Pa-s
Mix 1	0.737	0.3	0.011	1.197	000	0.40706	0.0149	0.215	33.82	1.15
Mix 2	0.727	0.31	0.0109	1.18	0+0	0.42641	0.015	0.24	19.51	0.87
Mix 3	0.748	0.29	0.0112	1.214	0-0	0.3877	0.015	0.175	94.65	2.05
Mix 4	0.748	0.299	0.011	1.192	+00	0.39973	0.0147	0.185	71.69	1.57
Mix 5	0.727	0.301	0.0111	1.202	-00	0.41403	0.0153	0.23	24.14	0.99
Mix 6	0.737	0.3	0.0113	1.197	00+	0.40706	0.0153	0.225	26.94	1.04
Mix 7	0.738	0.3	0.0108	1.197	00-	0.4065	0.0146	0.19	62.74	1.24

4.3.3.1 Flow measurement

The slump flow test was carried out using experimental set up described in the previous chapters, and high definition digital video recording on suited above the slump flow. The video captures are analyzed frame by frame using specialized video image processing software, Imaje J. In this way, the evolution of flow diameter vs. time was obtained. The flow velocity was computed by the ratios of change in diameter over specified time interval. It has been mentioned that the final setting time is related with the viscosity [Ferrara et al., 2008].

Table 4.3 Slump flow velocity for cement mortar from Mini slump video recording.

flow	cement mortar mixes-flow velocity in cm/sec;						
time,sec.	mix1	mix2	mix3	mix4	mix5	mix6	mix7
0	5.348	5.082	3.473	4.193	5.583	5.123	4.655
2	0.570	1.623	0.544	0.798	0.917	0.542	0.706
4	0.237	0.854	0.194	0.418	0.542	0.407	0.549
6	0.095	0.342	0.039	0.342	0.292	0.452	0.235
8	0.000	0.256	0.000	0.000	0.125	0.045	0.039
10	0.000	0.171	0.000	0.000	0.042	0.090	0.078
12	0.000	0.171	0.000	0.000	0.000	0.090	0.000
14	0.000	0.000	0.000	0.000	0.000	0.000	0.000

Figure 4.2 Flowability of cement mortar.
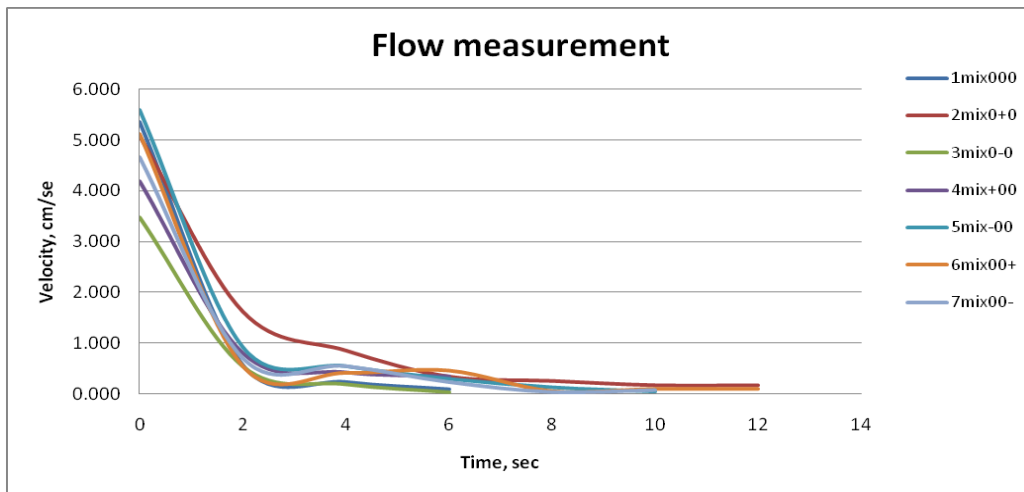
From the above results, it can be observed that changes in water has the most significant effect on the slump flow of cement mortar. The decrease in water results in the decrease in slump diameter. Changes in cement is the second most important affecting the fluidity of cement mortar. While the SP is the least because of its lowest mix ratio in the mix design.

4.3.4 Statistical analysis of experimental results from cement paste and mortar

The statistical software minitab-ANOVA was used to analyze the effects of variation on cement content, water content and amount of SP on the properties of the cement paste such as final flow diameter [D_{final}], and final flow time, [T_{final}].

The main effect plot and interaction plot as obtained from the several factor ANOVA are shown hereafter:

Main effect plot: the effect of a factor is defined as a change in response produced by a change in the level of the factor

Interaction effect plot: in some experiments, the difference in response between the level of one factor is not same at all level of the other factors. When this occurs, there is interaction between the factors.

A significant interaction can mask the significance of main effects. Consequently, when interaction is present, the main effects of the factors involved in the interaction may not have much meaning.

4.3.4.1 Cement paste

Final flow diameter

The Mini cone final slump flow diameter [D_{final}] i.e. the final spread of the cement paste, was mainly affected by the changes in the water and cement content.

Fig. 4.3 Main effect and interaction plot of D_{final} [m] vs. variations (cement, water, SP) [%]:
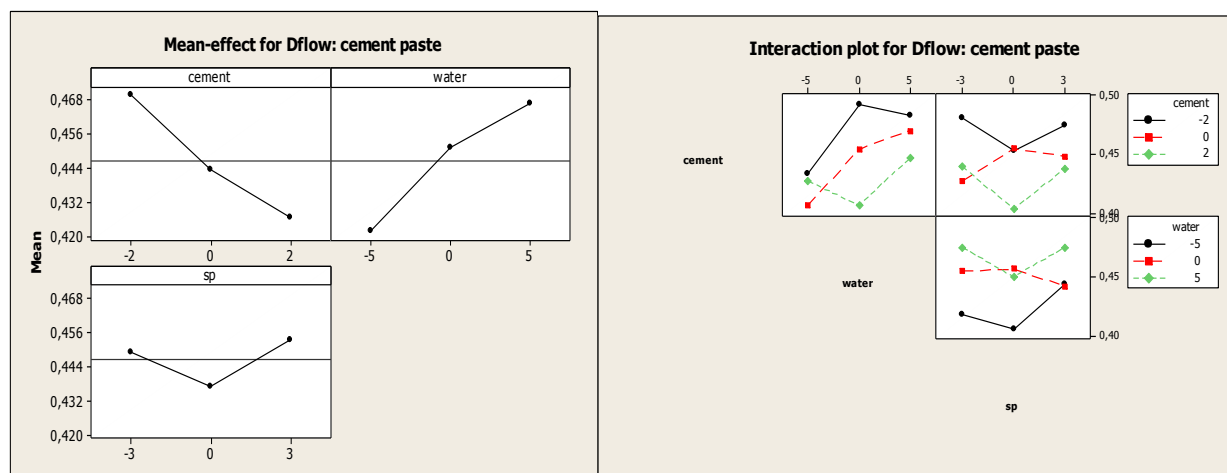
➢ The slump diameter decreases with an increase in cement content,

➢ The slump diameter increases with an increase in water content,

➢ The effect of the SP on the final diameter seems to negligible,

➢ The interaction among the cement and water, cement and SP, water and SP are shown. SP and water variations seems to have high interaction. Water and cement variations seems to have least interaction.

Final flow time

The Marsh cone final flow time, [T_{final}] i.e. the time cement paste volume flow out of Marsh cone, was mainly affected by the changes in the water and cement content.

Figure 4.4: Main and interaction effect Plot of T_{final} [sec] vs. variation (cement, water, SP) [%],
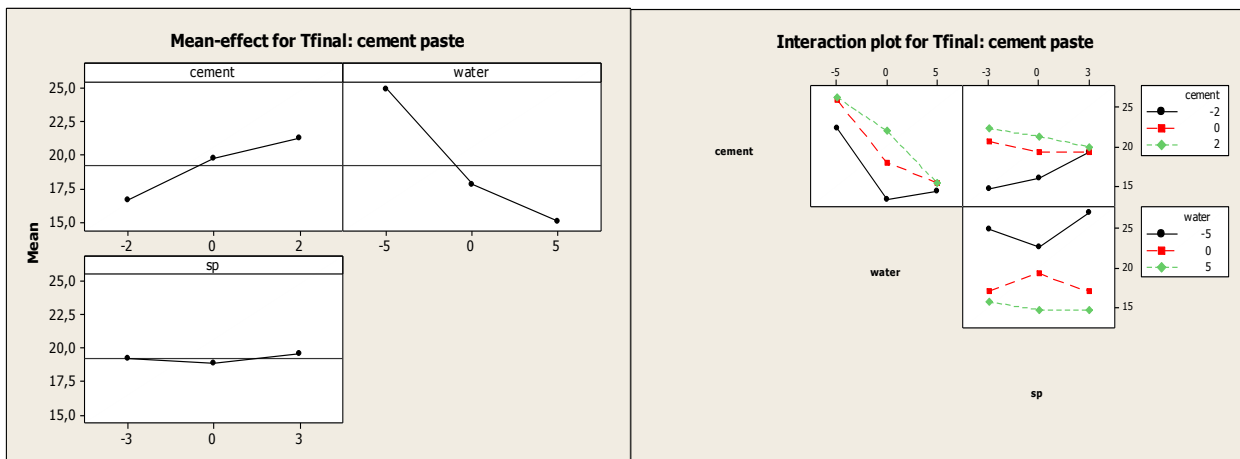
- The time to final spread increases with increase in the cement content,
- The time to final spread decreases with increase in cement content,
- The effect of the SP on the final diameter seems to be negligible,
- The interaction among the variation in cement and water, cement and SP, water and SP are shown. SP and cement seems to have high interaction. Water and cement variations seems to have least interaction.

Yield stress and viscosity

Figure 4.5 Main effect plot yield stress, N/m^2 and viscosity (Pa-s) vs. variations (c, w, sp) [%].
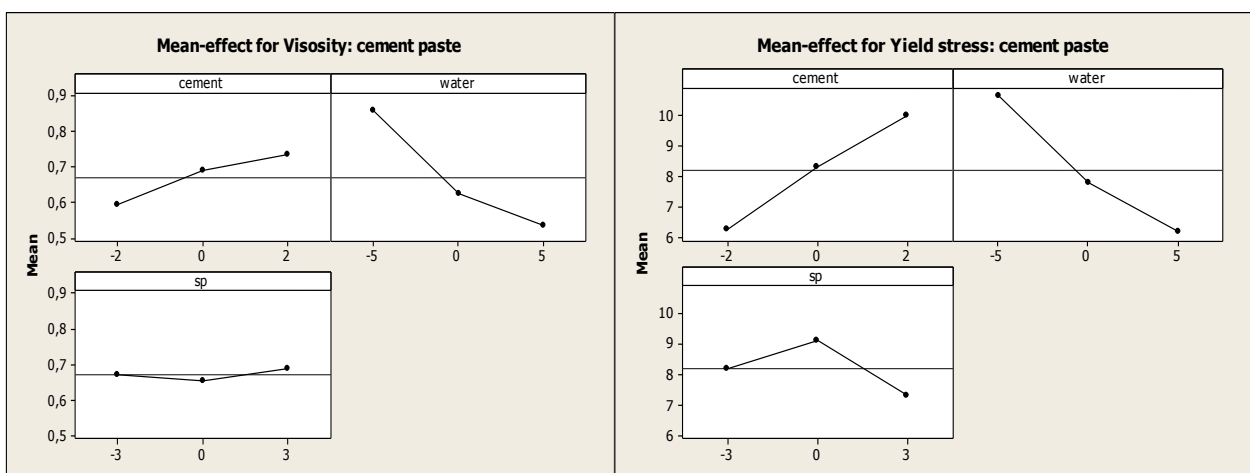
- The yield stress coherently increases with an increase in cement content!
- The yield stress decreases with an increase in water content.
- The effect of the SP on the final diameter is negligible.
- The viscosity increases with an increase in cement content.
- The viscosity decreases with an increase in water content.

4.3.4.2 Cement mortar

Final slump flow diameter

Figure 4.6 Main and interaction effect plot of D_{final} [m] vs. variations in (c, w, sp) [%]
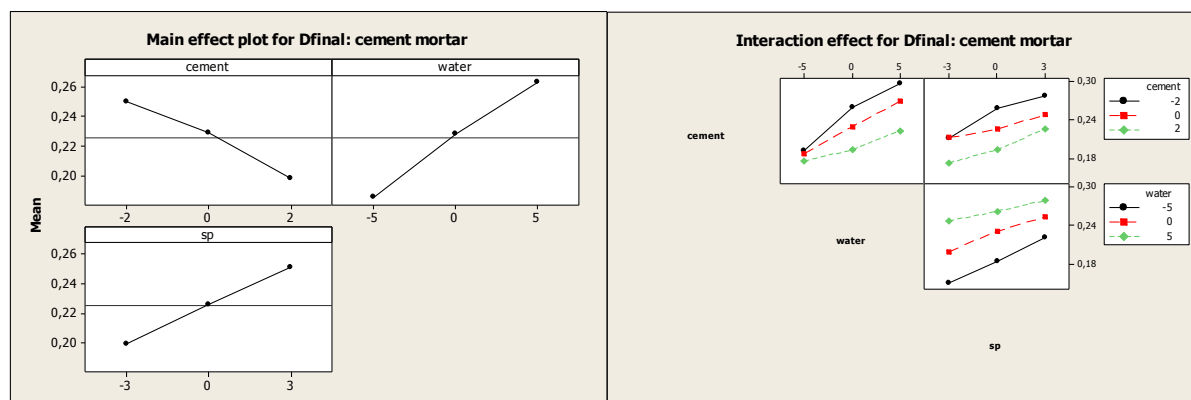
- ➤ The increase in cement content with decreases the final spread diameter.
- ➤ The increase in water content with increase the final spread diameter.
- ➤ The increase in SP content with increases the final spread diameter.
- ➤ The interaction among the variation in cement and water, cement and SP, water and SP are shown. It can be observed that there is no significant interactions between them as the effects of one is not dependent on another.

4.3.5 Comparison of cement paste and cement mortar

The yield stress and plasticity viscosity increase as the maximum particle size increases. the increased plastic viscosity is partly due to due to the increase inter particle contact and surface interlocking, as demonstrated by the fact that for two concrete with the same yield stress containing rounded and angular course aggregate, the plastic viscosity of the latter is higher.

4.4 Experimental results for self consolidating steel fiber reinforced concrete

4.4.1 Fresh state properties

The fresh state properties of SCSFRC as determined according to the methodology described in previous chapter are hereafter analyzed.

4.4.1.1 Final slump flow diameter and flow time

The final slump flow diameter and V-funnel flow time are shown in table 4.4.

Table 4.4 Final slump diameter and flow time for SCSFRC,

Mix Number	change in cemet,%	change in water,%	change in SP,%	final slump diameter,cm	Change in Diameter,%	V-funnel time, sec	Change Time, %
mix1	0%	0%	0%	60	0	8.4	0
mix2	0%	+5%	0%	80	33.33	6	-28.57
mix3	0%	-5%	0%	20	-66.67	-	-
mix4	+2%	0%	0%	56	6.67	11	30.95
mix5	-2%	0%	0%	62	3.33	8.5	1.19
mix6	0%	0%	+3%	68	13.33	6.9	-17.86
mix7	0%	0%	-3%	45	-25.00	10	19.05

From the above results, it can be observed that,

➢ Increase in water amount, decrease in cement content, increase in SP all results increase in final slump diameter of SCSFRC.

➢ Decrease in water amount, increase in cement content, decrease in SP results in decrease final slump diameter of SCSFRC.

➢ Increase in water amount, decrease in cement content, increase in SP all results in decrease in flow time of SCSFRC.

➢ Decrease in water amount, increase in cement content, decrease in SP all results in increase in flow time of SCSFRC.

Comparison of cement paste, mortar, and SCSFRC

Table 4.5 Comparison of cement paste, mortar and SCSFRC

mix no	Variation in slump D $_{final}$ [%]			variation in flow time, T $_{final}$, [%]		Remarks
	paste	mortar	SCSFRC	paste	SCSFRC	
mix1	0	0	0	0	0	Reference
mix2	5.494505	11.627907	33.33	-15.7895	-28.57	Ref+5%w
mix3	-5.49451	-18.60465	-66.67	21.05263	-	Ref-5%w
mix4	-8.79121	-13.95349	-6.67	26.31579	30.95	Ref+2%c
mix5	9.89011	6.9767442	3.33	-21.0526	1.19	Ref-2%c
mix6	2.417582	4.6511628	13.33	-15.7895	-17.86	Ref+3%sp
mix7	-2.74725	-11.62791	-25	5.263158	19.05	Ref-3%sp

Note: the effect of changes in cement, water or sp on the fresh parameters of cement paste, mortar and SCSFRC are shown above.

The fiber distribution along the channel is determined by washing fresh specimens. The channel length equal to 1500mm was divided into 9 parts and each part was washed with water for separating fiber content. The amount of fiber is weighted to determine the concentrations of fiber along the channel length.

Table 4.6a fiber distribution along SCSFRC flow,

Mix1: Reference mix: ±0% c; ± 0 % w; ±0% sp			Mix2: Reference mix + 5%w: ±0% c; +5% w; ± 0% sp		Mix3: Reference mix - 5%w: ±0 % c; -5% w; ± 0 % sp	
Slump D $_{final}$ = 60cm Flow time: 8.4sec			Slump D $_{final}$ = 80cm, Flow time: 6sec		Slump D $_{final}$ = 20cm, Flow time: ----	
Beam	Fiber	fiber	Fiber	fiber	Fiber	fiber
section	Weights	conc.	Weights	conc.	Weights	conc.
(cm)	(g)	(Kg/m^3)	(g)	(Kg/m^3)	(g)	(Kg/m^3)
8.3	57	37.92	45	29.94	67.12	44.66
25	73	48.57	115	76.51	58.9	39.19
41.7	65	43.25	71	47.24	54.27	36.11
58.4	77	51.23	98	65.20	62.68	41.70
75.1	72	47.90	83	55.22	59.23	39.41
91.8	73	48.57	82	54.56	62.49	41.58
108.5	76	50.57	90	59.88	56.42	37.54
125.2	50	33.27	119	79.17	56.32	37.47
141.9	66	43.91	108	71.86	58.9	39.19
	AVG	45.02	AVG	59.95	AVG	39.65
	STN. DEV	6.08	STN. DEV	15.52	STN. DEV	2.63
	Stn.Dev/Avg	0.14	Stn.Dev/Avg	0.25886	Stn.Dev/Avg	0.07

We can see the effect of increasing the water content on the fiber distribution. Increasing water content causes greater fiber gradient along the SCSFRC flow. This could be related to the increasing flowability due to higher water content. On the other hand, decreasing the water content cause the concrete very stiff and this also reduce the fiber dispersion in the channel. This can also be related to the fresh parameters life yield stress and viscosity through the experimental tests of slump cone tests, V-funnel tests on the SCSFRC and SCC as well as mini-cone and marsh cone tests on the cement paste and cement mortar.

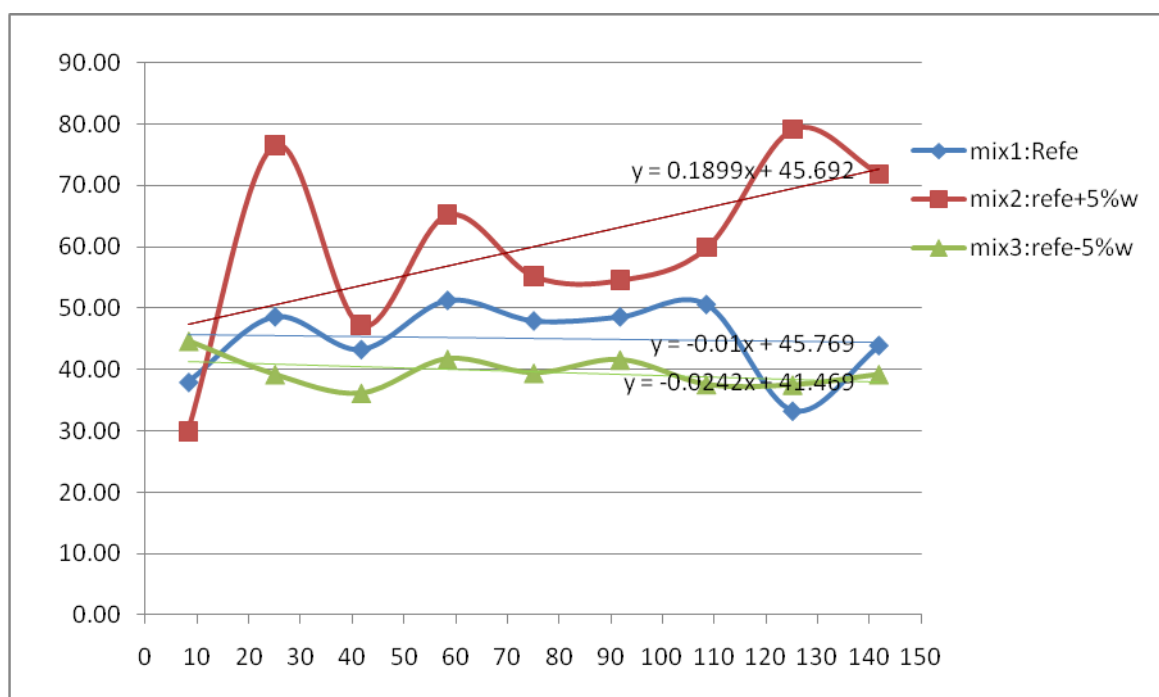Figure 4.7a plot of the fiber distribution along the flow of SCSFRC,

Table 4.6b fiber distribution along SCSFRC flow,

Mix1: Reference mix:			Mix4: Reference mix + 2%c:		Mix5: Reference mix - 2%c:	
±0 % c; ± 0% w; ± 0 sp			+ 2% c; ± 0% w; ± 0% sp		- 2% c; ± 0% w; ± 0% sp	
Slump D_{final}= 60cm Flow time: 8.4sec			Slump D_{final}= 56cm Flow time: 11sec		Slump D_{final}= 62cm Flow time: 8.5sec	
beam	Fiber	fiber	Fiber	fiber	Fiber	fiber
section	Weights	conc.	Weights	conc.	Weights	conc.
(cm)	(g)	(Kg/m^3)	(g)	(Kg/m^3)	(g)	(Kg/m^3)
8.3	57	37.92	76	50.57	91	60.55
25	73	48.57	80	53.23	79	52.56
41.7	65	43.25	81	53.89	81	53.89
58.4	77	51.23	73	48.57	76	50.57
75.1	72	47.90	77	51.23	82	54.56
91.8	73	48.57	73	48.57	80	53.23
108.5	76	50.57	80	53.23	75	49.90
125.2	50	33.27	78	51.90	77	51.23
141.9	66	43.91	77	51.23	81	53.89
	AVG	45.02	AVG	51.38	AVG	53.37
	STN. DEV	6.08	STN. DEV	1.93	STN. DEV	3.13
	Stn.Dev/Avg	0.14	Stn.Dev/Avg	0.04	Stn.Dev/Avg	0.06

Figure 4.7b plot of the fiber distribution along the flow of SCSFRC
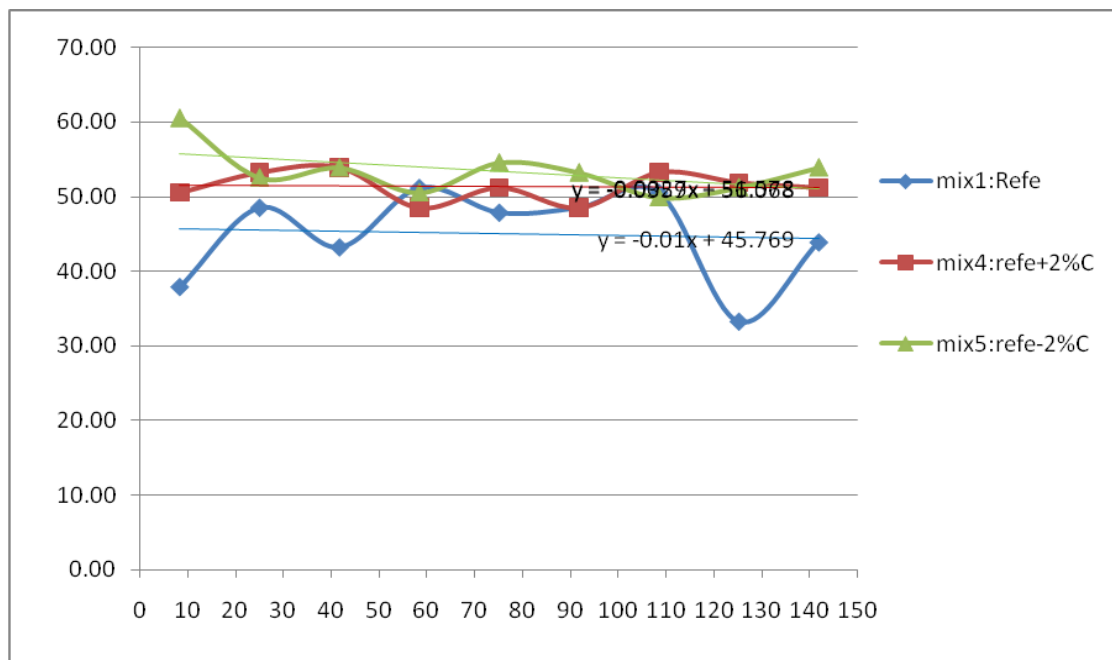
Table 4.6c fiber distribution along SCSFRC flow,

Mix1: Reference mix:			Mix6: Reference mix + 3%SP:		Mix7: Reference mix - 3%SP:	
±0 % c; ± 0 % w; ± 0% sp			±0% c; ±0% w; +3% sp		±0% c; ± 0% w; -3% sp	
Slump D $_{final}$= 60cm Flow time: 8.4sec			Slump D $_{final}$= 68cm Flow time: 6.9sec		Slump D $_{final}$= 45cm Flow time: 10sec	
beam	Fiber	fiber	Fiber	fiber	Fiber	fiber
section	Weights	conc.	Weights	conc.	Weights	conc.
(cm)	(g)	(Kg/m^3)	(g)	(Kg/m^3)	(g)	(Kg/m^3)
8.3	57	37.92	50	33.2668	72	47.90
25	73	48.57	71	47.2389	77	51.23
41.7	65	43.25	75	49.9002	86	57.22
58.4	77	51.23	82	54.5576	73	48.57
75.1	72	47.90	91	60.5456	85	56.55
91.8	73	48.57	68	45.2428	81	53.89
108.5	76	50.57	68	45.2428	78	51.90
125.2	50	33.27	78	51.8962	77	51.23
141.9	66	43.91	65	43.2468	76	50.57
	AVG	45.02	AVG	47.9042	AVG	52.12
	STN. DEV	6.08	STN. DEV	7.7018	STN. DEV	3.23
	Stn.Dev/Avg	0.14	Stn.Dev/Avg	0.1608	Stn.Dev/Avg	0.06

73

Figure 4.7c plot of the fiber distribution along the flow of SCSFRC
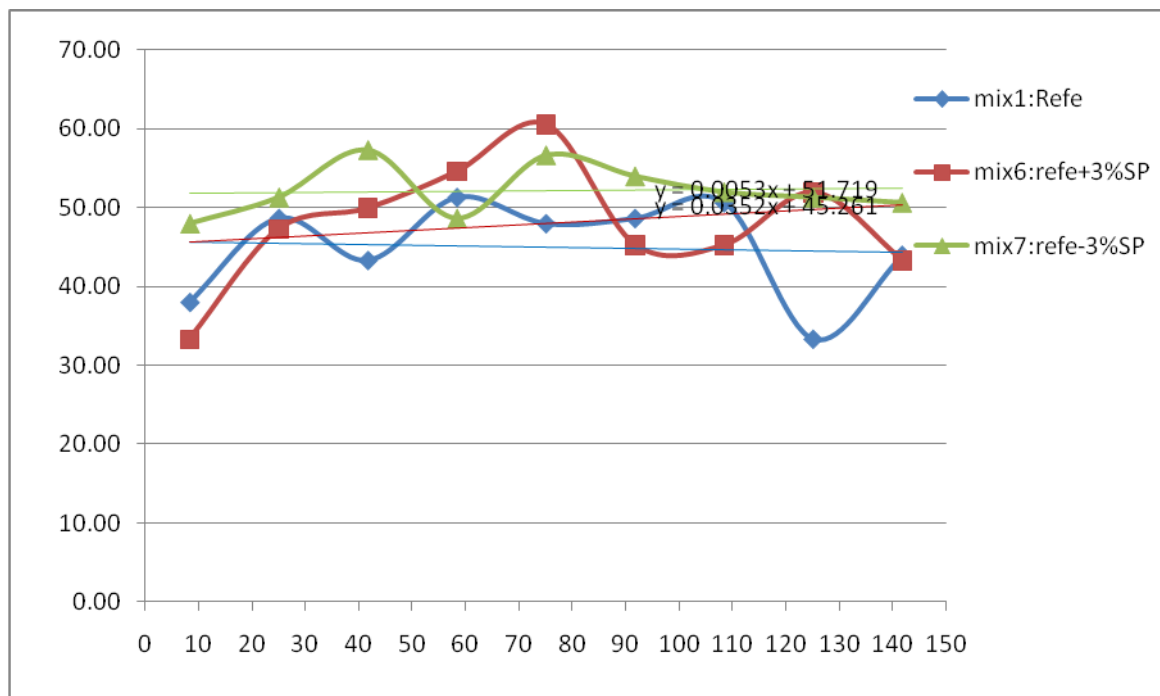
Fiber segregation index (FSI)

The fiber distributions along the SCSFRC flow directions depends on the fresh characteristics which on its hand a functions mix design. For the above seven different mixes of SCSFRC the fiber concentrations are computed in the nine sections of beam samples as shown on the above figures.

The fiber segregations index mathematically computed as the slope of the trend line of fiber concentration along the SCSFRC flow,

Table 4.7 fiber distribution along SCSFRC flow- fiber segregation index (FSI),

Mix no.,	Fiber segregation index	FSI kg/m³/m
mix1	Slope of the trend line	-0.01
mix2	Slope of the trend line	0.1899
mix3	Slope of the trend line	-0.0242
mix4	Slope of the trend line	-0.0027
mix5	Slope of the trend line	-0.0359
mix6	Slope of the trend line	0.0352
mix7	Slope of the trend line	0.0053

Note: mix number 2 of SCSFRC, i.e. with more water, had relatively higher fiber segregation due to higher concentrations difference along the its section i.e. higher slope of FSI.

4.4.1.3 Fiber dynamic distribution: free flow

The ability of the free flowing SCSFRC mixture to distribute the fiber uniformly on the horizontal plate of Abrahams cone is determined as follows.

Table 4.8a: Mix 1and mix2

sectional	Mix1: Reference mix			Mix2: Reference mix + 5%w		
Diameter	fiber, g	Vol., dm^3	Con., g/dm^3	fiber, g	Vol., dm^3	Con., g/dm^3
>50 cm	50	0.8412	59.436	82	2.445	33.540
20 cm- 50 cm	146	3.6454	40.050	119	2.463	48.322
< 20 cm	50	1.0084	49.586	57	0.587	97.025
		Avg	49.691		Avg	59.629
		Stn.Dev	9.693		Stn.Dev	33.219

Table 4.8b: Mix4 and mix5

Sectional	Mix4: Reference mix + 2%c			Mix5: Reference mix - 2%c		
Diameter	fiber, g	Vol., dm^3	Con., g/dm^3	fiber, g	Vol., dm^3	Con., g/dm^3
>50 cm	29	0.451	64.328	33	1.034	31.918
20 cm- 50 cm	170	3.899	43.603	160	3.512	45.554
< 20 cm	58	1.145	50.638	63	0.949	66.401
		Avg	52.856		Avg	47.958
		Stn.Dev	10.539		Stn.Dev	17.367

Table 4.8c: Mix6 and mix7

Sectional	Mix6: Reference mix + 3%sp			Mix7: Reference mix - 3%sp		
Diameter	fiber, g	Vol.,dm^3	Con.,g/dm^3	fiber, g	Vol.,dm^3	Con.,g/dm^3
>50 cm	47	1.574	29.865	0	0	0
20 cm- 50 cm	139	3.123	44.511	148	3.792	39.026
< 20 cm	54	0.798	67.635	109	1.703	64.018
		Avg	47.337		Avg	51.522
		Stn.Dev	19.043		Stn.Dev	17.672

Note:

The concentrations of the fibers are in g/dm^3 which is equivalent to kg/m^3.

The fiber segregations are shown in the following in the following graphs. When the slope of the fiber concentrations along the flow i.e. trend line from the graph is near to horizontal, the fiber distributions were more uniform.

Figure 4.8a: dynamic segregation for the for mix 1 and 2
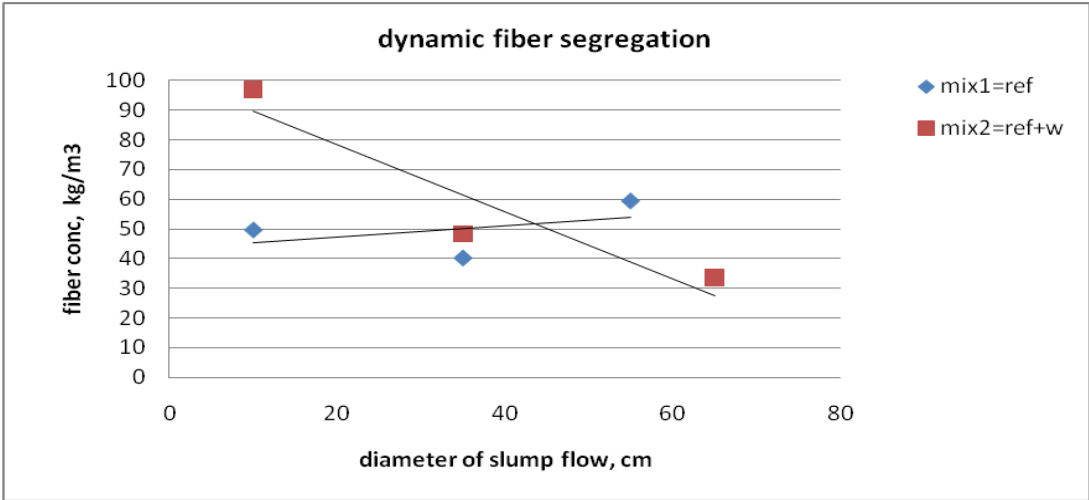
Figure 4.8b: dynamic segregation for the for mix 1 + 4 + 5
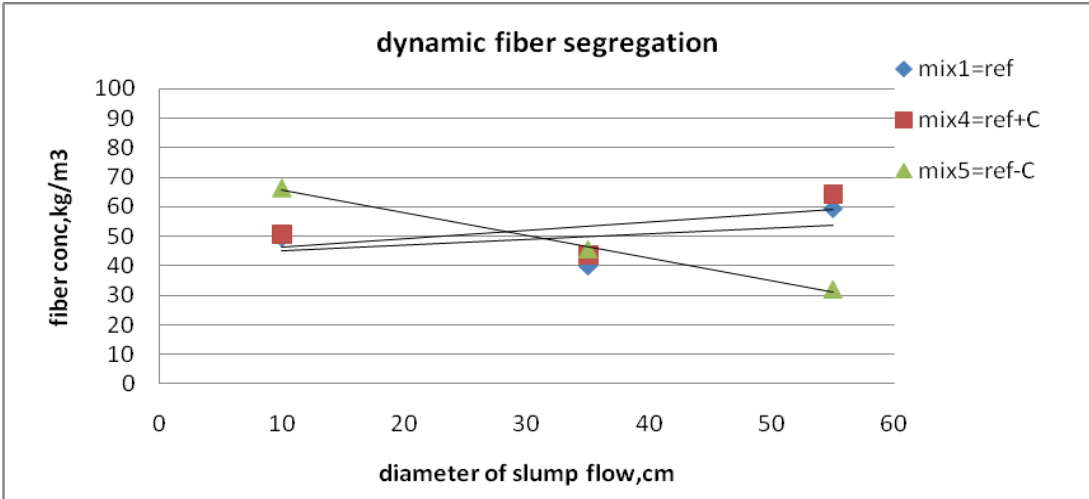
Figure 4.8c: dynamic segregation for the for mix 1 + 6 + 7
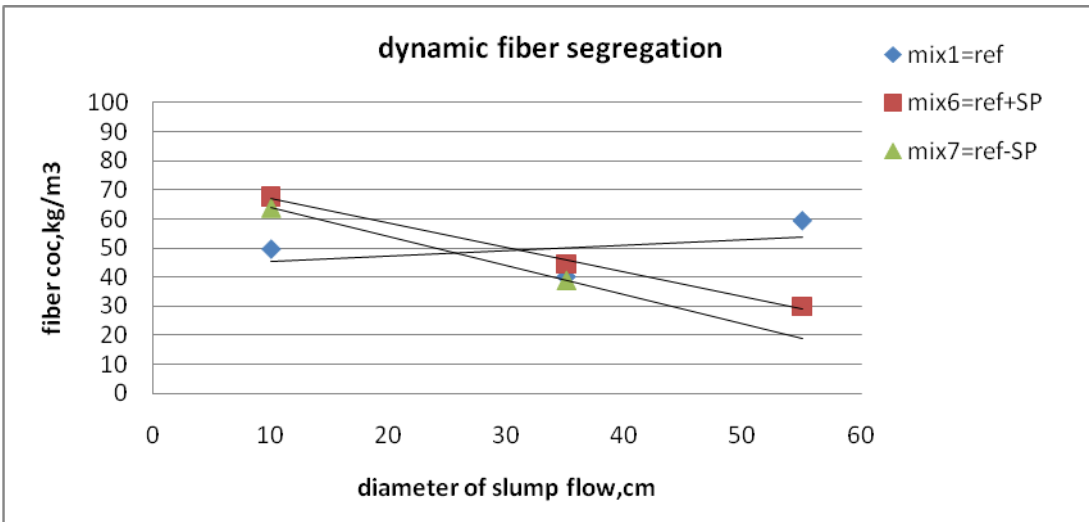
Note: the fiber distribution along te diameter section can be estimated from the slope of the straight line joining the concentrations of each specimen.

Fiber segregation index (FSI)

Dynamic segregation along the radial flow direction has been computed as the slope of the trend obtained from experimental data.

Table 4.9 slope of the trend life for FSI

mix no.,	Fiber segregation index	FSI kg/m^3/m
mix1	Slope of the trend line	0.1943
mix2	Slope of the trend line	-1.1325
mix3	-	-
mix4	Slope of the trend line	0.2802
mix5	Slope of the trend line	-0.7691
mix6	Slope of the trend line	-0.8429
mix7	Slope of the trend line	-0.9997

Note: the fiber segregation index is very high in the case of mix2 which means there were significant variation in concentrations along the flow. The mix 2 of SCSFRC has 5% more water content to mix1.

4.5 Fiber dispersions and orientations in the hardened state

4.5.1 Magnetic probe test: non-destructive measurement

The magnetic test was performed on the hardened beam specimen of SCSFRC for estimating the steel fiber concentrations and orientations. this is non-destructive methods performed on the hardened specimen.

4.5.1.1 Beams

Fiber concentrations- the fiber concentrations are directly proportional to the measurement of the inductance from the magnetic circuit. For each beam length, the test was performed on the nine equal section of a beam numbered from 1 to 9. The following are the plot of inductance vs the section of beam.

Figure 4.9: The sections of the beam and flow of SCSFRC.
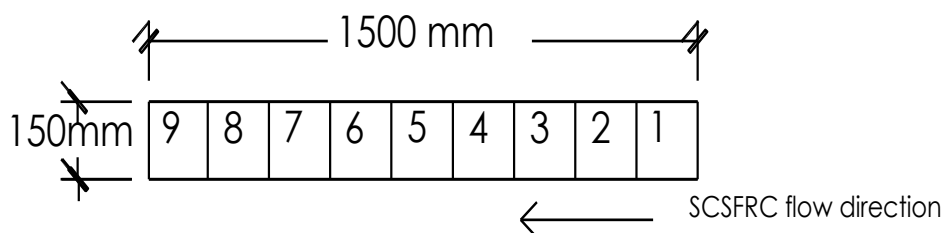
4.5.1.1.1 Fiber concentrations: the measured concentrations my the magnetic probe test as function of the measured inductance were shown below.

Figure 4.10a: Plot of mean inductance for mix1, mix2, mix3
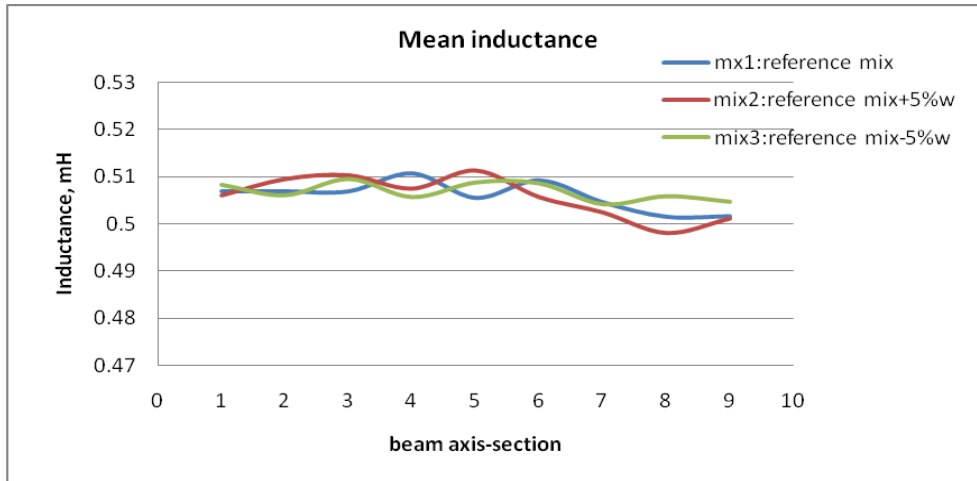
Figure 4.10b: Plot of mean inductance for mix1, mix4, mix5
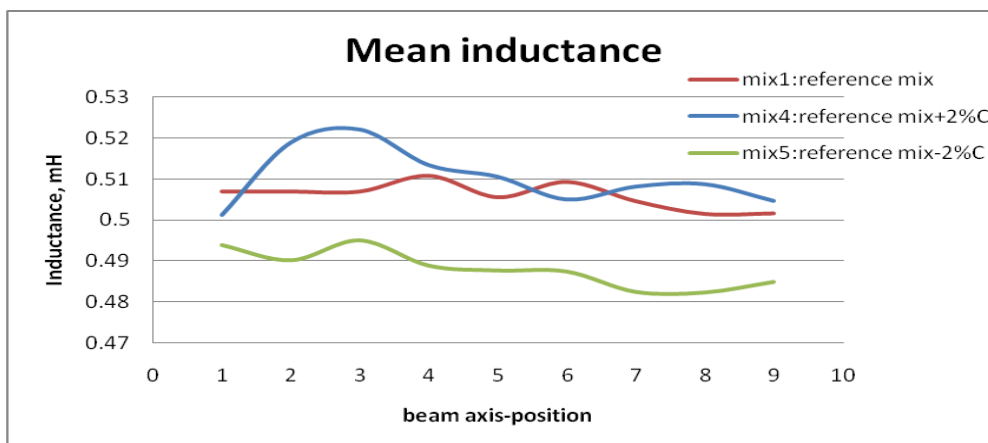
Figure 4.10c: Plot of mean inductance for mix1, mix6, mix7
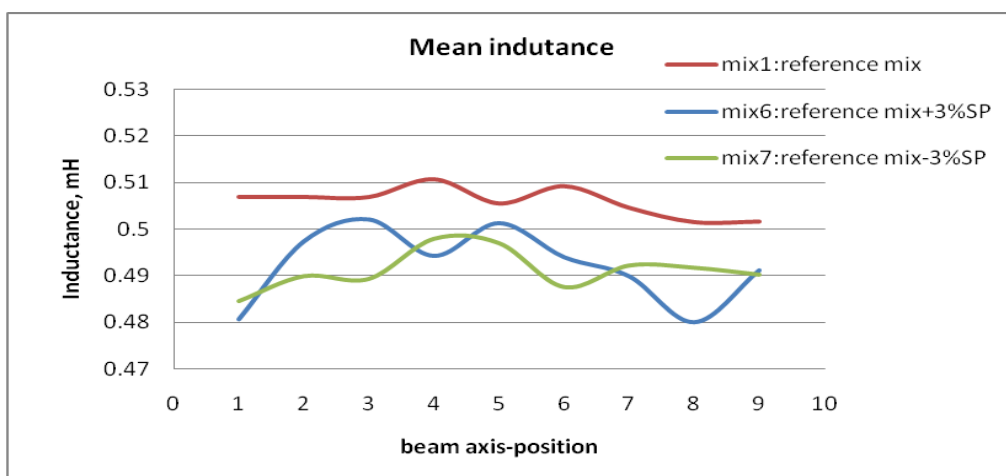
4.5.1.1.2 Fiber orientation: the magnetic test was performed in four direction, i.e EW (East west), NE (North east), NS (North south), NW (North west) on top and bottom surface of the beam specimen and the average plot values are the following.

Figure 4.11: plot of inductance with direction NS, EW, NE, NW.

Mix1:   ±0 % c; ± 0% w; ± 0% sp   Mix2:   ±0 % c; +5% w; ± 0% sp
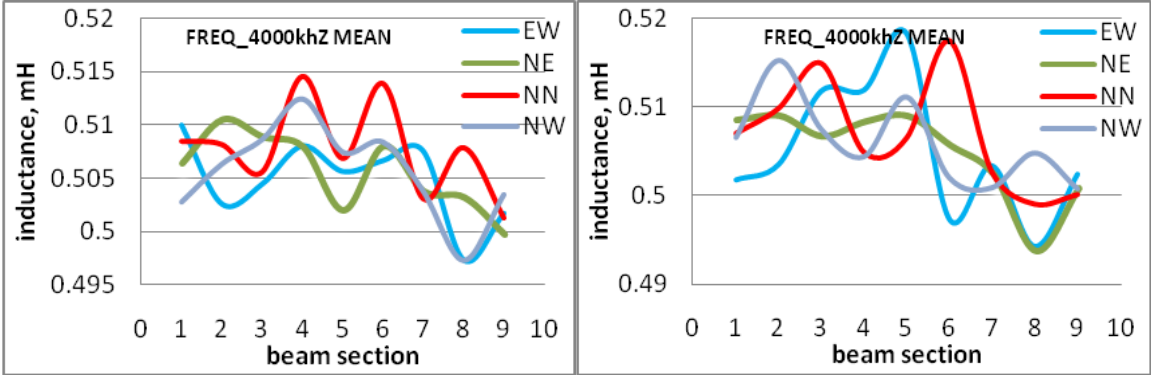
Mix3:   ±0 % c; -5% w; ± 0 %sp   Mix4:   +2 % c; ± 0% w; ± 0 %sp
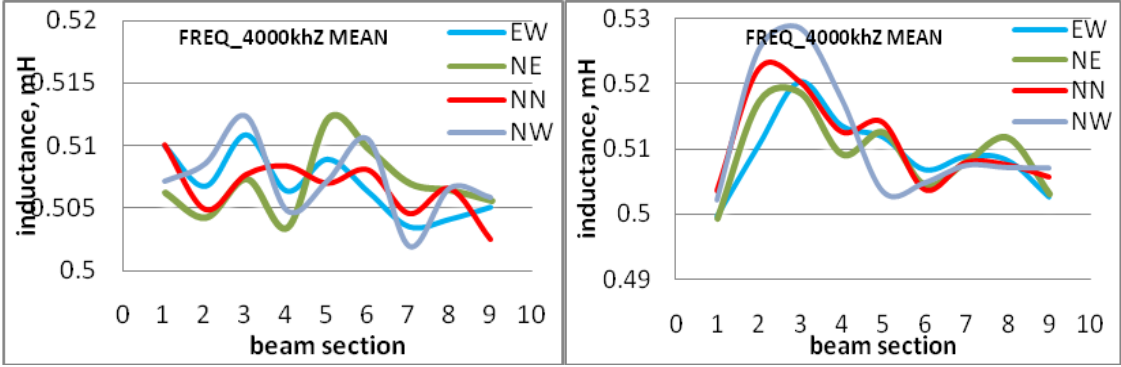
Mix5:   -2 % c; ± 0% w; ± 0% sp   Mix6:   ±0 % c; ± 0% w; +3% sp
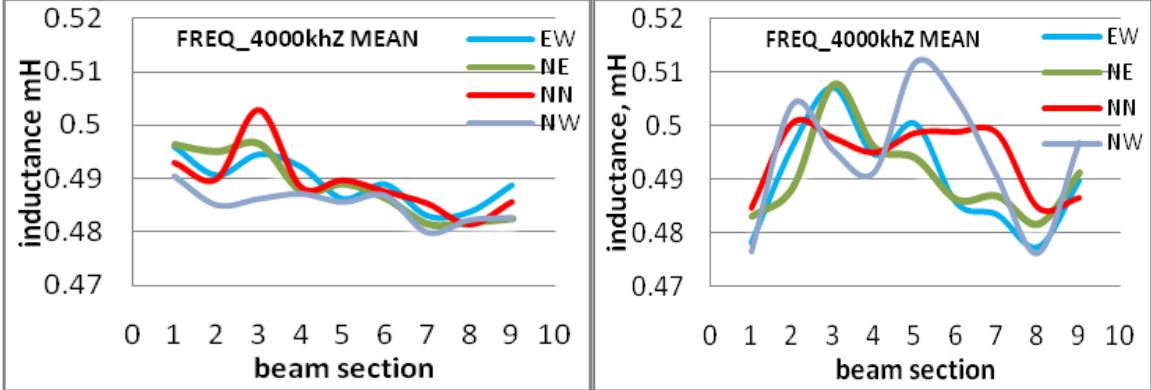
Mix7:   ±0 % c; ± 0% w; -3% sp
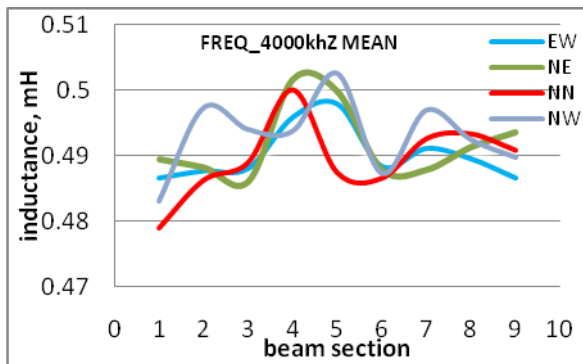
Table 4.10: fibers orientations in the beam specimens,

Section	BEAM1	BEAM2	BEAM3	BEAM4	BEAM5	BEAM6	BEAM7
1	→	↙	↓	↓	↙	→	↙
2	↙	↘	↘	↘	↙	↘	↘
3	↙	↓	↘	↘	↓	↙	↘
4	↓	→	↓	↘	→	↙	↙
5	↘	→	↙	↓	↓	↘	↘
6	↓	↓	↘	→	→	↘	→
7	→	→	↙	→	↓	↓	↘
8	↓	↘	↘	↙	→	↓	↓
9	↘	→	↘	↘	→	→	↙

The direction with highest magnitude of the inductance was marked,

Note: Assumed direction,

NS	NE	EW	NW
↓	↙	→	↘

The fibers were generally oriented in direction of flow with more common NS, NW, NE and less common EW as shown in the table 4.10.

The fibers in mix2 are more random than mix 3 in orientation. This seems to be the higher amount of water in mix2 results in the more viscous mix. In mix3 the concrete is more stiffer and tends to orients the fibers concentrations.

In addition, the fibers in mix4 is more oriented than in mix 5 which seems also related to the more amount of cement content in mix4.

80

4.5.1.2 Cylinders

The test was performed on the cylinder in the hardened state as shown below. The test was performed three sections of the cylinder as follows: top section, mid-section, middle section.

Figure 4.13: cylindrical samples with magnetic probe.

The values of measured inductance were written in table 4.11.

Table 4.11 the measure inductance along the cylinder specimen.

Cylinders, section	Level,m	mix1	mix2	mix3	mix4	mix5	mix6	mix7
top	1	20	0.498977	0.4922	0.496999	0.498849	0.49837	0.49846	0.498475
middle	2	12	0.49992	0.4935	0.49763	0.499375	0.49791	0.497999	0.498248
bottom	3	3	0.49756	0.4943	0.497065	0.500609	0.50075	0.498948	0.497365

Figure 4.14a Measured inductance along the cylinder axis,
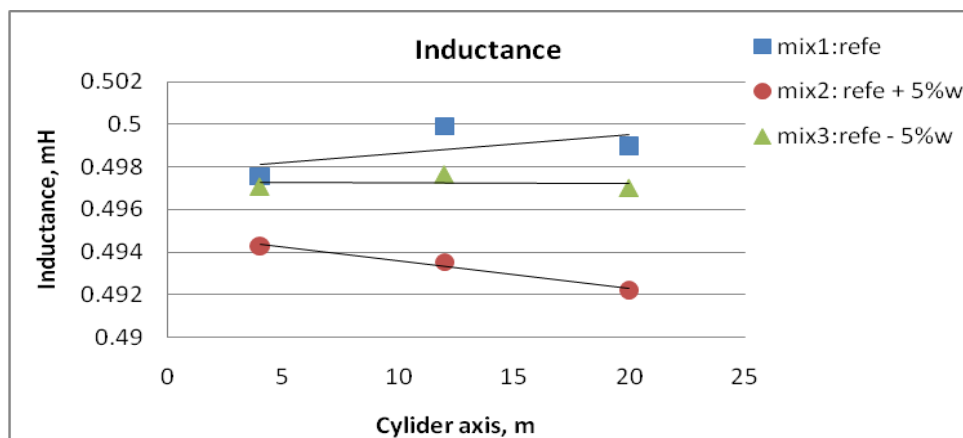
Note: the mix numer 2 has more fiber segregation from measured inductance. The correlations between measured inductance and actual concentrations has been explained in chapter 3.

Figure 4.14b Measured inductance along the cylinder axis,
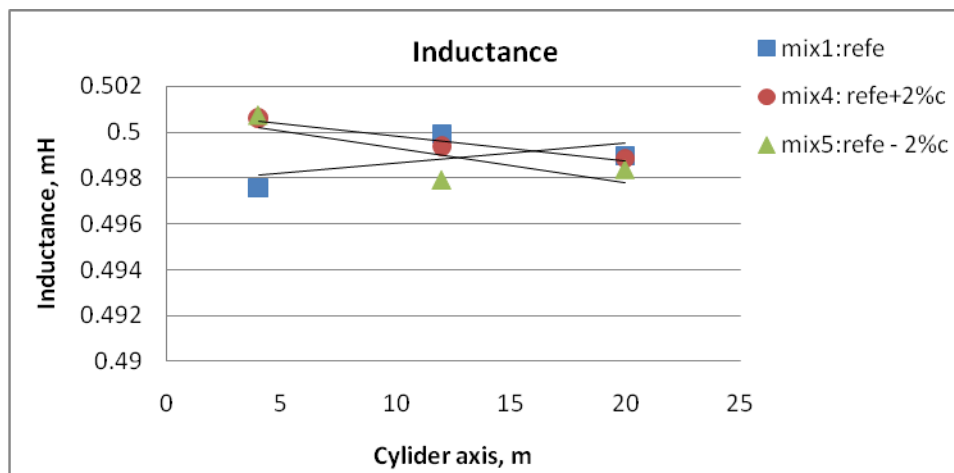
Figure 4.14c Measured inductance along the cylinder axis,
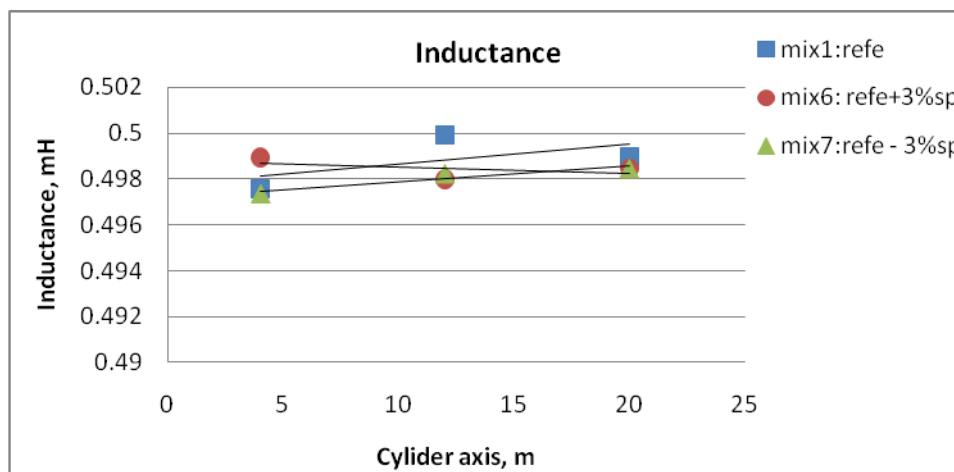
Note: the inclination of the trend line in the above plot means to be the fibers distribuiton along the channel.

4.5.2 Correlations of fiber concentrations and magnetic probe test

The actual fiber concentrations were measured in the beams and cylinder specimen either in fresh or hardened state. Correlations between the actual fiber concentration and corresponding measured inductance as measured by magnetic probe we shown in the following figures.

4.5.2.1 Crushing of cylinder specimen

In order to measure fiber concentrations along the length of the cylindrical specimen, the specimen was divided into three equal parts. Each parts was crushed with grinding machine hammer and the fibers were separated from the concrete rubble. The fibers were weighed for each part: top section, middle section and bottom section.

Figure 4.15: the steel fiber as crashed out of hardened concrete and collected in a can.

The weight of fibers from each part of cylinders were registered in the following tables 4.12 and the concentrations of the fiber is computed by dividing the weight of the steel fiber in each section of the cylinder specimen by the volume of the same section.

Table 4.12 : the measure weight of steel fiber out of all specimen.

Cylinder	section	mix1,g	mix2,g	mix3,g	mix4,g	mix5,g	mix6,g	mix7,g
top	1	17.8	8.4	13.82	14.92	18.62	17.52	20.07
middle	2	20.89	8.1	12.09	20.37	20.25	15.65	19.02
bottom	3	17.89	18.9	15.14	22.61	23.68	23.71	19.5

Table 4.13: Computed concentration of steel fiber of specimens.

Cylinder	section	Concentrations of steel fiber, kg/m3						
section	Level,cm	mix1	mix2	mix3	mix4	mix5	mix6	mix7
top	20	44.26	20.89	34.37	37.10	46.30	43.57	49.91
middle	12	51.95	20.14	30.07	50.66	50.36	38.92	47.30
bottom	4	44.49	47.00	37.65	56.23	58.89	58.96	48.49
	AVG	46.90	29.34	34.03	48.00	51.85	47.15	48.57
	StDev.	4.37	15.30	3.80	9.84	6.42	10.49	1.31

Figure 4.16a plot of the segregation along the horizontal cylinder axis
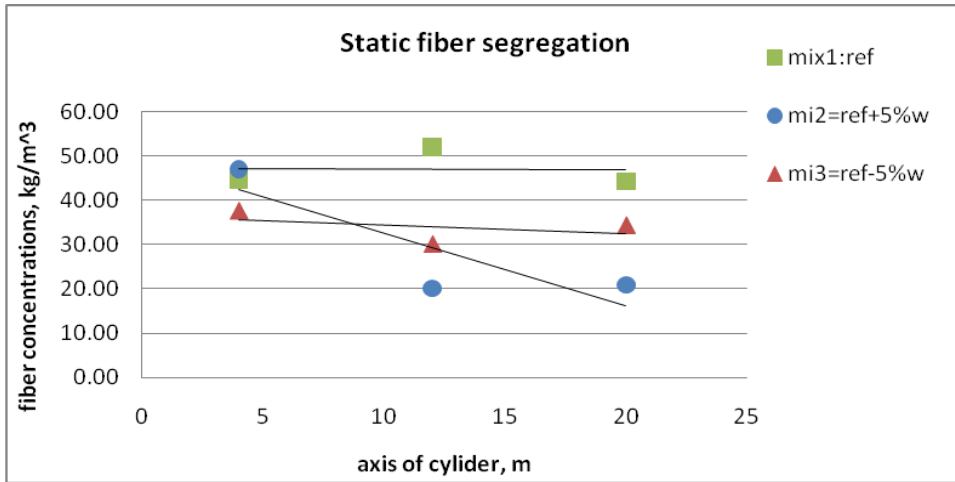
Figure 4.16b plot of the segregation along the horizontal cylinder axis
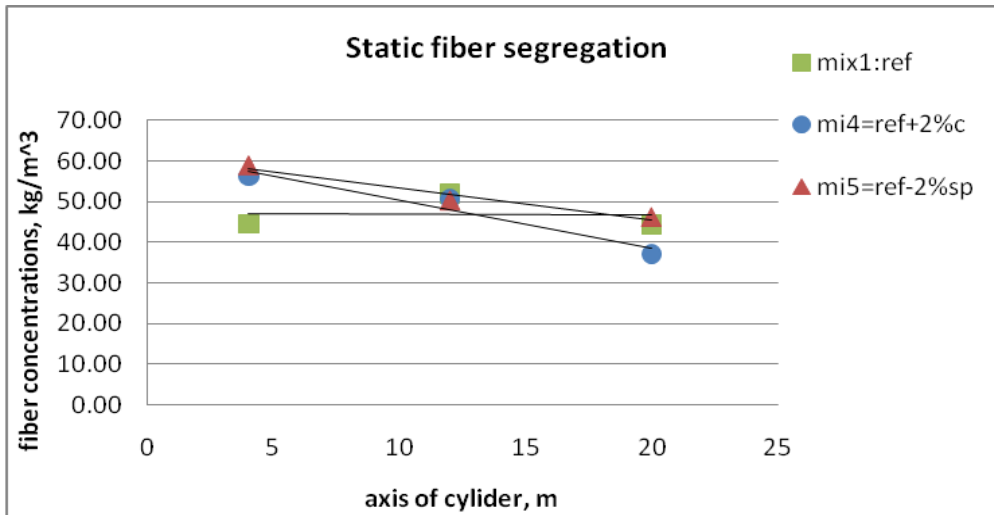
Figure 4.16c plot of the segregation along the horizontal cylinder axis

84
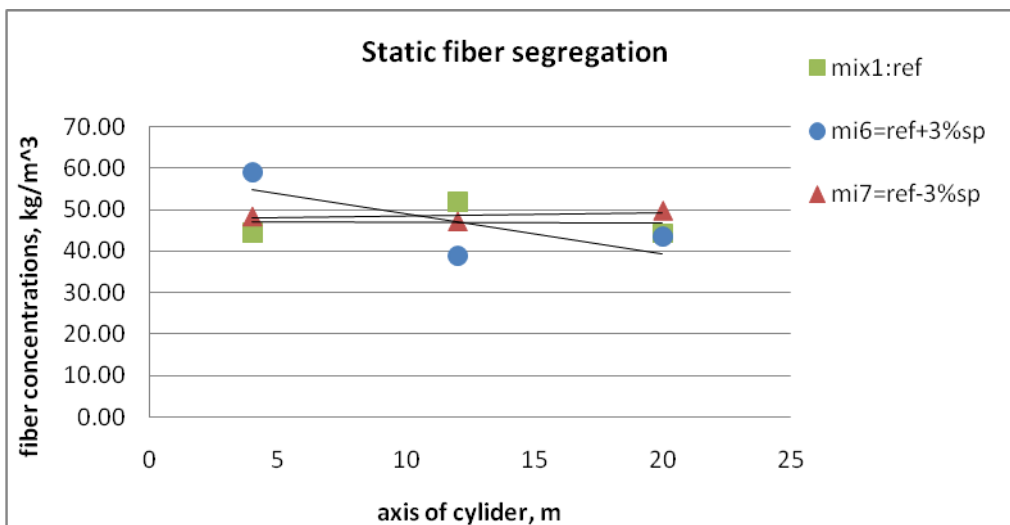
4.5.2.2 Static fiber segregation

The fiber distributions along the height of the cylinder from the top to the bottom. We have three section, top, middle, and bottom, each with 8cm high. the amount of steel fiber concentrations are computed in each section by crushing the specimens.

The static fiber segregations index (FSI) is mathematically computed as the slope of the trend line of fiber concentration along the specimen,

Table 4.14 calculations of static fiber segregation cylinder specimen

mix no.,	**Fiber segregation** index	**FSI** kg/m3/m
mix1	Slope of trend line	-0.014
mix2	Slope of trend line	-1.632
mix3	Slope of trend line	-0.2052
mix4	Slope of trend line	-1.1952
mix5	Slope of trend line	-0.7864
mix6	Slope of trend line	-0.9621
mix7	Slope of trend line	0.0886

Note: mix 2 of SCSFRC, i.e. with 5% more water, has more fiber segregation along the section which can be seen from the higher FSI slope.

4.5.2.3 Correlations of cylinder fiber concentrations

The actual fiber concentrations were measured in the beams and cylinder specimen either in fresh and hardened state. Correlations between the actual fiber concentration and corresponding inductance as measured by magnetic probe we shown in the following figures.

First, the correlation for the all the cylinders were developed. Figure 4.17a shows that measurement of all the inductance and actual concentrations of steel fibers for all specimen and 21 points were shown. The remaining figure shows the graph for individual cylinders separately. Here, the correlations was acceptable since we have had an overlap in the section while the measurement of the inductances were taken in contrast with the actual fiber concentrations.
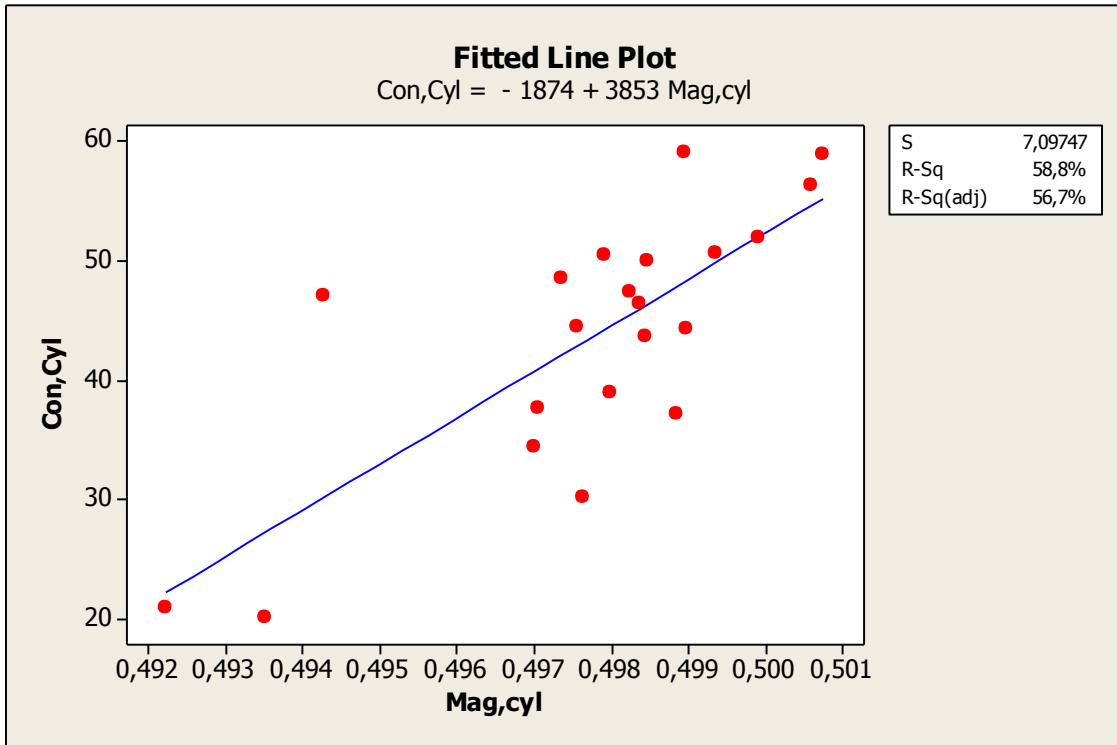
Figure 4.17a Correlations of the fiber concentrations and measured inductance for all cylinders.
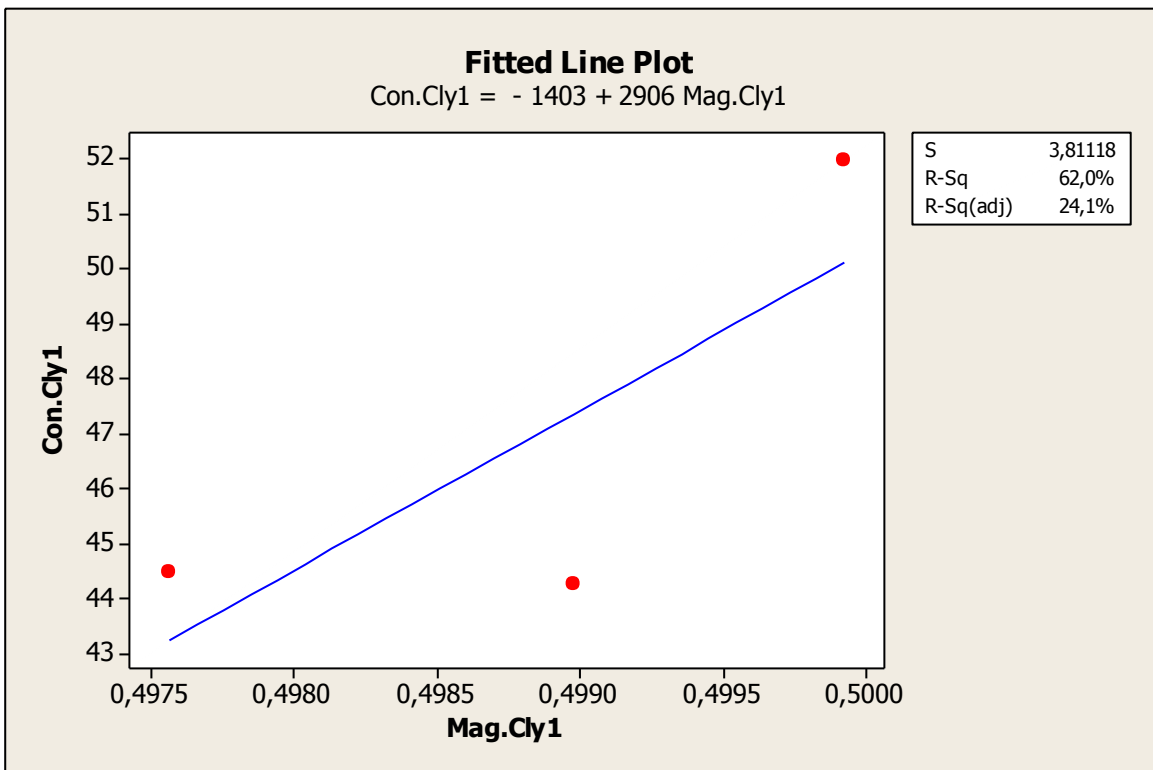

Figure 4.17b Correlations of the fiber concentrations and measured inductance for cylinder 1/ mix1.
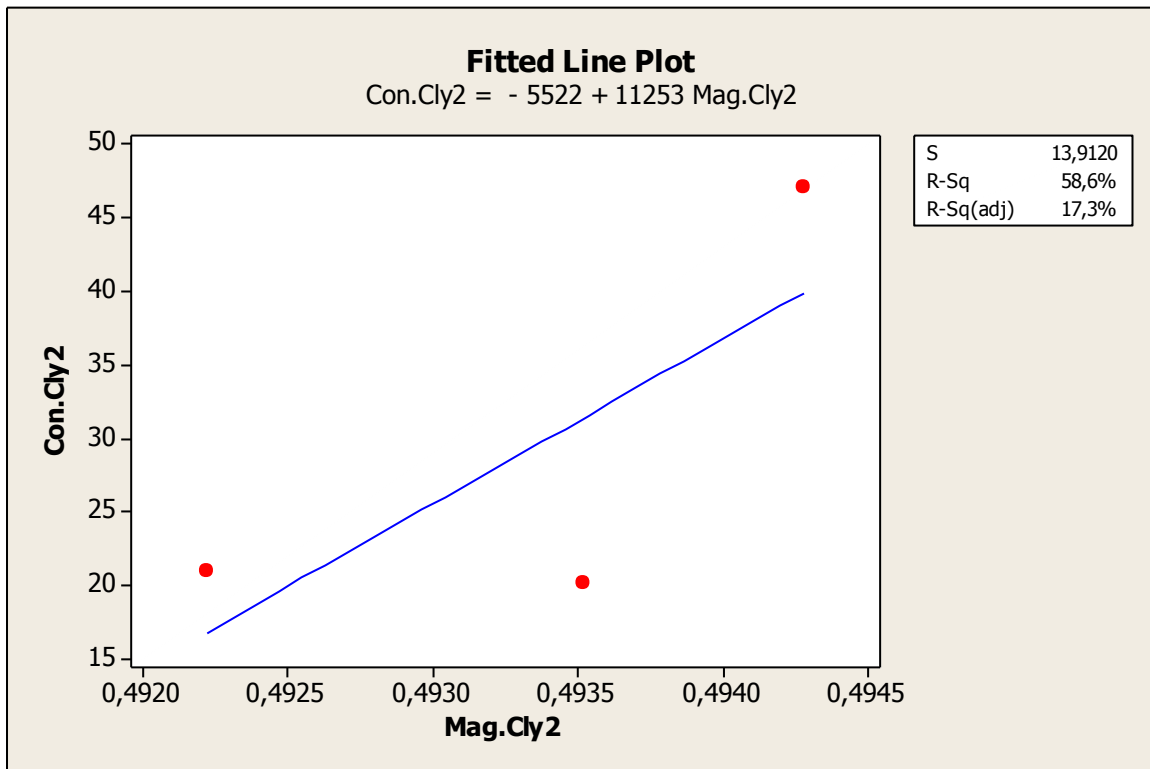
Figure 4.17c Correlations of the fiber concentrations and measured inductance for cylinder2/mix2.
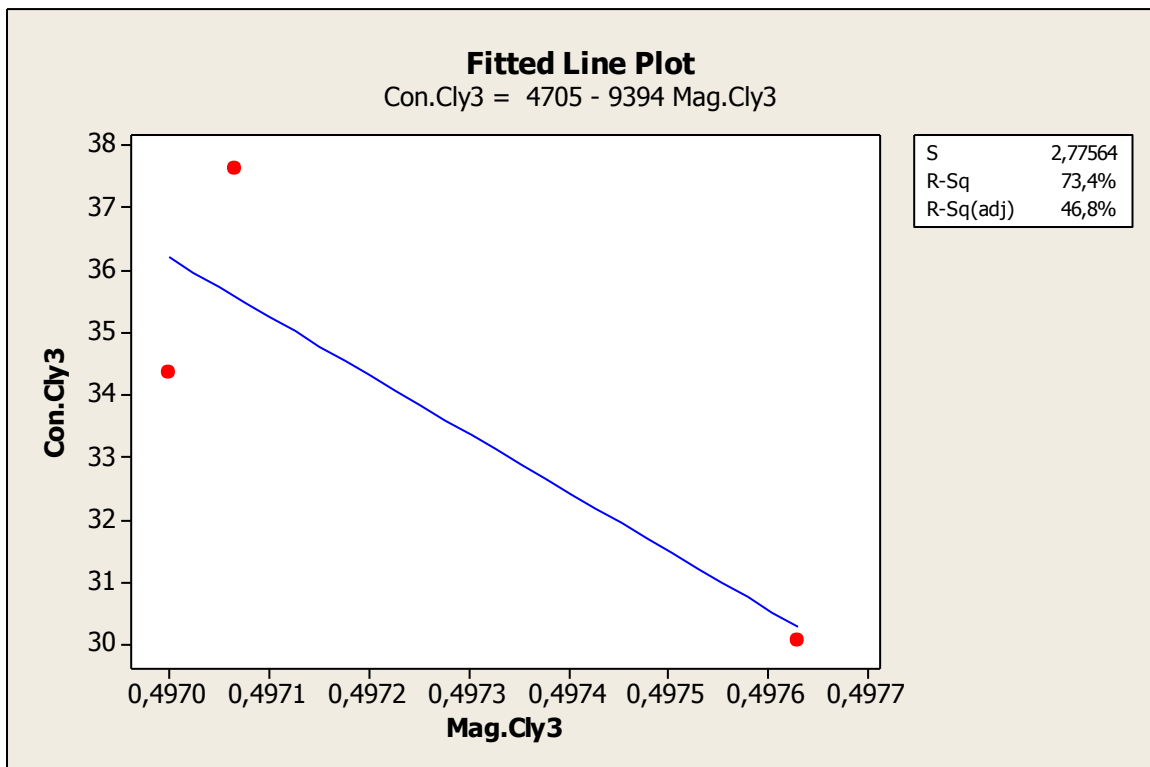

Figure 4.17d Correlations of the fiber concentrations and measured inductance for cylinder3/mix3.
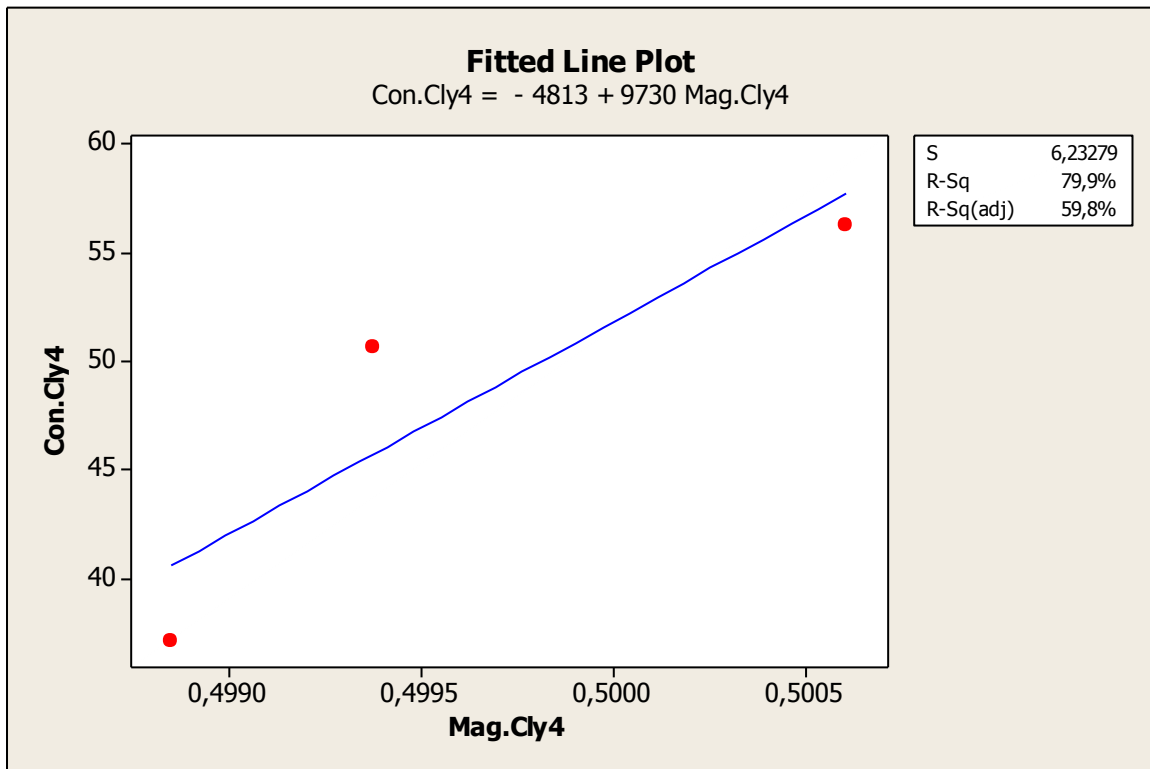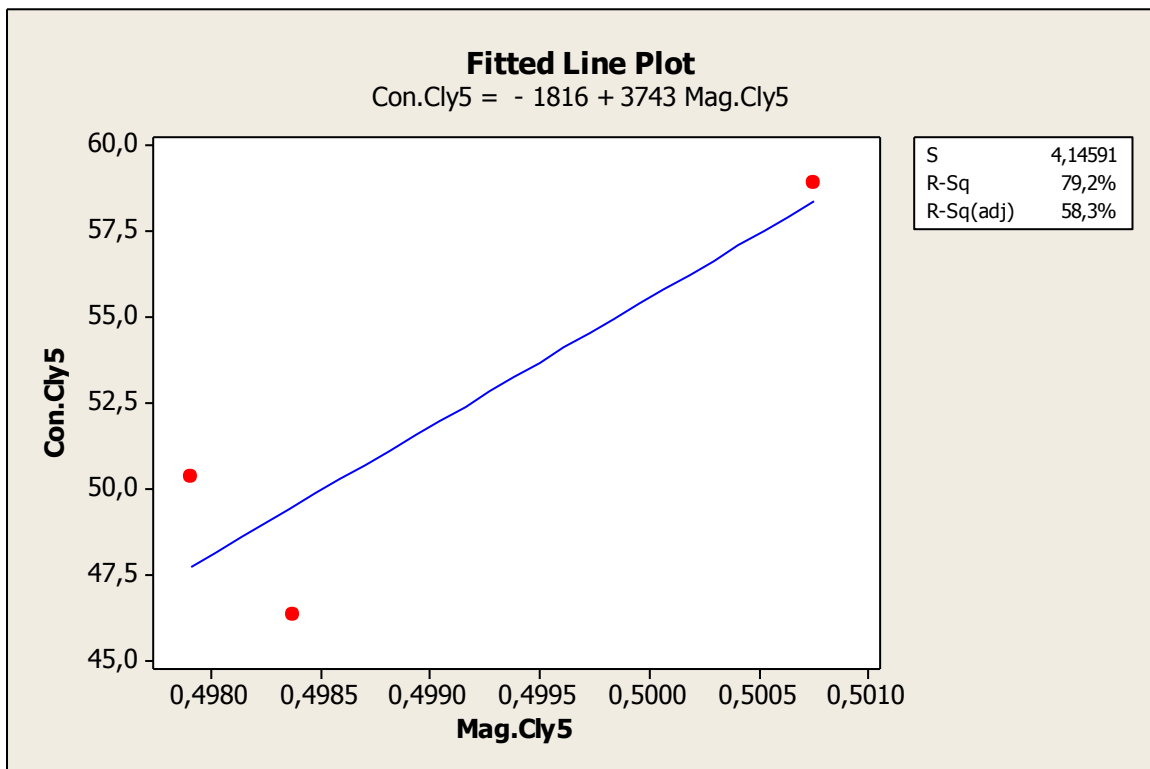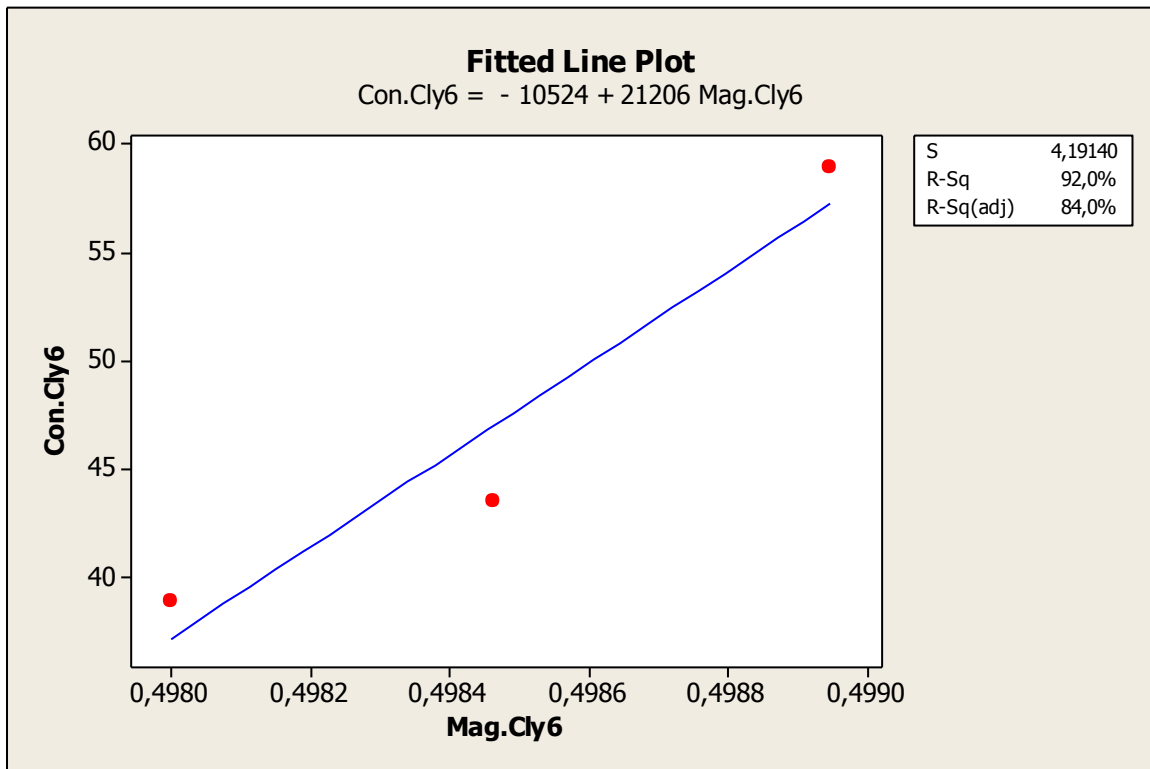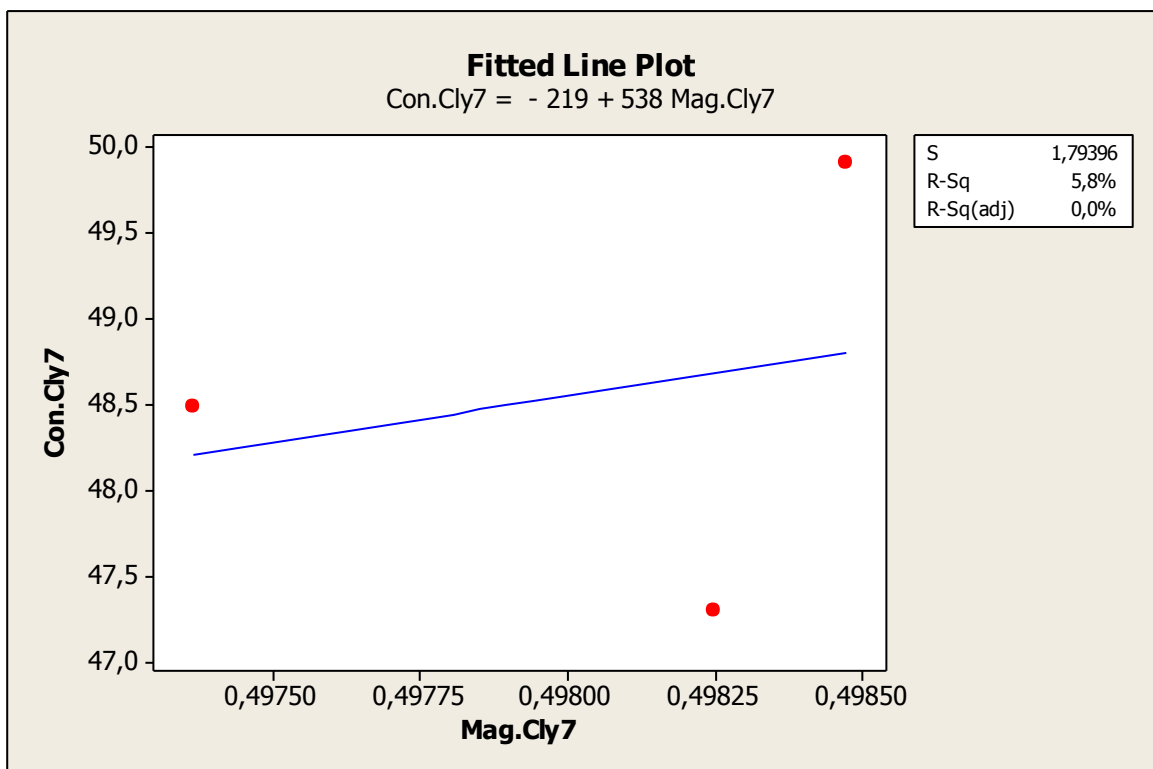
Figure 4.17e Correlations of the fiber concentrations and measured inductance for cylinder4/mix4.

Figure 4.17f Correlations of the fiber concentrations and measured inductance for cylinder5/mix5.

Figure 4.17g Correlations of the fiber concentrations and measured inductance for cylinder6/mix6.

Figure 4.17h Correlations of the fiber concentrations and measured inductance for cylinder7/mix7.

4.5.2.4 Correlations of beam fiber concentrations

The actual concentrations of fibers in hardened beam specimens were correlated to the measured inductance on equivalent specimen of same mix design as shown below.
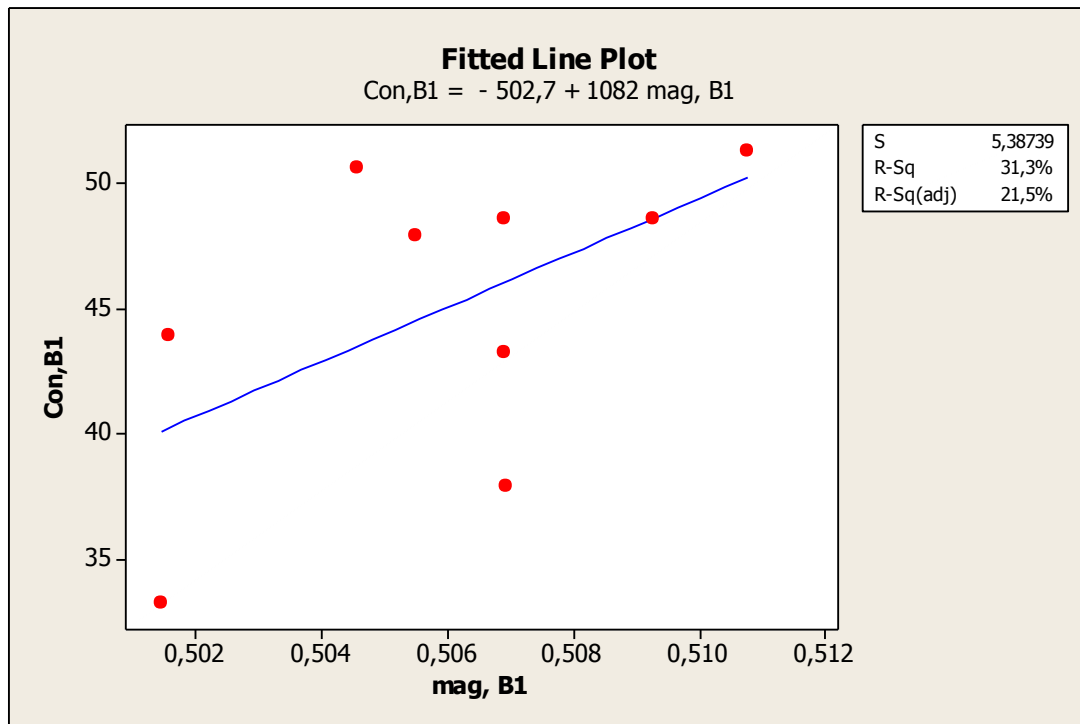

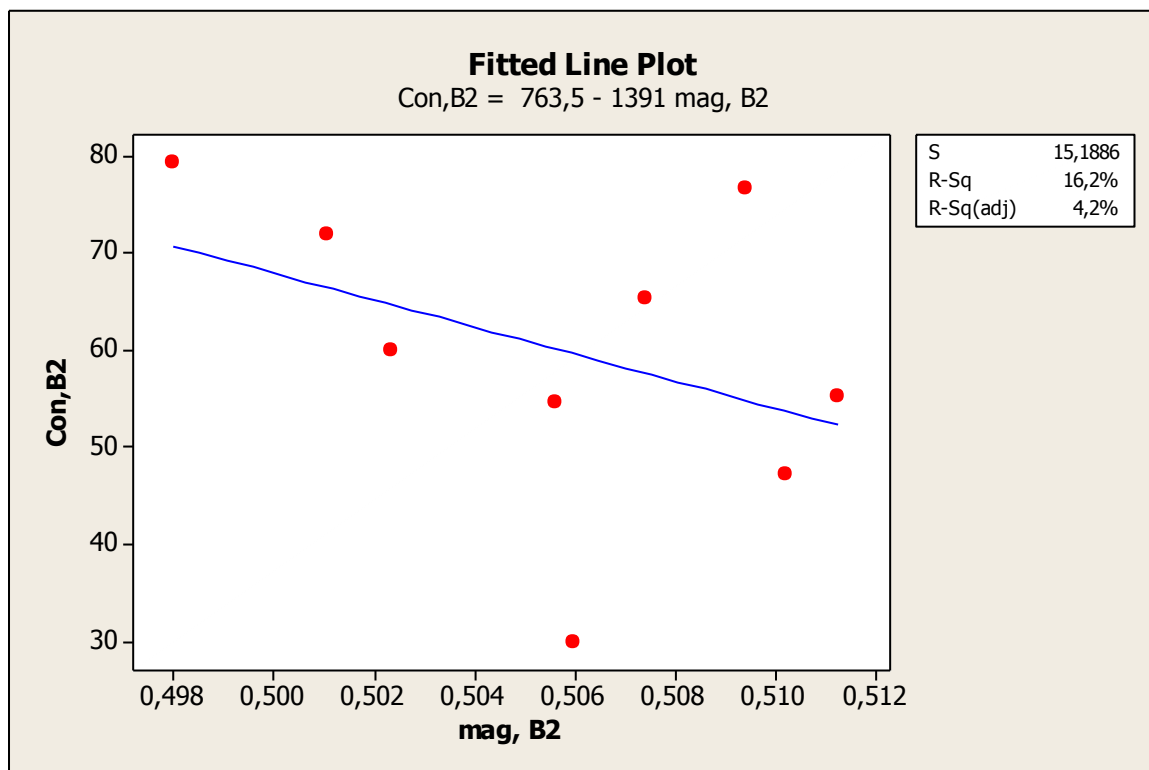Figure 4.18a Correlations of the fiber concentrations and measured inductance for beam1/mix1.

Figure 4.18b Correlations of the fiber concentrations and measured inductance for beam2/mix2.
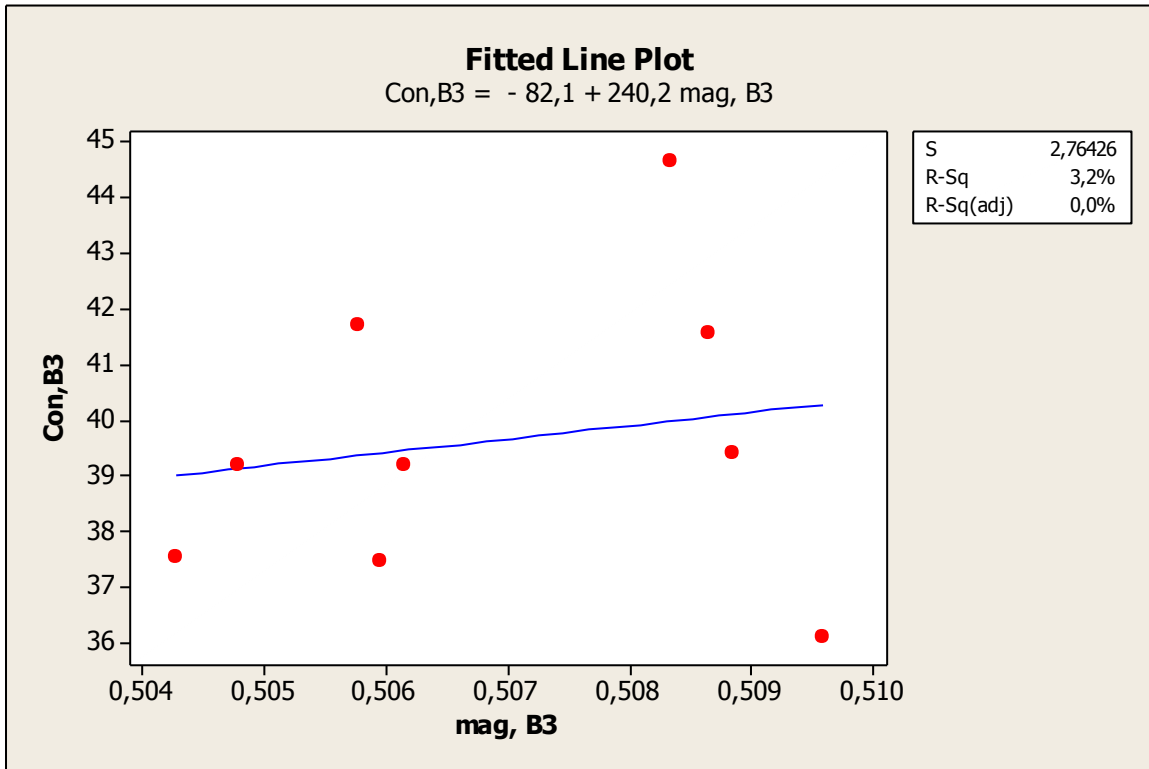
Figure 4.18c Correlations of the fiber concentrations and measured inductance for beam3/mix3.
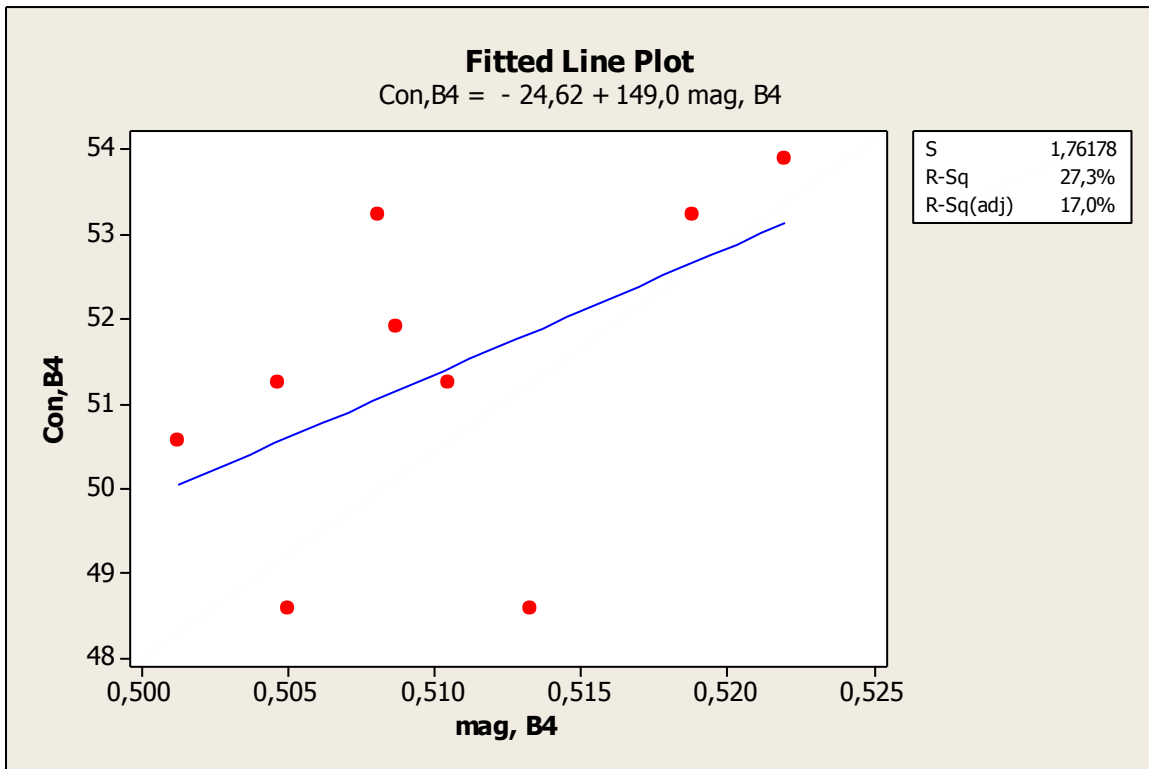

Figure 4.18d Correlations of the fiber concentrations and measured inductance for beam4/mix4.

Figure 4.18e Correlations of the fiber concentrations and measured inductance for beam5/mix5.

Figure 4.18f Correlations of the fiber concentrations and measured inductance for beam6/mix6.
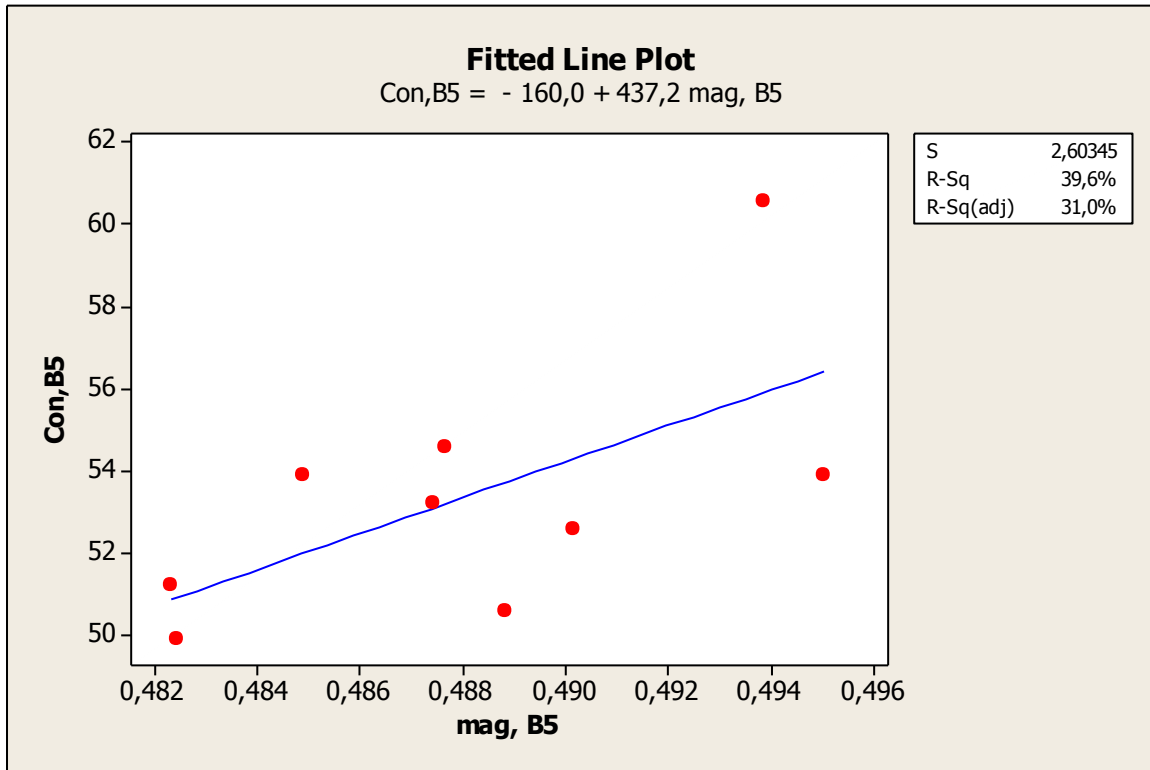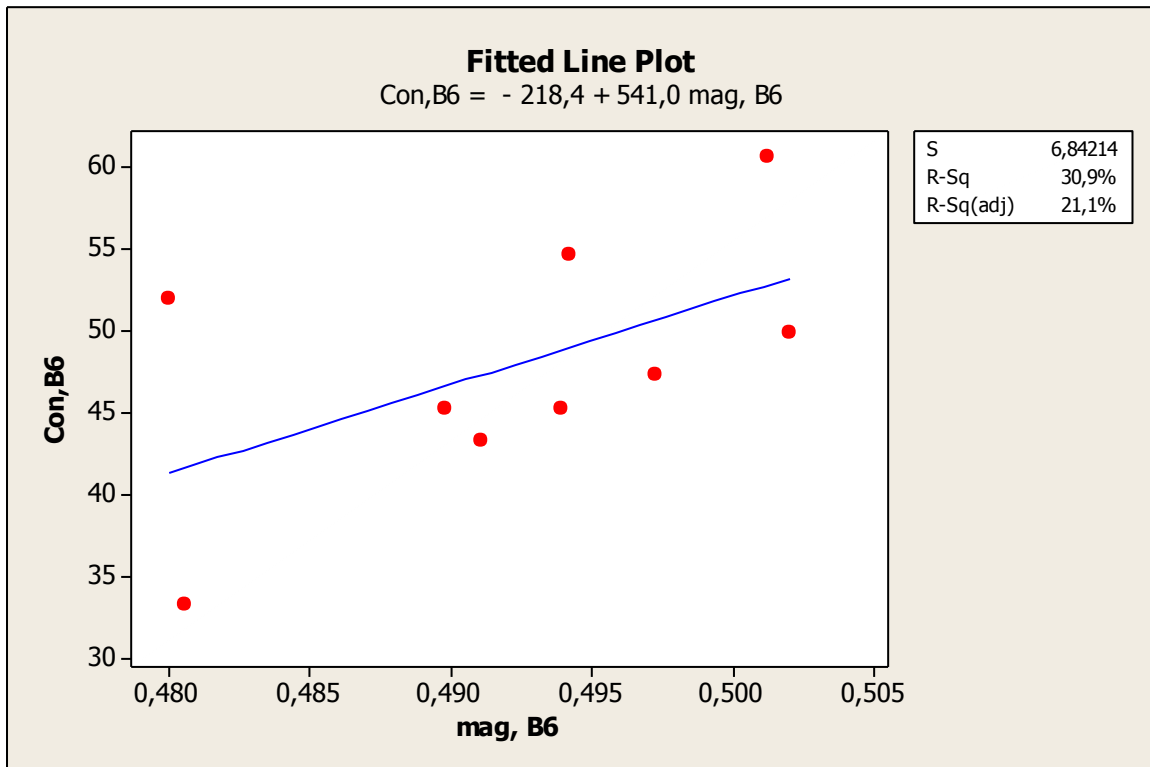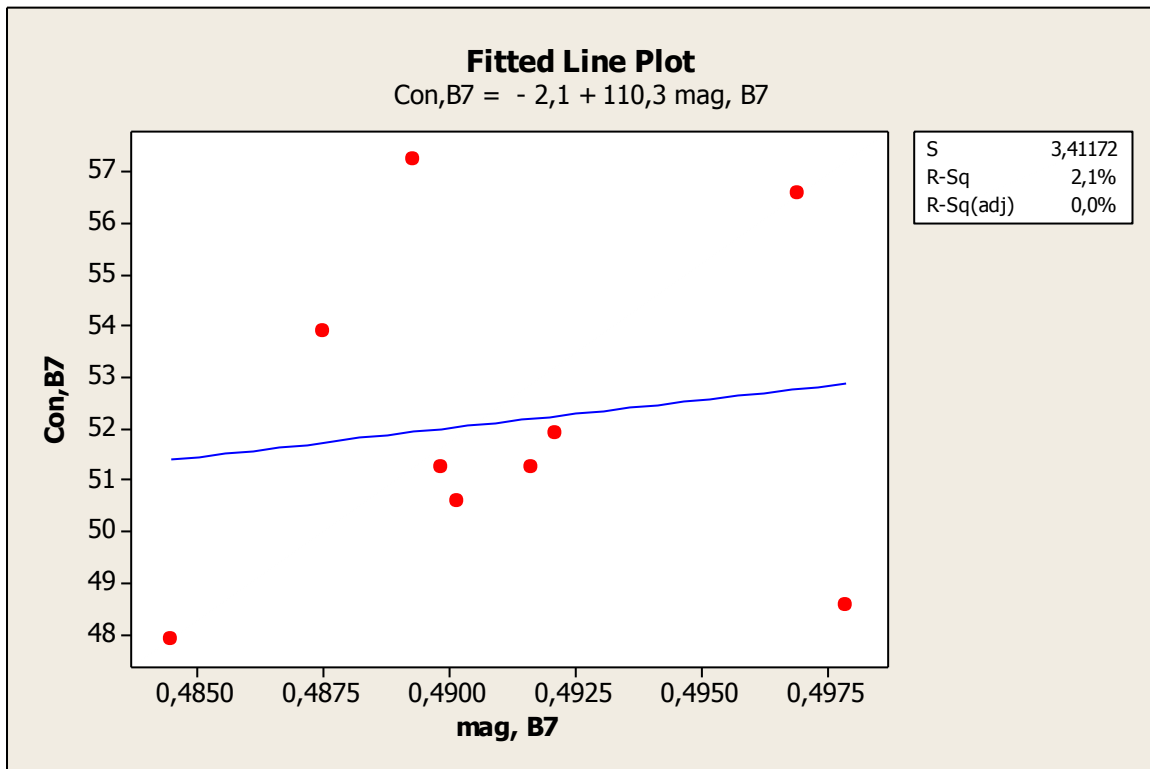
Figure 4.18g Correlations of the fiber concentrations and measured inductance for beam7/mix7.
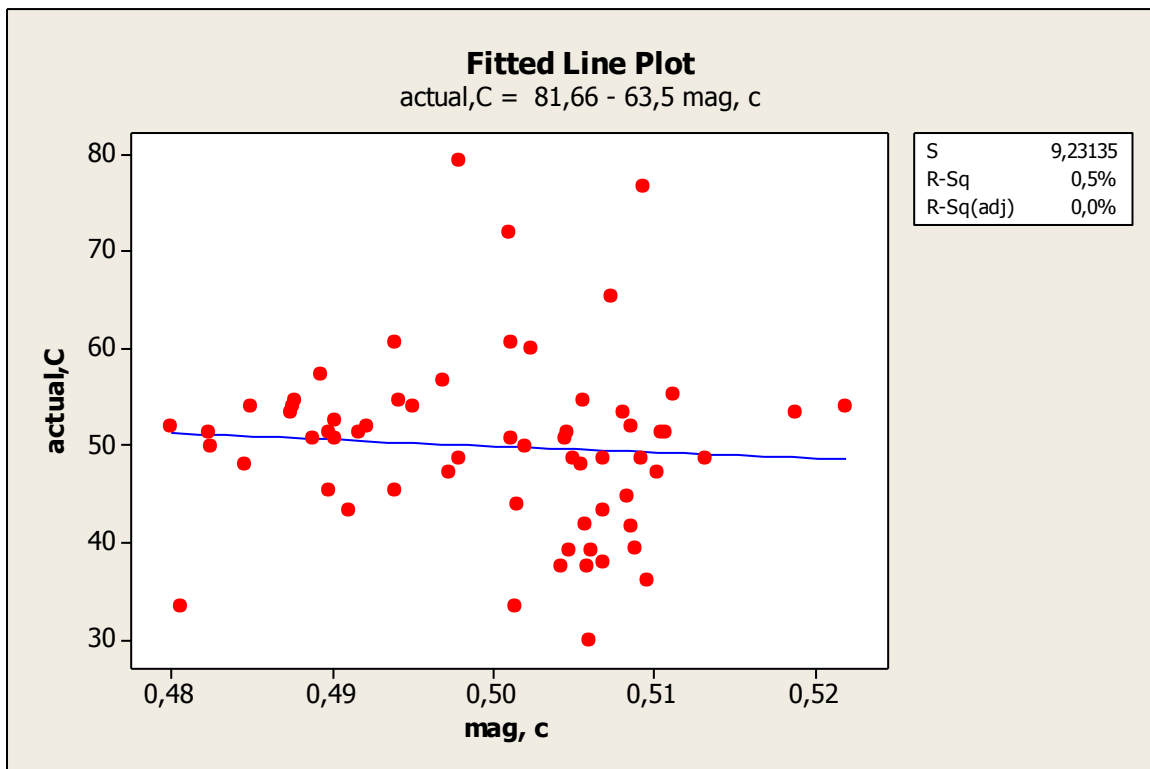

Figure 4.18e Correlations of the fiber concentrations and measured inductance for all beams..

4.6 Hardened state properties

The hardened state properties are determined from the tests conducted on the specimen casted from the fresh mixes. We have started with the non destructive magnetic test and perform mechanical destructive tests such as bending test and crushing test.

4.6.1 Results from the bending tests

The bending tests were performed on beam specimens obtained from longer 1500 mm beams as described in detail in previous chapter. The plots of nominal stress, $\sigma_N = \dfrac{P/2\,\ell}{bh^2/6}$ [with P total applied load, ℓ loading span, b and h beam width and depth] vs. Crack Opening Displacement (COD), measured across the constant bending moment region over a 200 mm gauge length are shown in the figure below. They clearly show to what extent the fibers were oriented by the fresh concrete flow and were able to affect the mechanical performance of the material.

The set up for the four bending test was shown in figure 4.16.

Figure 4.16 bending test set up,

. From the measured nominal stress vs. COD curve, besides the first cracking strength, the following post cracking equivalent stresses were computed.

➤ feq1, in the COD range 0.3mm-0.5mm;

➤ feq2, in the COD range 0.96mm-1.44mm; COD limits come from 0.02h +- 20% where h is the specimen depth (60 mm).

Mix 1: Reference mix: 0% c, 0% w, 0% sp.

Figure 4.17a, plot of nominal stress vs. COD

Mix2: Reference mix + 5%w   Mix3: reference mix – 5%w
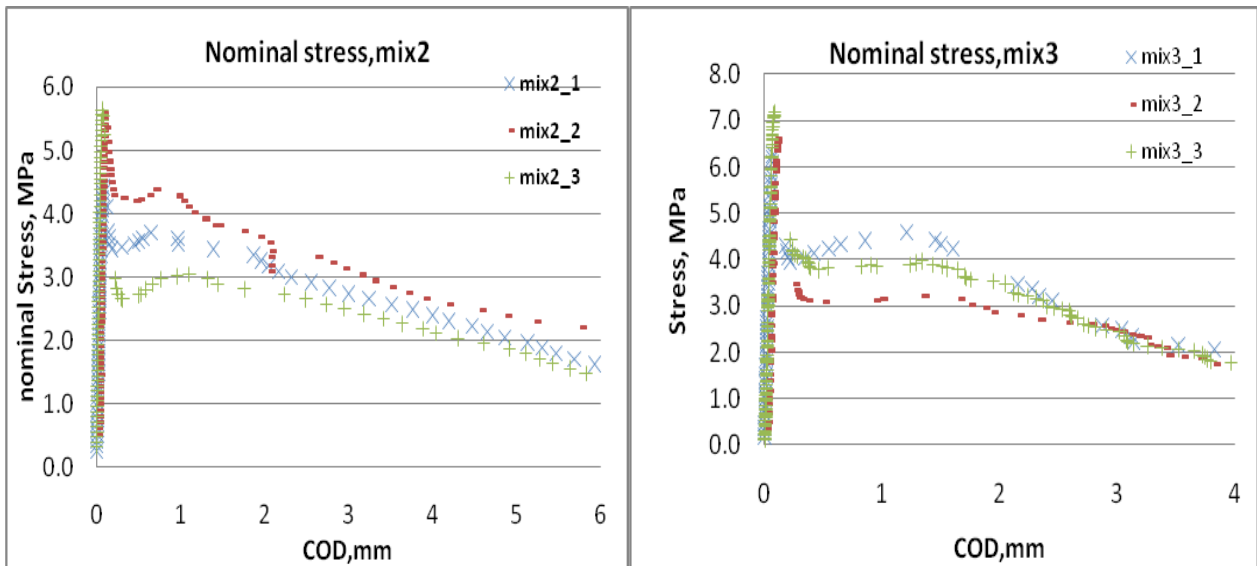
Figure 4.17b, plot of nominal stress vs. COD,

Note: mix3 has higher peak stress,

Mix4: reference mix + 2%c   Mix5: reference mix - 2%C,
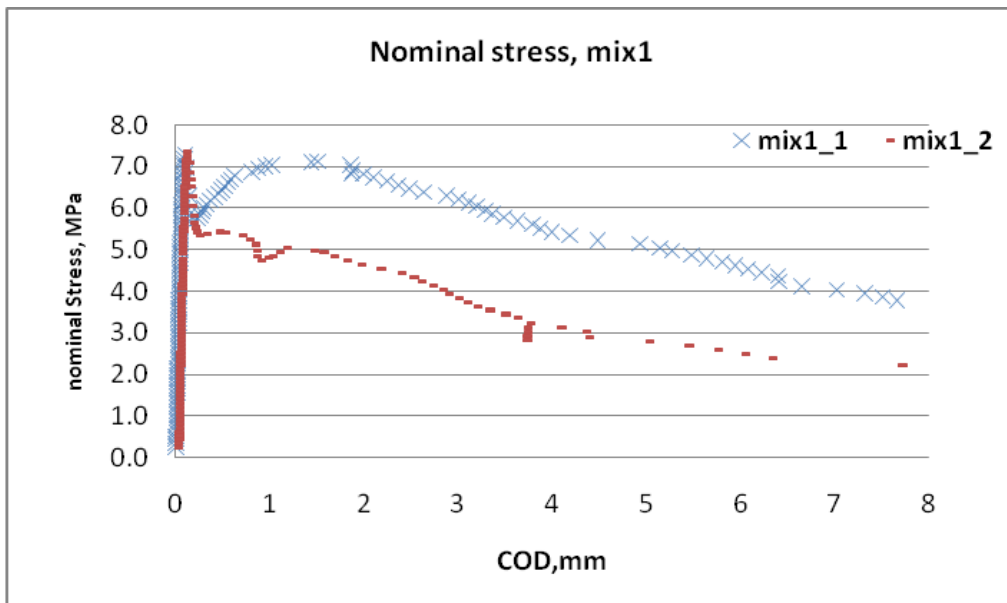

Figure 4.17c, plot of nominal stress vs. COD

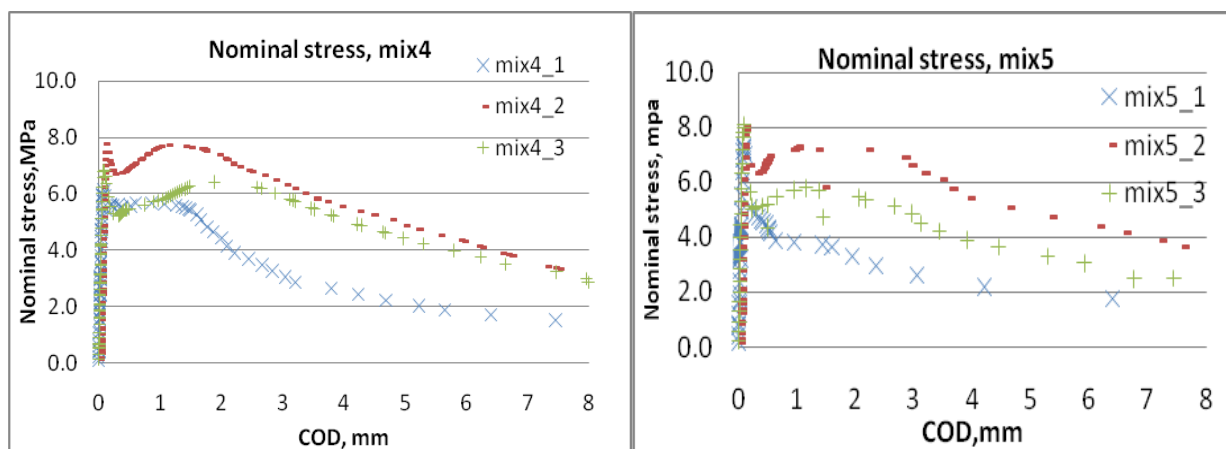Mix6: reference mix + 3%SP,   Mix7: reference mix – 3%SP,
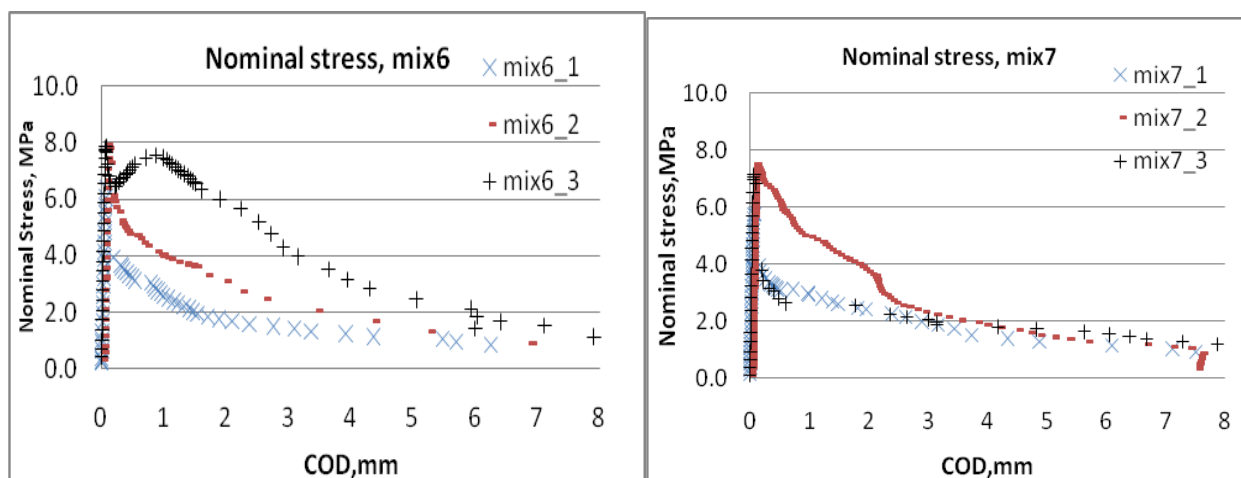

Figure 4.17d, plot of nominal stress vs. COD

✓ Increase in water content results in decreasing residual strength

✓ Increase in cement content increases the residual bending strength.

Table 4.15   Summary of f_{eq1}, f_{eq2}, f_{lt} and peak COD

Beam section	feq,1: N/mm² [0.3-0.5 mm]	feq,2 : N/mm² [0.02h±20%]	σN peak: N/mm² [COD peak]	COD peak (mm)
B1_1	6.259912	7.068361	7.29	0.101
B1_2	5.402179	4.980731	7.35	0.0905
B2_1	3.513679	3.485099	4.42	0.084
B2_2	4.222307	3.996243	5.59	0.0735
B2_3	2.692366	2.997362	5.64	0.066
B3_1	4.156226	4.564654	6.46	0.079
B3_2	3.102912	3.174124	6.60	0.095
B3_3	3.839377	3.89544	7.18	0.085
B4_1	5.555477	5.58035	6.15	0.0715
B4_2	6.866948	7.709162	7.78	0.09
B4_3	5.379461	5.981668	6.90	0.0795
B5_1	4.55158	3.763101	7.31	0.0905
B5_2	6.616255	7.221045	8.05	0.083
B5_3	5.123513	5.750099	8.08	0.0895
B6_1	3.385589	2.333722	6.36	0.77
B6_2	4.849779	3.812035	7.90	0.079
B6_3	6.886985	7.051741	7.86	0.0695
B7_1	3.187475	2.791575	5.83	0.069
B7_2	6.371369	4.644524	7.50	0.0875
B7_3	2.967565	2.62	7.14	0.067

The peak stress from the above plot is dependent on the matrix strength, i.e. the mid design paremeters. The fibers activated after the cracking occurred in the sectio of the beam. Therefore, the post-cracking determined the number of fibers on the cracked surface.

4.6.2 Comparison for the section of beams

The fiber dispersion and orientations can then be determined since it is the concentrations and oreientations of fibers which significantly affetspost-cracking flexural strength.
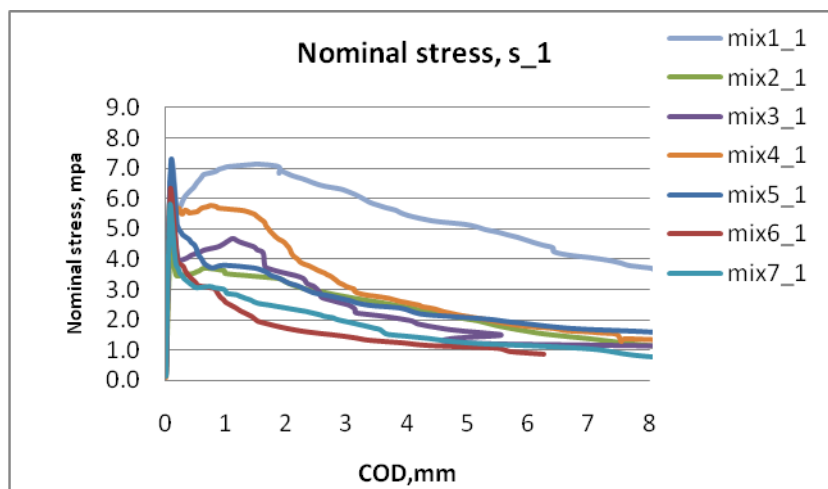

Figure 4.18a plot of nominal stress for first section of beams vs. nominal stress
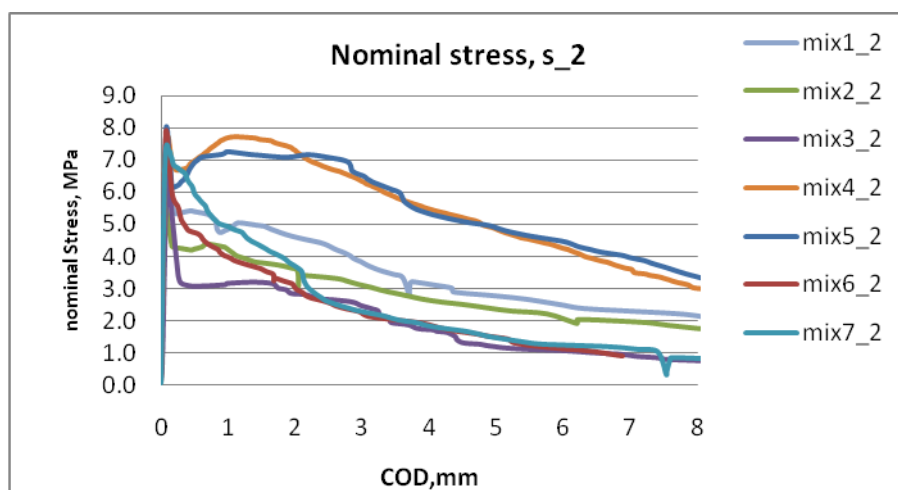
Figure 4.18b plot of nominal stress for middle section of beams vs. nominal stress
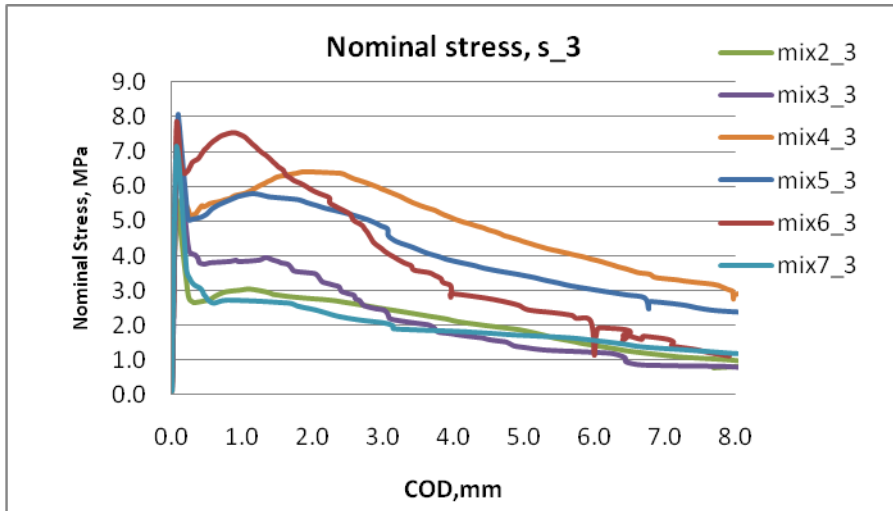
Figure 4.18c plot of nominal stress for last section of beams vs. nominal stress

4.6.3 Correlation of Nominal stress vs. fiber counting

The number of fibers on the fracture surface was counted from the results of bending tests. It has to be remarked that in the specific number of fibers on the fracture surface information about the orientations of fibers is already embedded, [Soroushian and Lee]. In fact , from specific number of fibers per unit area, Nf, the orientation factors α has been calculated.

The following three figures shows that the plot of reference mix nominal stress with reference to the mix variations with water, cement, SP.
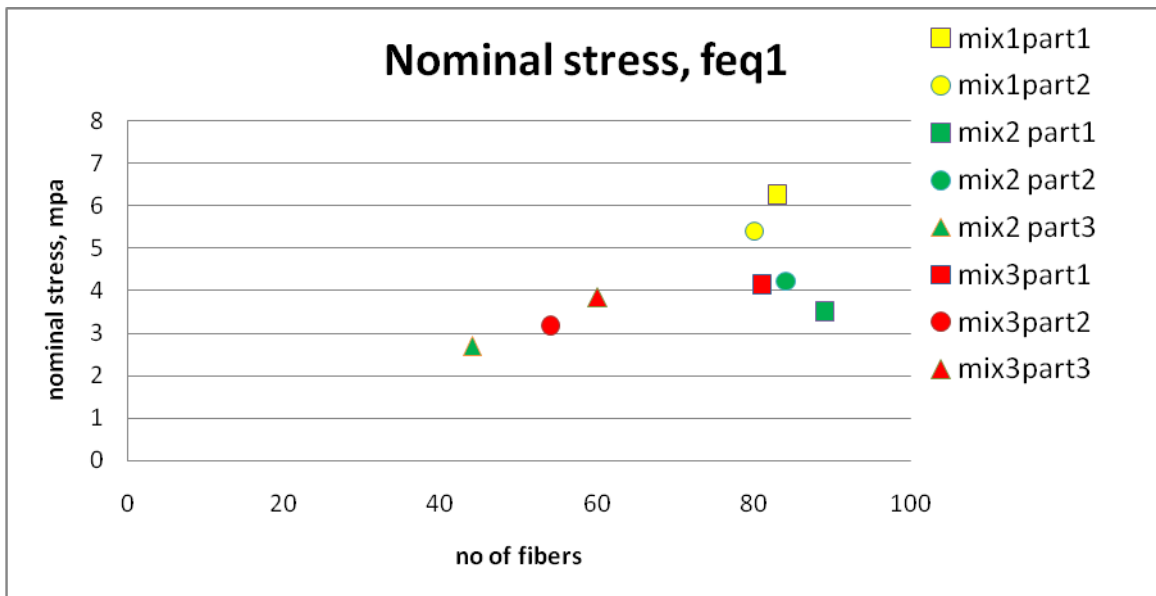
Figure 4.19a correlations of number of fibers with nominal stress, feq1
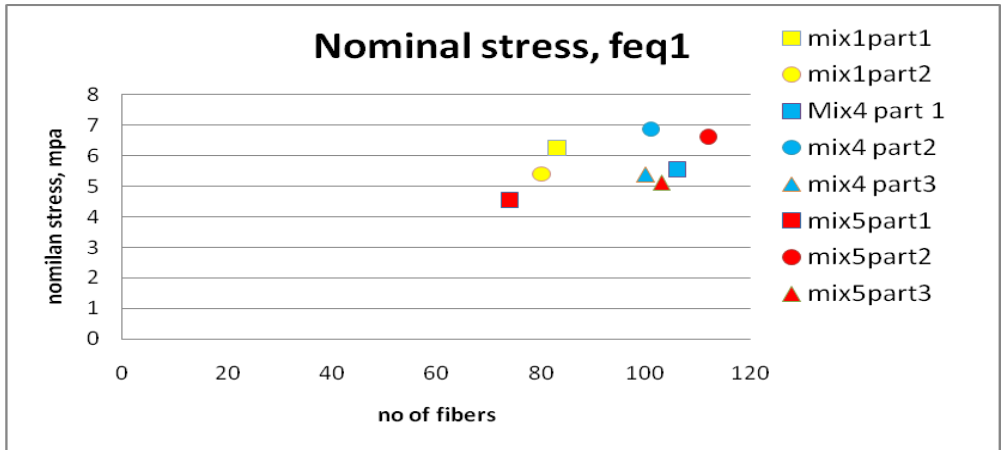
Figure 4.19b correlations of number of fibers with nominal stress, feq1
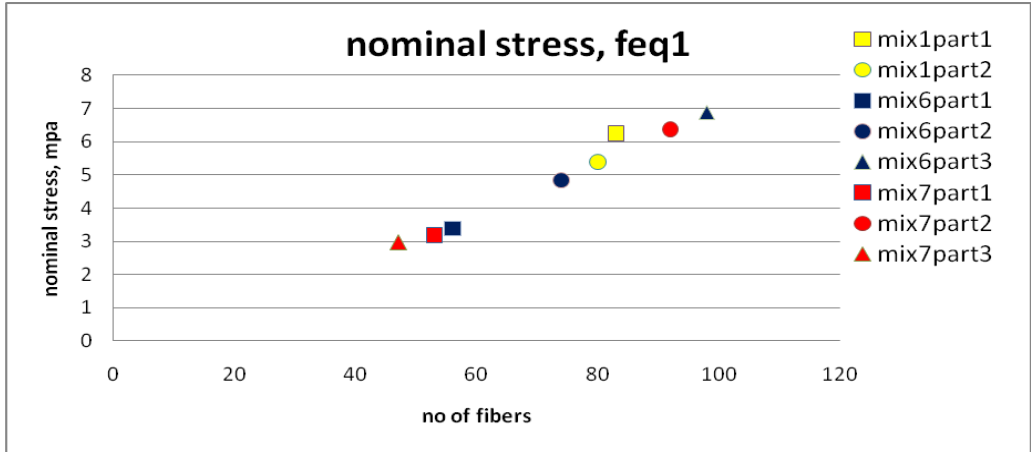
Figure 4.19c correlations of number of fibers with nominal stress, feq1
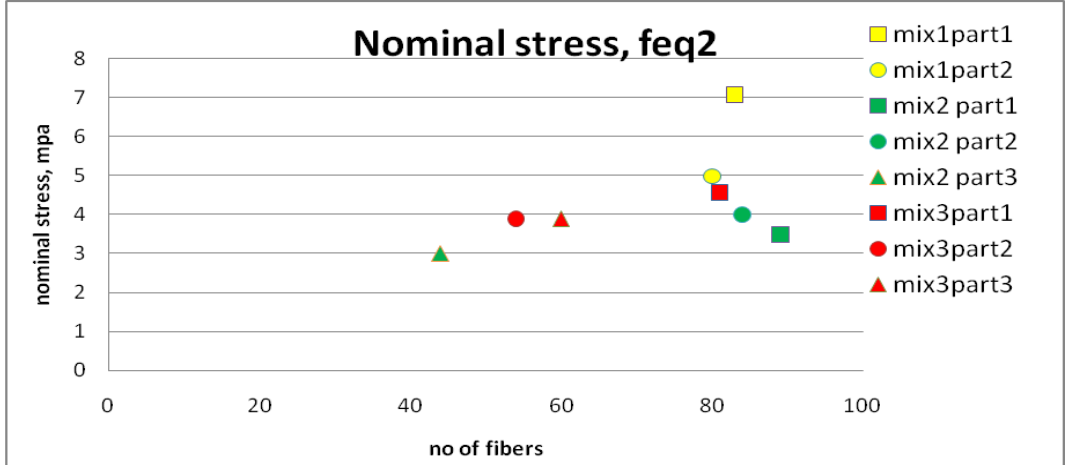
Figure 4.19d correlations of number of fibers with nominal stress, feq2
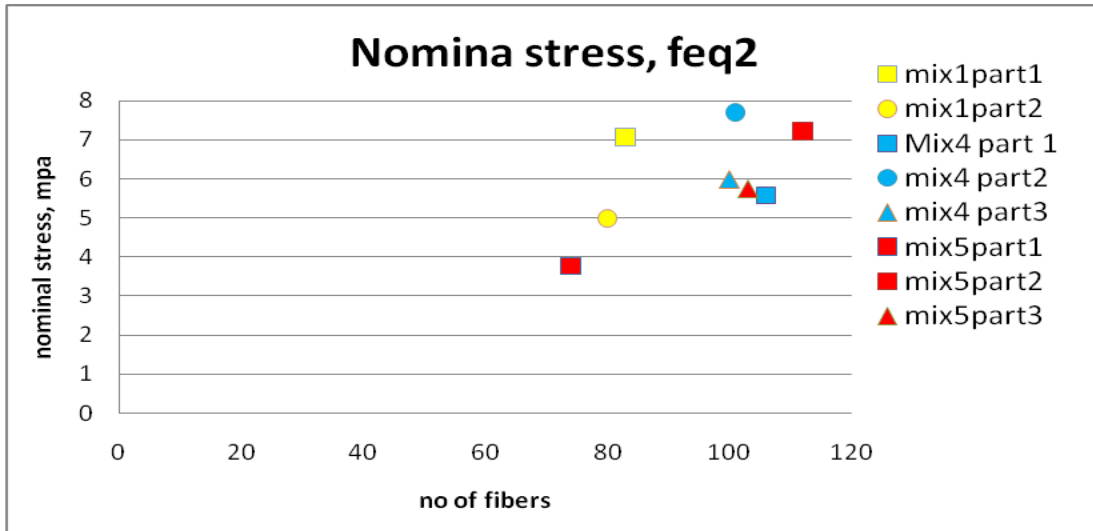
Figure 4.19e correlations of number of fibers with nominal stress, feq2
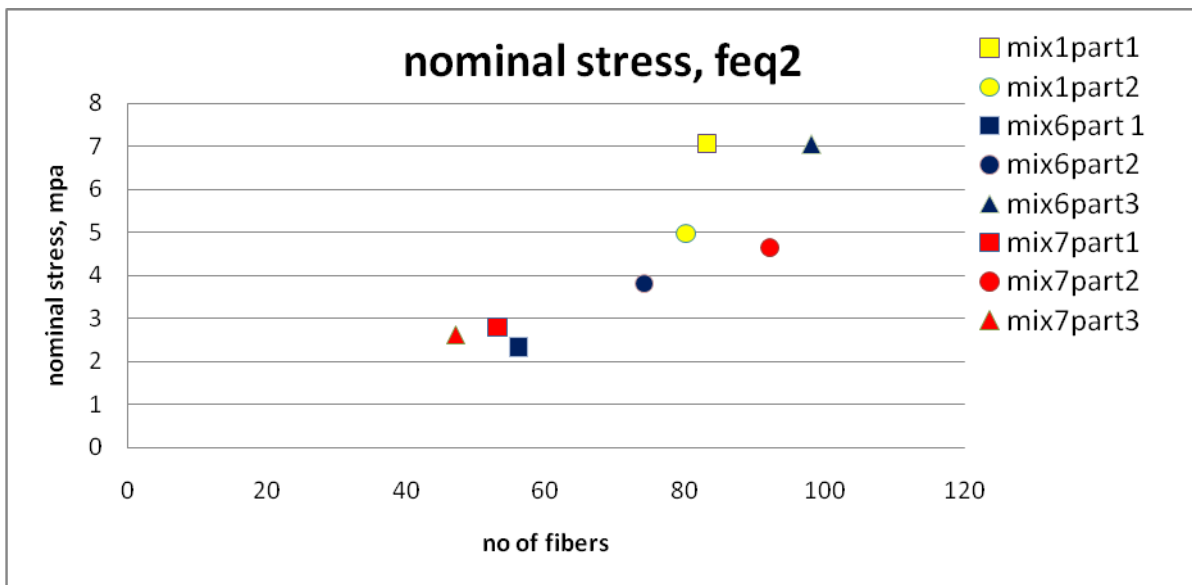
Figure 4.19f correlations of number of fibers with nominal stress, feq2

Finding:

➢ the post-cracking flexural strength seems to be directly increases with increase in the number of fibers.

➢ The higher the numnber of fibers on the section, the higher is the corresponding strength.

➢ the sensitivity of the flexural strength to the cement variation, water variations and sp variations can be concluded from the plot.

4.6.4 Results from the compressive strength tests

The experimental results from the compressive tests were shown in the table 4.16

Table 4.16 compressive strength value as function of mix variation

Mix. No.	casted dates	cube number	dimensions, mm			weight kg	max. P KN	Compres Stress,Mpa
			length	depth	width			
1	20/05/2010	no1	150	153	150	8.209	1291.5	56.27
2	14/06/2010	no2	150	148	150	7.632	1093	49.23
3	21/06/2010	no3	150	151	150	8.1895	1330.5	58.74
4	21/06/2010	no4	150	150	150	7.9105	1327.5	59.00
5	24/06/2010	no5	150	150	150	8.071	1279	56.84
6	28/06/2010	no6	150	151	150	8.0595	1307	57.70
7	28/06/2010	no7	150	133	150	7.587	1240.5	62.18

Note:

➢ Increase in water content significantly reduces the compressive strength.

4.6.5 Results from the tensile splitting tests

The results from the tensile splitting tests, are shown in the following tables 4.17,

Table 4.17 splitting tensile strength value for mixes

| Mix. No.	specimen date	cylinder number	dimensions,mm		weight kg	max. P load, KN	Tesile Stress,Mpa	average stress,mpa	
			diameter	height					
1	20/05/2010	no1_1	77	80	0.866	46.18	4.773	4.1434511	mix1
		no1_2	77	81	0.877	34.43	3.514		
2	14/06/2010	no2	77	87	0.951	30.56	2.904	2.9041798	mix2
3	21/06/2010	no3_1	77	91	1.004	55.94	5.082	5.0046349	mix3
		no3_2	77	88	0.967	52.44	4.927		
4	21/06/2010	no4_1	77	83	0.895	29.25	2.914	2.9136486	mix4
5	24/06/2010	no5_1	77	77	95	59.81	6.422	5.0952017	mix5
		no5_2	77	95	91	43.3	3.768		
6	28/06/2010	no6_1	77	127	1.43	75.6	4.922	5.5886766	mix6
		no6_2	77	125	1.372	94.58	6.256		
7	28/06/2010	no7_1	77	77	0.837	41.43	4.449	4.4485001	mix7

Note:

✓ The decrease in water content decreases the amount tensile strength since the peak strength is dependent on the matrix strength.

CHAPTER 5 CONCLUSION AND FUTURE DEVELOPMENTS

5.1 Conclusion

The observations about the investigated robustness of self consolidating steel fiber reinforced concrete in fresh and hardened state were presented as follows.

5.1.1 Fresh state properties

The rheological parameters of cement paste, cement mortar**,** self-compacting concrete and self consolidating steel fiber reinforced concrete were analyzed considering the variation in amount of cement, water and sp. They were instrumental to assess sensitivity of the flowability, segregation resistance, passing ability fiber dispersion and orientations to the variations of mix constituents. This allow to develop dedicated rheological quality control procedures for the qualification and acceptance of the material as well as for the assessment of the robustness in fresh state performance.

From the obtained results, it can be concluded that changes in water content is most important since it changes the fresh parameters like fluidity, workability and fiber segregations significantly. The effect of moisture available in the aggregates needs to be considered very carefully. The cement content variation also affects the fresh properties. Increasing the amount of cement makes the concrete more viscous and reduces workability. Anyways, the cement content is usually weighed more accurately with an acceptable errors.

5.1.2 Hardened state properties.

The hardened state properties of SCSFRC are affected by variations in cement content, water content, and admixture. Toughness parameters always depends on the fiber dispersion and orientation. Similar to the fresh state properties, changes in the mix constituents affects the fiber dispersion and orientations and dispersion. Other properties like compressive strength, tensile splitting strength are mainly affected by the water cement ratios in the mix design. Moreover, the fibers distribution or segregation in the SCSFRC mixes were mainly affected by the changes in water content.

5.2 Future developments.

This research project provides useful information also to develop quality control procedure in field of applications of self compacting steel fiber reinforced concrete.

REFERENCES

Abrishami, H.H. and Mitchell. D.: "Influence of steel fibers on tension stiffening", ACI Structural Journal, 94 (6), 1997, pp. 769-776.

Aoude, H., Cook, W. D. and Mitchell, D.: "Tensile behaviour of reinforced concrete specimens constructed with steel fibers and SCC", in Fiber Reinforced Concrete: Design and Applications, Proceedings of the 7th International RILEM Symposium BEFIB 2008, R. Gettu, ed., 17-19 September 2008, Chennai, India, RILEM PRO 60, RILEM Pubs, pp. 689-698.

Aoude, H., Cook, W.D. and Mitchell, D.: "Behavior of columns constructed with fibers and self-consolidating concrete", ACI Structural Journal, 106 (3), 2009, pp. 349-357.

Armelin. H.S., and Banthia, N.: "Predicting the flexural post-cracking performance of steel fibre reinforced concrete from the pullout of single fibers", ACI Materials Journal, 94 (1), 1997,

A.B. Yu, R.P. Zou, N. Standish, Packing of ternary mixtures of non-spherical particles, Journal of the American Ceramic Society, 75 (10), 1992.

Balaguru, P. N. and Shah. S.P.: "Fiber reinforced cement composites", Mc Graw Hill, Singapore New York, (1992), 530 pp.

Bamonte, P., Felicetti, R. and Gambarova, P.G.: "Mechanical properties of self-compacting concrete at high temperature and after cooling", in S.P. Shah, ed., proc. SCC2008, The Third North American Conference on the Design and Use of Self-Consolidating Concrete, November 10-12 2008, Chicago, IL, USA.

Barragàn, B., Zerbino, R., Gettu, R., Soriano, M., de la Cruz, C., Giaccio, G. and Bravo, M., "Development and application of steel fiber reinforced self-compacting concrete", in M. di Prisco et al. (eds.) BEFIB 2004, Proc. 6th Int. RILEM Symp., Varenna, Italy, 20-22 Sept. 2004, Rilem Pubs.

Bayasi, M.Z. and Soroushian, P.: "Effect of Steel fiber reinforcement on fresh mix properties of concrete", ACI Materials Journal, 89 (4), 1992, pp. 369-374.

Bindiganavile, V., Banthia, N. and Aarup, B.: "Impact response of ultra-high strength fiber reinforced cement composites", ACI Materials Journal, 99 (6), 2002, pp. 543-548.

Biolzi, G., Guerrini, G.L. and Bertolini, L.: "Cementitious materials with hybrid fibers exposed to high temperatures", in M. di Prisco et al. (eds.) BEFIB 2004, Proc. 6th Int. RILEM Symp., Varenna, Italy, 20-22 Sept. 2004, Rilem Pubs.,pp. 635-646.

Bonen, D., and Shah, S. P., "Fresh and Hardened Properties of Self-Consolidating Concrete," *Progress in Structural Engineering and Materials*, V. 7, 2005

Buratti, N: and Mazzotti, C.: "Long term behaviour of self compacting fibre-reinforced concrete beams", Proceedings 2nd International Symposium on the Design Performance and Use of SCC, SCC2009, C. Shi et al., eds, Beijing, 5-7 June 2009, RILEM Pro 65, 551-561.

Carlsward, J. and Emborg, M.: "Prediction of stress development and cracking in steel fibre reinforced self compacting concrete overlays due to restrained shrinkage", in ACI SP Self Consolidating Fiber Reinforced Concrete, Corina M. Aldea and L. Ferrara eds., to appear.

Caverzan, A.: "High strain rate uniaxial tensile constitutive behavior in fiber reinforced cementitious composites", PhD Thesis, 2010, Politecnico di Milano, 158 pp.

Chalencon, F:, Orgeas, L., Dumont, P.J.J., Foray, G., Cavaillé, J.Y., Maire, E. and Rolland du Roscoat, S. (2010): "Lubricated compression and X-ray microtomography to analyse the rheology of a fibre-reinforced mortar", Rheologica Acta, 49,

Cheung, A.K. and Leung, C.K.Y.: "Experimental study on the bond between steel reinforcement and self-

compacting high strength fiber reinforced cementitious composites", in Fiber Reinforced Concrete: Design and Applications, Proceedings of the 7th International RILEM Symposium BEFIB 2008, R. Gettu, ed., 17-19 September 2008, Chennai, India, RILEM PRO 60, RILEM Pubs, pp. 667-678.

Colombo, M., di Prisco, M., Felicetti, R.: « Mechanical properties of steel fibre reinforced concrete exposed at high temperatures", Materials and Structures, 43, 2010, pp. 475-491.

Cremonesi, M., Ferrara, L. and Frangi, A.: "Rheological properties of cementitious composites: identification through field tests and Computational Fluid Dynamics modelling", submitted for publication to BAC 2010, July 2010, Portugal.

Cunha, V.M.C.F., Barros, J.A.O. and Sena Cruz, J.M.: "Tensile behavior of steel fiber reinforced self-compacting concrete", in ACI SP Self Consolidating Fiber Reinforced Concrete, Corina M. Aldea and L. Ferrara eds., to appear.

Cunha, V.M.C.F., Barros, J.A.O. and Sena-Cruz, J.: "Modelling the influence of age of steel fiber reinforced self-compacting concrete on its compressive behaviour", Materials and Structures, 41, 2008, pp. 465-478.

Cunha, V.M.C.F., Barros, J.A.O. and Sena-Cruz, J.M.: "Pull.out behavior of steel fibers in self-compacting concrete", ASCE Journal of Materials in Civil Engineering, 22 (1), 2010, pp. 1-9.

Dhonde, H.B., Mo, Y.L., Hsu, T.T.C., and Vogel, J.: "Fresh and hardened state properties of self-consolidating fiber-reinforced concrete", *ACI Materials Journal*, 104 (45), 2007.

di Prisco, C., di Prisco, M., Mauri, M. and Scola, M.: "A new design for stabilizing round slopes", *Proceedings of the Fib Conference, Naples, June 2006* (paper 823-CD-Rom).

Domone, P., Yongmo, X. and Banfill, P.F.G.: Developments of the two-point workability test for high performance concrete", Magazine of concrete research, 51 (3), 1999, pp. 171-179.

Domone, P.L.: "A review of the hardened mechanical properties of self compacting concrete", Cement and Concrete Composites, 2007, 29, pp. 1-12.

Douglas, J.F. and Garboczi, E.J.: "Intrinsic viscosity and the polarizability of particles having a wide range of shapes", Advances in Chemical Physics, XCI, Wiley, New York, 1995, pp. 2265-2270.

EFNARC, "European Guidelines for Self-Compacting Concrete: Specification, Production and Use," www.efnarc.org, 2005.

Faifer, M., Ottoboni, R., Toscani, S., Ferrara, L.: Steel Fiber Reinforced Concrete Characterization Based on a Magnetic Probe, accepted for publication in Proceedings of IMTC10, IEEE Intrumentation and Measurement Technology Conference, Austin TX, May 2010.

Felicetti, R., Ferrara L.: "The effect of steel fibre on concrete conductivity and its connection to on-site material assessment", Proceedings of Befib 2008, 7th International RILEM Symposium on Fiber Reinforced Concrete, R. Gettu ed., Chennai, India, 17-19 September 2008, pp. 525-536.

Ferec, J., Ausias, G., Heuzey, M.C., Carreau, P.J.: "Modeling fiber interactions in semiconcentrated fiber suspensions", *Journal of Rheology,* 53 (1), 2009, pp. 49-72.

Ferrara, L. and Meda, A.: "Relationships between fibre distribution, workability and the mechanical properties of SFRC applied to precast roof elements", Materials and Structures, 2006, 39, pp. 411-420.

Ferrara, L., Dozio, D. and di Prisco, M. : "On the connections between fresh state behavior, fiber dispersion and toughness properties of steel fiber reinforced concrete", Preoceedings of HPFRCC5, A. Naaman and H.W. Reinhardt eds., Mainz (Germany), July 13-15 2007, RILEM Pubs. PRO 53, pp. 249-258.

Ferrara, L., Park, Y.D., Shah, S.P.: "A method for mix-design of fiber reinforced self compacting concrete", Cement and Concrete Research, 37, 2007.

Ferrara, L., Ozyurt, N.: "Mix-design optimization of steel fiber reinforced SCC", Proceedings 3rd North American Conference on SCC, S.P. Shah ed., Chicago, 10-12 November 2008, CD_Rom, paper n° 1124.

Ferrara, L., Park, Y.D. and Shah, S.P. :Correlation among fresh state behaviour, fiber dispersion and toughness properties of SFRCs, ASCE Journal of Materials in Civil Engineering, 20 (7), 2008, pp. 493-501.

Ferrara, L.: "Statistical properties of steam-cured plant-produced SCC for prestressed precast applications", Proceedings SCC2009, 2nd International Symposium on Design, performance and use of Self-Consolidating Concrete, Beijing, 5-8 June 2009, C. Shi et al. eds., RILEM Pubs. S.a.r.l., RILEM PRO 65, pp. 483-494.

Ferrara, L., Ozyurt, N. and di Prisco, M.: "High mechanical performance of fiber reinforced cementitious composites: the role of "casting-flow" induced fiber orientation", accepted for publication on Materials and Structures, April 2010, available on line, DOI 10.1617/s11527-010-9613-9

Ferrara, L., Tregger, N., Shah, S.P.: "Flow-induced fiber orientation in SCSFRC: monitoring and prediction", accepted for publication in Proceedings of SCC2010, 4th International RILEM Symposium on Self-Compacting Concrete and 4th North American Conference on the Design and Use of SCC, Montreal, Canada, 26-29 September 2010.

Ferrara, L., di Prisco, M., Lamperti, M.G.L.: "Identification of the stress-crack opening behavior of HPFRCC: the role of flow-induced fiber orientation", *Proceeedings FraMCoS 7*, 7th International Conference of Fracture Mechanics of Concrete and Cocnrete Structures, B.H. Oh et al., eds., Jiejiu, South Korea, 23-28 May 2010, pp. 1541-1550

Forgeron, D. and Omer, A.: "Flow characteristics of macro-synthetic fiber reinforced self consolidating concrete", in ACI SP Self Consolidating Fiber Reinforced Concrete, Corina M. Aldea and L. Ferrara eds., to appear.

F. De Larrard, Concrete mixture proportioning. A scientific approach, E&FN Spoon, 1999
Ghanbari, A. and Karihaloo, B.L.: "Prediction of the plastic viscosity of self-compacting steel fiber reinforced concrete", Cement and Concrete Research, 39 (12), 2009,

Ghanbari, A. and Karihaloo, B.L.: "Prediction of the plastic viscosity of self-compacting steel fiber reinforced concrete", Cement and Concrete Research, 39 (12), 2009, pp. 1209-1216

Greenough, T. and Nehdi, M.: "Shear behaviour of fiber.reinforced self-consolidating concrete slender beams", ACI Structural Journal, 105 (5), 2008, pp. 468-477.

Groth, P.: "Steel fibre reinforced SCC", Final report of task 6, Brite Euram project (BE 96-3801) – rational production and improved working environment through using SCC.

Gunez, D.Z., Scirocco, R., Mewis, J., Vermart, J.: "Flow induiced orientationj of non spherical particles: effect of aspect ratio and medium rheology", Journal of Non Newtonian Fluid Mechanics, 155, 2008, pp. 39-50.

He, X. and Yang, Q.: "Research on impact properties of flexible fiber reinforced self-compcating concrete in middle-low intensity", in C. Shi et al., eds, Proceedings 2nd International Symposium on the Design Performance and Use of SCC, SCC2009, Beijing, 5-7 June 2009, RILEM Pro 65, 577-585.

Hegger, J., Rauscher, S., Lange, J. and Zell, M.: „Fiber orientation in ultra high performance concrete", in Fiber Reinforced Concrete: Design and Applications, Proceedings of the 7th International RILEM Symposium BEFIB 2008, R. Gettu, ed., 17-19 September 2008, Chennai, India, RILEM PRO 60, RILEM Pubs, pp. 191-199.

Hela, R. and Hibertova, M. : « Research of effect of fibre reinforcement at characteristics of lightweight self compacting concrete », in G. De Schutter and V. Boel, eds., Proc. SCC2007, 5th International RILEM Symposium on Self-Compacting Concrete, 3-5 September 2007, Gent, Belgium, Rilem Pubs, PRO 54, pp. 845-850.

Jiang, Z., Banthia, N. and Delbar, S.: "Effect of cellulose fibers on properties of self-compacting concrete with high volume mineral admixtures", in C. Shi et al., eds, Proceedings 2nd International Symposium on the Design Performance and Use of SCC, SCC2009, Beijing, 5-7 June 2009, RILEM Pro 65, 495-505.

Jonhson W. Rigueira, Emilio García-Taengua, and Pedro Serna-Ros : "Self-Consolidating Concrete Robustness in Continuous Production Regarding Fresh and Hardened State Properties

J.F. Lataste, M. Behloul, D. Breysse "Characterisation of fibres distribution in a steel fibre reinforced concrete with electrical resistivity measurements" NDT & E International, Volume 41(8), 2008, Pages 638-647

J. Walraven. Self-compacting concrete. Challenge for designer and researcher. In the S.P. Shah, editor, The 2nd North American Conference on the Design and Use of Self-Consolidating (SCC) and the 4th International RILEM Symposium on Self-Compacting Concrete, volume 1, pages 341-446, Chicago, 2005.

Keshtkar, M., Heuzey, M.C., Carreau, P.J.: "Rheological behaviour of fiber filled model suspensions: effect of fiber flexibility", *Journal of Rheology,* 53 (1), 2009, pp. 631-650.

Khayat, K., Assaad, J., and Daczko, J., "Comparison of field-oriented test method to assess dynamic stability of self-consolidating concrete", ACI Materials Journal, 101 (2), 2004, pp. 168-176.

Kooiman, A.G: "Modelling steel fibre reinforced concrete for structural design", PhD thesis, Department of Structural and Building Engineering, Delft University of Technology, 2000.

Krage, G. and Wallevik, O.H., "Rheology of synthetic fiber reinforced SCC", in in G. De Schutter and V. Boel, eds., Proc. SCC2007, 5th International RILEM Symposium on Self-Compacting Concrete, 3-5 September 2007, Gent, Belgium, Rilem Pubs, PRO 54, pp.347-352.

Kwon, S.H., Ferron, R.P., Akkaya, Y. and Shah, S.P.: "Cracking of fiber reinforced self-compacting concrete due to restrained shrinkage", International Journal of Concrete Structures and Materials, 1 (1), 2007, pp.3~9.

K.H. Khayat and Y. Roussel: "Testing and performance of fiber-reinforced, self-consolidating concrete", Materials and Structures, 33 (6), 2000.

Ma, W.K.A., Chinesta, F., Ammar, A. and Mackley, M.R.: "Rheological modeling of carbon nanotube aggregate suspensions"*, Journal of Rheology,* 52 (6), 2008, pp. 1311-1330.

Markovic, U., Grunewald, S., Walraven, J., van Mier, J.G.M.: "Characterization of bond between steel fibers and concrete – conventional fibre reinforced concrete vs. self-compacting fibre reinforced concrete", in Proc. Third International Symposium "Bond in Concrete-from research to standards", G. Balazs ed., Budapest, 2002, Publishing Company of the Budapest University of Technology, pp. 520-528.

Martinie, L., Rossi, P. and Roussel, N.: "Rheology of fiber reinforced cementitious materials: classification and prediction", Cement and Concrete Research, 40 (2), 2010,

Mechtcherine, V, Shyshko, S., "Simulating the behaviour of fresh concrete using distinct element method", Proceedings 5th International RILEM Symposium on Self Compacting Concrete, G. De Schutter ed., Ghent, Belgium, 3-5 September 2007, RILEM Pubs. sarl, PRO 54, pp. 467-472

Mohammed, R.N. and Elliot, K. S.: "Behaviour of steel fiber self compacting concrete under biaxial loading", in G. De Schutter and V. Boel, eds., Proc. SCC2007, 5th International RILEM Symposium on Self-Compacting Concrete, 3-5 September 2007, Gent, Belgium, Rilem Pubs, PRO 54, pp. 1079-1091.

Moses, K.B., Advani, S.G., Rheinhardt, A.: "Investigation of fiber motion near solid boundaries in single shear flow", Rheological Acta, 2001, 40, pp. 296-306.

Moncef Nedhi and J.D. Ladanchuk , "Fiber Synergy in Fiber-Reinforced Self-Consolidating Concrete", *ACI Materials Journal,* V.101, No 6, Nov-Dec 2004,pp. 403-422.

Naaman, A.E., Wongtanakitcharoen, T. and Hauser, G.: "Influence of different fibers on plastic shrinkage cracking of concrete", ACI Materials Journal, 102 (1), 2005, pp. 49-58.

Okumara H., Ozawa K. And Ouchi M. Self-compacting concrete, Structural Concrete, 2000, 1, No.1, Mar., 3-17.

Ozyurt, N., Woo, L.Y., Mason, T.O. and Shah, S.P.: "Monitoring fiber dispersion in fiber reinforced cementitious materials: comparison of AC Impedance Spectroscopy and Image Analysis", ACI Materials Journal 103 (5), 2006, pp. 340-347.

Ozyurt, N., Mason, T.O. & Shah, S.P.: "Non destructive monitoring of fiber orientation using AC-IS: an industrial scale application", Cement and Concrete Research, 36, 2006, pp. 1653-1660.

Ozyurt, N., Mason, T.O. and Shah, S.P.: "Correlation of fiber dispersion, rheology and mechanical performance of FRCs", Cement and Concrete Composites, 29, 2007

Ozyurt, N., Tregger, N., Ferrara, L., Sedan, I. and Shah, S.P.: "Adapting fresh state properties of fiber reinforced cementitious material for high performance thin-section elements", Proceedings Rheo-Iceland 2009, 3rd International RILEM Symposium on Rheology of cement suspensions such as fresh concrete, O. H. Wallevik et al., eds. RILEM Pubs. S.a.r.l. RILEM PRO 68, pp. 313-321.

Patankar, N.A., Joseph, D.D.: "Modelling and numerical simulation of particulate flow by Eulerian Lagrangian approach", International Journal of Mutiphase Flow, 27, 2001, pp. 1659-1684.

Pereira, E.N.B., Barros, J.A.O. and Camoes, A.: "Steel fiber reinforced self-compacting concrete: experimental research and numerical simulation", ASCE Journal of Structural Engineering, 134 (8), 2008, pp. 1310-1321.

Petrie, C.J.S.: The rheology of fiber suspensions", Journal of Non Netwonian Fluid Mechanics, 87, 1999, pp. 369-402.

Pons, G., Mouret, M., Alcantara, M. and Granju, J.L.: "Mechanical behaviour of self-compacting concrete with hybrid fiber reinforcement", Materials and Structures, 2007, 40, pp. 201-210.

prEN12350-8, Testing fresh concrete – part 8 – Self compacting concrete – slump flow test.

prEN12350-9, Testing fresh concrete – part 8 – Self compacting concrete – V-funnel test.

prEN12350-10, Testing fresh concrete – part 8 – Self compacting concrete – L-box test.

prEN12350-12, Testing fresh concrete – part 8 – Self compacting concrete – J-ring test.

Romano, G.Q., Silva, F.A., Toledo Filho, R., Fairbairn, E.M.R. and Battista, R.C.: "Mechanical characterization of steel fiber reinforced self-compacting refractory concrete", in G. De Schutter and V. Boel, eds., Proc. SCC2007, 5th International RILEM Symposium on Self-Compacting Concrete, 3-5 September 2007, Gent, Belgium, Rilem Pubs, PRO 54, pp.881-886.

Roussel, N., and LeRoy, R., "The Marsh cone: a test or a rheological apparatus", Cement and Concrete Research, 35, 2005, pp. 823-830.

Roussel, N., Geiker, M., Dufour, F., Thrane, L.N., Szabo, P: "Computational modeling of concrete flow: general overview, Cement and Concrete Research, 37, 2007, pp. 1298-1307.

Romualdi, J.P. & Mandel, J.A. 1964. Tensile strength of concrete affected by uniformly dispersed and closely spaced short lengths of wire reinforcement, *Journal of the American Concrete Institute* 61: 657-672.

Shen, L., Struble, L. and Lange, D.: "Modeling static segregation of Self-Consolidating Concrete", ACI Materials Journal, 106 (4), 2009, pp. 367-374.

Shen, L., Struble, L. and Lange, D.: "Modeling dynamic segregation of Self-Consolidating Concrete", ACI

Materials Journal, 106 (4), 2009, pp. 375-380.

Soroushian, P. & Lee, C.D.: "Distribution and orientation of fibers in steel fiber reinforced concrete", ACI Materials Journal, 87 (5), 1990, pp. 433-439.

Stahli, P., Custer, R. and van Mier, J.G.M.: On flow properties, fibre distribution, fibre orientation and flexural behaviour of FRC, Materials and Structures, 41 (1), 2008, pp. 189-196.

Suresh Babu, T., Seshagiri Rao, M.V. and Rama Seshu, D.: "A study on the flexural behaviour of glass fiber reinforced self compacting concrete", in Fiber Reinforced Concrete: Design and Applications, Proceedings of the 7th International RILEM Symposium BEFIB 2008, R. Gettu, ed., 17-19 September 2008, Chennai, India, RILEM PRO 60, RILEM Pubs, pp. 793-802.

S. Grunewald, "Performance based design of self compacting steel fiber reinforced concrete", PhD Thesis, Delft University of Technology, 2004.

Tregger, N., Ferrara, L., Shah, S.P.: "Identifying cement rheological properties from the mini-slump-flow test", ACI Materials Journal, vol. 105, n° 6, November-December 2008.

Torrents, J. M., Mason,, T. O., Peled, A., Shah, S. P., and Garboczi, E. J., "Analisys of the impedance spectra of short conductive fiber-reinforced composites", *Journal of Materials Sciences,* 36 2001, pp. 4003-4012.

Torrijos, M.C., Barragan, B.E. and Zerbino, R.L.: "Physical-mechanical properties, and mesostructure of plain and fibre reinforced self-compacting concrete", Construction and Building Materials, 22, 2008, pp. 1780-1788.

Van Damme, S.; Franchois, A.; De Zutter, D.; Taerwe, L.; "Nondestructive determination of the steel fiber content in concrete slabs with an open-ended coaxial probe"; IEEE Transactions on Geoscience and Remote Sensing, 42 (11), pp. 2511 –2521

Vandewalle, L., Heriman, G. and van Rickstal F.: "Fibre orientaiton in self-compacting fibre reinforced concrete", n Fiber Reinforced Concrete: Design andf Applications, Proceedings of the 7th International RILEM Symposium BEFIB 2008, R. Gettu, ed., 17-19 September 2008, Chennai, India, RILEM PRO 60, RILEM Pubs, pp. 719-728

Voigt, T., Van Bui, K. and Shah, S.P.: "Drying shrinkage of concrete reinforced with fibers and welded-wire fabric", *ACI Materials Journal*, 101, (2), 2004, pp. 233-241.

V.K. Bui, J. Akkaya, S.P. Shah, Rheological model for self-consolidating concrete, ACI Materials Journal, 99 (6), 2002, pp. 549-559.

Yardimci, M.Y., Baradan, B. and Tasdemir, M.A.: "Studies on the relation between fiber orientation and flexural performance of SFRSCC", in Fiber Reinforced Concrete: Design and Applications, Proceedings of the 7th International RILEM Symposium BEFIB 2008, R. Gettu, ed., 17-19 September 2008, Chennai, India, RILEM PRO 60, RILEM Pubs, pp. 711-718

Yin, W.S., Su, E.C.M., Mansur, M.A. and Hsu, T.C.H.: "Biaxial tests on plain and fiber concrete", ACI Materials Journal, 86 (3), 1989, pp. 236-243.